DOI: 10.14750/ME.2018.004

Institute of Applied Mechanics
Faculty of Mechanical
Engineering and Informatics
University of Miskolc

Static and dynamic analyses of composite beams with interlayer slip

Ákos József Lengyel

PhD Thesis

István Sályi Doctoral School
Main Topic Group: Fundamental Sciences in Mechanical Engineering
Topic Group: Mechanics of Solid Bodies

Head of Doctoral School:
Miklós Tisza
Doctor of Science, Full Professor

Head of the Main Topic Group:
István Páczelt
Member of the Hungarian Academy of Sciences, Professor Emeritus

Head of the Topic Group:
György Szeidl
Doctor of Science, Professor Emeritus

Scientific Supervisor:
István Ecsedi
Professor Emeritus

Miskolc
2017

DOI: 10.14750/ME.2018.004

Contents

Declaration

The author hereby declares that the work in this thesis contains no material previously published or written by another person and no part of the thesis has been submitted, either in the same or different form to any other university for a PhD degree.

The author confirms that the work presented in this thesis is his own and appropriate credit is given in the text when (and where) reference is made to the work of others.

Miskolc, 26 January 2017

Ákos József Lengyel

Nomenclature

Here the most important notations are gathered in alphabetical order, although each notation is described in the text when first used.

Greek symbols

α_i	linear thermal expansion coefficient of the i-th layer
β	angle of the curved composite beam
γ_{xy}, γ_{xz}, γ_{yz}	shearing strains in Cartesian coordinate-system $Oxyz$
$\gamma_{r\varphi}$, $\gamma_{\varphi z}$, γ_{rz}	shearing strains in cylindrical coordinate-system $Or\varphi z$
ε_x, ε_y, ε_z	normal strains in $Oxyz$
ε_r, ε_φ	normal strains in $Or\varphi z$
ϑ	uniform temperature
ϑ_0	reference temperature
Θ	angle of the radial distributed line load on curved beams
κ_i	shear correction factor of the i-th layer
Π	total potential energy
ρ_i	mass density of the i-th layer
σ_y, σ_z	normal stresses in $Oxyz$
σ_φ	normal stress in $Or\varphi z$
τ_{yz}	shearing stress in $Oxyz$
$\tau_{r\varphi}$	shearing stress in $Or\varphi z$
ϕ_i	cross-sectional rotation of the i-layer
φ	tangential coordinate in $Or\varphi z$
ω_j	j-th eigenfrequency of the composite beam

Latin symbols

A	cross-section of the whole composite beam
A_i	cross-section of the i-th layer
∂A_{12}	common boundary of A_1 and A_2
b_i	width of the i-th layer
B	spatial domain occupied by the whole composite beam
B_i	spatial domain occupied by the i-th layer
∂B_{12}	common boundary surface of B_1 and B_2
c	distance between C_1 and C_2
c_i	distance between C and C_i
C	origin of the coordinate-system $Oxyz$, E-weighted centre of the whole beam cross-section
C_i	centre of the i-th layer

$\mathbf{e}_x$, $\mathbf{e}_y$, $\mathbf{e}_z$	unit vectors of $Oxyz$
$\mathbf{e}_r$, $\mathbf{e}_\varphi$, $\mathbf{e}_z$,	unit vectors of $Or\varphi z$
E_i	elastic modulus of the i-th layer
f, f_y	distributed line load in $Oxyz$
f_r, f_φ	distributed line load in $Or\varphi z$
F, $\tilde{F}$, F_1, F_2	concentrated force as loading
F_j^{cr}	j-th buckling load
G_i	shear modulus of the i-th layer
h_i	height of the i-th layer
H	Heaviside function
i	number of the layer
I_i	second moment of area of the i-th layer
k	slip modulus
L	length of the beam
m	distributed bending moment
M	total bending moment
$\tilde{M}$	bending moment as loading
M_i	internal bending moment in the i-th layer
N	total axial force
N_i	internal axial force in the i-th layer
Q	interlayer shear force
r	radial coordinate in $Or\varphi z$
r_a	radial coordinate of the outer boundary of the curved composite beam
r_b	radial coordinate of the inner boundary of the curved composite beam
r_c	radial coordinate of the common boundary of the layers of the curved beam
s	interlayer slip
S_i	cross-sectional shear force of the curved composite beam
t	time
T	uniform temperature change
$\mathbf{u}$	displacement field
u	horizontal displacement of the cross-section in $Oxyz$, radial displacement in $Or\varphi z$
U	strain energy
v	vertical displacement of the cross-section in $Oxyz$, tangential displacement in $Or\varphi z$
V	cross-sectional shear force
w	displacement in z direction
w_i	displacement of centreline of the i-th layer in z direction
W	work of the loading
x	horizontal coordinate of the cross-section
y	vertical coordinate of the cross-section
z	coordinate along the beam in $Oxyz$, coordinate perpendicular to the plane of symmetry of the curved beam in $Or\varphi z$

Chapter 1

Introduction

Layered composite structures, especially layered beams are widely applied in building and bridge engineering since the advantages of the layers made of different elastic materials can be well married, while their disadvantages can be reduced or eliminated. Therefore it is very important to understand the mechanical behaviour of the layered composite beams and the influence of the connection between the layers for the mechanical properties. In some cases it is assumed that the connection is perfect both in normal and tangential direction and this assumption provides satisfying results for these problems. The theory of this kind of composite beams is well developed. However, in a lot of other cases it is necessary to deviate from this assumption. Namely the beam components are generally joined to each other by different shear connectors such as nails, studs, screws or rivets. Because of the elastic deformation of these connectors two phenomena can occur among the layers. In normal direction the beam components may be divorce and in tangential direction an interlayer slip can happen. The experiments and measurements have proven that the effects of these phenomena cannot be neglected in a number of cases. This thesis is restricted to that problems when the connection is perfect in normal direction (the divorce of the layers is not allowed) but there is interlayer slip in tangential direction.

One of the most commonly used configuration is shown in Fig. 1.1. This type of composite beam is widely applied in the bridge industry. Its cross-section consists of a concrete slab with steel reinforcement and a steel joist. A large amount of studies and researches, which we are going to outlined in Section 1.1, deal with this configuration and its mechanical behaviour. Composite structures are also utilized as floor and wall elements, e.g. timber-concrete elements composed of thin concrete plates attached to wood studs by means of shear connectors. The common property of these structural elements is the interlayer slip. Our analyses are not restricted to the above mentioned configurations. The considered composite beam and the assumptions are going to appear at the start of each corresponding chapter.

1.1 Literature review

The first analytical works analysing the behaviour of composite beams with weak shear connection appeared in the 40's and 50's [1–3]. The pioneering and most cited work is definitely paper by Newmark et al. [1]. Their model, which is called the Newmark's model in the literature, used the following assumptions (i) the layers have linear elastic materials, (ii) the layers separately follow the Euler-Bernoulli beam theory, (iii) the vertical separation of the layers is not allowed. The problem was governed by a linear differen-

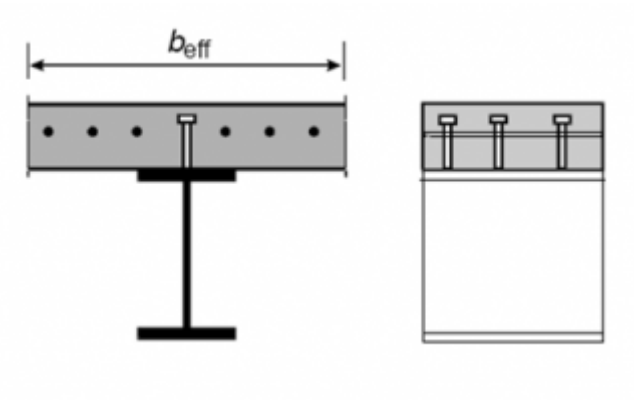

Figure 1.1. Frequently used composite cross-section with interlayer slip.

tial equation of second order in the longitudinal force resisted by the top element, and the other unknowns were the longitudinal force and the expression for moment along the beam.

In the late 60's, Goodman and Popov [4] further developed the Newmark's model and extended it for three-layered wood beams with interlayer slip. They deduced a differential equation of fourth order in the deflection and also contained the expression of the moment along the beam (the latter one is only unknown in the case of indeterminate beam). They consider the problem with one concentrated force applied at mid span and two concentrated force at third points. Adekola [5] proposed a model which took into account the vertical separation (it is also called uplift) of the layers and frictional effects. For the computations Adekola applied the finite difference method to solve the problem numerically. Other researchers further investigated the influence of the uplift [6–8]. They computed the error caused by neglecting the uplift in the Newmark's model and determined that the effect of the uplift can be ignored since the order of this error is a few percent.

Girhammar and Gopu [9] proposed a formulation for the exact first- and second-order analyses of composite beam-columns with partial shear interaction subjected to transverse and axial loading. In this study the authors extended the Newmark's model with taking into account axial loading. The governing differential equation was of the sixth order in vertical displacement. Ecsedi and Baksa [10] also deduced the governing equation of the problem in terms of the slip and the vertical displacement. Previous researches including the work of Newmark et al. [1] always assumed no axial force on the composite beam. Girhammar and Pan [11] developed a model for the exact and approximate analysis for composite beams with interlayer slip subjected to general dynamic load.

Some study dealt with the behaviour of continuous composite beams with interlayer slip in the linear-elastic range [12–14]. Plum and Horne [12] investigated a two-span continuous beam subjected to two equal point loads at the centres of the two span. They proposed closed-form solutions for the deflection, for the longitudinal force in the top element, for the slip, for the slip strain and for the redundant moment at the internal support. A two-span and a three-span continuous beam were analysed by Jasim [13]. The two-span continuous beam was subjected to both distributed line load and point loads at mid-spans, whilst the three-span continuous beam had a point load at the centre of the internal span. Jasim and Atalla [14] provided a simplified solution to determine the deflection of a continuous composite beam. However, the formulation can be derived for the continuous beams based on the Newmark's model, the computations can easily

become lengthy and difficult.

Interesting fact that the significant applications of the finite element method (FEM) for the problem of composite beams with partial shear interaction were carried out around the millennium, although the behaviour of this type of beams had been investigated for 50 years. The finite element satisfying the least regularity to describe the partial shear interaction problem is the 8 degrees of freedom (dof) finite element, for which the lengthwise interpolation functions are cubic for the transverse deformation and linear for the axial deformations defined at the centroids of the top and bottom elements. Application of this element leads to a curvature locking problem, which causes numerical instabilities for high values of the stiffness of the shear connection [15, 16]. The consequences of this phenomenon have been described by Prathap and Naganarayanan [17]. The spurious oscillatory trends that occur in related multi-field problems in engineering numerical methods have been quantified by Dall'Asta and Zona [18]. Some researchers examined the possibilities to avoid the locking phenomenon. Dall'Asta and Zona [16, 18] proposed to introduce further nodes at midspan of the element. A 10dof element was provided by Daniels and Crisinel [19]. Previously Arizumi, Hamada and Kajita considered a 12dof finite element in [20]. Dall'Asta, Leoni and Zona further increased the degrees of freedom to 16 [21, 22]. Salary, Spacone et al. [23, 24] proposed a finite element formulation based on the force method. Ayoub and Filippou [25, 26] derived displacement-stress mixed elements. Dall'Asta and Zona [27] also considered the possibility of utilizing a three-field mixed formulation.

Faella et al. [28, 29] developed a stiffness element with 6 dof which are the vertical displacement, the rotation and the slip at both ends. To obtain the stiffness matrix the flexibility matrix was inverted for the case of a simply supported beam. The flexibility coefficients had already been derived by Consenza and Pecce [30]. The determination of the stiffness matrix based on the Newmark's model, thus this method is able to provide the same results as the solution of the governing equation of the partial shear interaction problem. All the above mentioned study dealt with the problem of composite beams with interlayer slip in linear-elastic range. In this thesis the problem of the considered composite beams is also analysed in the linear-elastic range.

Therefore we note that a number of studies investigated the problem of composite beams with weak shear connection by means of non-linear modelling but in the following only the significant publications are mentioned. Many researchers further extended the Newmark's model taking into account material non-linearities. Several tests have been carried out on simply supported and continuous beams in order to compare the real behaviour of the beams with the modelling. Test results have been published in [31–34]. Some investigators analysed the behaviour of composite beams at ultimate loads only [35, 36]. Yam and Chapman [37] proposed a modelling method taking into account material non-linearities based on the Newmark's model. For the solution of the problem a step-by-step method of numerical integration was used. They utilized the results in [38, 39]. The ductility of composite beams was investigated by Rotter and Ansourian [40, 41]. Ansourian [31] introduced a finite element technique including realistic material properties for steel and concrete but the solution did not provide a general and robust technique. Finite difference method was applied in [42, 43]. In these studies the material non-linearities were assumed only for the shear connectors, the material of the layers behaved in linear-elastic way. A mixed formulation was derived by Oehlers and Sved [44]. They assumed that the beam layers behaved elastic, whilst the connection was plastic. Fabbrocino et al. [45] derived a formulation to analyse the behaviour of a simply supported

composite beam (shown in Fig. 1.1) in the sagging moment region. During the solution they used the finite difference method. These authors further developed the considered formulation to extend it to the hogging moment region [46]. They also assumed interlayer slip between the concrete and the steel reinforcement in the top layer. In [47] the authors had analysed a continuous beam with the previously developed method, and one year later they also published a study on the ductility of composite beams in the hogging moment regions [48].

The composite beams made of a concrete slab combined with a steel joist are the most frequently used in the bridge and building industry. Amongst these type of composite beams perhaps the most significant one is shown in Fig. 1.1. It follows that many works deal with steel-concrete composite beams including the effect of the time-dependent behaviour of concrete taking into account the interlayer slip. The thesis is not restricted to this pair of materials and does not consider the time-dependent behaviour of concrete, therefore only the most important publications are mentioned in the following. Bradford and Gilbert [49] applied a relaxation solution for the steel joist and the so-called age-adjusted effective modulus method for the concrete assuming full shear interaction between the layers. The same authors further developed their model with the influence of the partial shear interaction in [50, 51]. Tarantino and Dezi [52] proposed a new formulation based on two discretization, one in the time domain and one in the spatial domain along the beam axis. They used the step-by-step procedure to model the time-dependent behaviour of concrete. The same authors further developed the previous study for continuous beams applying the flexibility method [53, 54]. This method was used in [55] including simplified creep models, such as the age-adjusted effective modulus method, the effective modulus method and the mean stress method. Few years later Dezi, Leoni and Tarantino [56] carried out a comparison between their previously published models. They found that the age-adjusted effective modulus method provided good results under static actions, while shrinkage effects should be modelled by dint of the mean stress method. A lot of investigators utilized FEM solutions to describe the time-dependent behaviour of concrete, e.g. [57–60]. The only closed form solution for the problem of steel-concrete composite beams was proposed by Mola et al. [61]. They used the flexibility approach for a simply supported beam with various loading conditions and the behaviour of concrete was modelled by the age-adjusted effective modulus method. Numerical models [62] and stiffness element [29] were also investigated for the problem of time analysis of steel-concrete composite beams with partial shear interaction.

An excellent thesis was carried out by Ranzi [63] on composite beams with partial shear interaction. The author utilized and further developed several models mentioned above. Namely general solution was derived for two- and for m-layered composite beams with interlayer slip in linear elastic range. Some stiffness elements were also described to analyse the problem of steel-concrete composite beams. The author summarized several theories of material non-linearity which were also applied. Finally time analyses were introduced including the time-dependent behaviour of concrete assuming both full and partial shear interaction between the layers. The steel-concrete composite beam analysed by Ranzi had the cross-section shown in Fig. 1.1. The author also provided a detailed and useful literature review.

Other beam theories were adopted for investigation of composite beams with interlayer slip as well. The Timoshenko beam theory was used in [64]. Murakami [64] formulated boundary value problems by means of the principle of virtual work. Combining the development of finite elements with the Timoshenko beam theory was also analysed in

[65–70]. Recently several works have also revealed utilizing higher order beam theories for the problem of composite beams with partial shear interaction [71–74].

There exist several works in connection with the dynamic analysis of composite beams with interlayer slip [11, 75–78]. An exact and an approximate analysis of composite members with partial interaction and subjected to general dynamic loading were presented by Girhammar and Pan [11]. Adam et al. [75] analysed the flexural vibration of composite beams with interlayer slip using the Euler-Bernoulli beam theory. The governing sixth-order initial-boundary value problem was solved by separating the dynamic response in a quasi-static and in a complementary dynamic response. Heuer and Adam extended the previous model for composite beams made of piezoelectric materials in [76]. The partial differential equations and general solutions for the deflection and internal actions and the pertaining consistent boundary conditions were presented for composite Euler–Bernoulli members with interlayer slip subjected to general dynamic loading in [77]. Wu et al. [78] derived the governing differential equations of motion for the partial-interaction composite members with axial force. All these works neglected the influence of the axial and rotary inertia.

The elastic stability problems of composite beams with weak shear connection were also investigated [79–83]. Challamel and Girhammar [79] analysed the lateral-torsional stability of vertically layered composite beams with interlayer slip based on a variational approach. An analytical method was presented for the delamination buckling using the Timoshenko beam theory by Chen and Qiao [80]. Grognec et al. [81] utilized the Timoshenko beam theory as well. Schnabl and Planinc [82] presented a detailed analysis of the influence of boundary conditions and axial deformation on the critical buckling loads and the same authors took into account the effect of the transverse shear deformation on the buckling [83].

Although a lot of papers were published in connection with layered curved beams with perfect shear connection, only a few works counted the influence of the interlayer slip [84–86]. For out-of plane deformation and loads the time dependent creep and shrinkage behaviour of horizontally curved steel-concrete composite beams with partial shear interaction were analysed by Liu et al. [84]. Erkmen et al. [85] developed a total Lagrangian finite element formulation for elastic analysis of steel-concrete curved composite beams. A three-dimensional finite element model is used to simulate composite steel-concrete curved beams subjected to combined flexure and torsion [86]. Tan and Uy gave a detailed description of the torsion induced vertical slip [86].

1.2 Objectives

According to the literature review one can see that a number of investigators dealt with the static analysis of composite beams with interlayer slip to determine the governing equation of the problem. In many cases the analysis led to a higher order differential equation the solution of which is often difficult and cumbersome. Thus it is my

Objective 1 to provide an analytical method for the solution of the governing equation the application of which is handy and needs less computations. In connection with this objective I draw up the following items:

- to write the governing equation of the problem in terms of the slip and shear force function,

- to deduce the so-called fundamental solutions for the problem by means of both the Euler-Bernoulli and the Timoshenko beam theory,
- to apply the developed solutions for various beams and boundary conditions and compare with results derived from other studies and from FEM solution.

The overview of the literature shows the lack of researches in accordance with composite beams with interlayer slip under the action of thermal loading. My

Objective 2 is to take into account the effect of thermal loading with the help of the following items:

- to derive the governing equation of the problem in terms of the slip and shear force function using the Euler-Bernoulli beam theory and the Duhamel-Neumann's law,
- to determine the solution of the governing equation with various boundary conditions,
- to provide formulae for the computation of the stresses.

A very important question is the stability analysis of composite beams with weak shear connection.

Objective 3 is to analyse the buckling of the composite beams, namely

- I aim to determine the buckling load based on the principle of minimum potential energy,
- I also intend to deduce the buckling load by dint of exact analysis to compare with the variational method,
- My further purpose is to give the function of the buckling load in terms of the slip modulus.

However, there are many studies on vibration analysis of composite beams in relation to the free flexural vibration, these works neglect the effect of the rotary and axial inertia. My

Objective 4 consists of the following items:

- to deduce the equations of motion including the d'Alembert forces taking into account the rotary and axial inertia
- to provide a closed form solution for the eigenfrequencies of the composite beam.

The literature contains a number of researches analysing layered curved composite beams with perfect shear connection, but there exist only a few works on the effect of the partial shear interaction. The

Objective 5 of the thesis includes

- developing an analytical method based on the principle of minimum potential energy to describe the behaviour of curved composite beams with interlayer slip,
- writing a Rayleigh-Betti type reciprocity relation for the considered curved composite beams.

Chapter 2

Analytical solutions for two-layered composite beams with interlayer slip

In this chapter we are going to introduce a novel analytical method for two-layered composite beams with interlayer slip to provide the deflection, the rotation, the slip, the bending moment, the shear force and the normal force function of the considered beam. In the first case it is assumed that the beam components separately follow the requirements of the Euler-Bernoulli hypothesis, while in the second case the beam components satisfy the requirements of the Timoshenko beam theory. Each method is based on the fundamental solutions.

2.1 Fundamental solutions for an Euler-Bernoulli composite beam

This section deals with two-layered beam with interlayer slip giving an analytical solution for the deflection, the cross-sectional rotation, the slip and the internal forces. The presented solution is based on the fundamental solutions. The fundamental solutions satisfy all the field equations and their initial values are zero except only one of them. A linear combination of the fundamental solutions which are fitted to the given loading and boundary conditions gives the solution of the considered static equilibrium problem.

2.1.1 Governing equations

The considered two-layered composite beam made of linear elastic materials is shown in Fig. 2.1. The plane yz is the plane of symmetry for the geometrical and material properties and the loading conditions. The cross-section of the beam component B_i is A_i $(i = 1, 2)$ and the common boundary surface of B_1 and B_2 is $\partial B_{12} = \partial A_{12} \times (0, L)$ as illustrated in Fig. 2.1. Here, L is the length of the two-layered beam and ∂A_{12} is the common boundary of A_1 and A_2. It is assumed that the connection in normal direction between B_1 and B_2 is perfect, but in the displacement it may have jump in axial direction which is called interlayer slip. The origin O of the rectangular coordinate system $Oxyz$ coincide the E-weighted centre of the cross-section at $z = 0$ [10]. The centre of A_i is C_i $(i = 1, 2)$ and E_i is the Young modulus of the layer B_i. It is known, that

$$c_1 = \left|\overrightarrow{CC_1}\right| = \frac{A_2 E_2}{\langle AE \rangle} c, \qquad c_2 = \left|\overrightarrow{CC_2}\right| = \frac{A_1 E_1}{\langle AE \rangle} c, \tag{2.1}$$

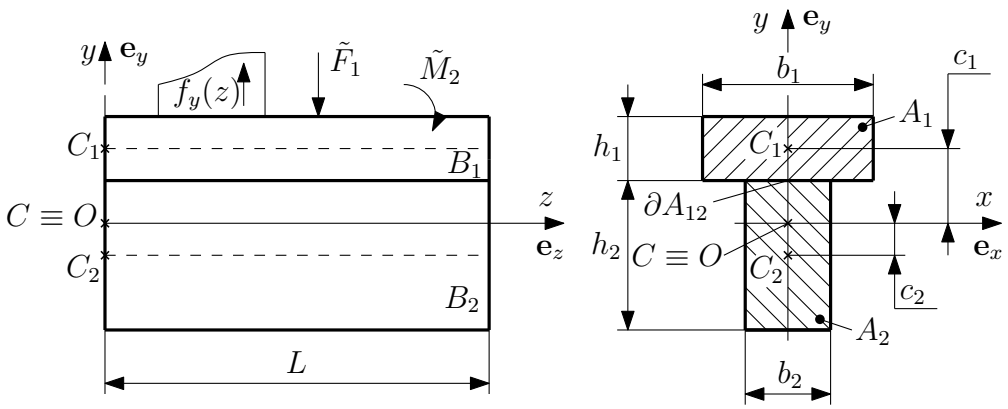

Figure 2.1. Two-layered beam with imperfect shear connection.

$$\langle AE \rangle = A_1 E_1 + A_2 E_2, \qquad c = c_1 + c_2. \tag{2.2}$$

According to the Euler-Bernoulli beam theory for the displacement field we have

$$\mathbf{u}(x,y,z) = u(x,y,z)\mathbf{e}_x + v(x,y,z)\mathbf{e}_y + w(x,y,z)\mathbf{e}_z, \tag{2.3}$$

$$u = 0, \qquad v = v(z), \qquad w(x,y,z) = w_i(z) - y\frac{\mathrm{d}v}{\mathrm{d}z}, \qquad (x,y,z) \in B_i, \quad (i = 1,2), \tag{2.4}$$

and the cross-sectional rotation can be computed as

$$\phi = -\frac{\mathrm{d}v}{\mathrm{d}z}. \tag{2.5}$$

Utilising the constitutive equations of elasticity and the Hooke's law we obtain

$$\sigma_z = E_i \varepsilon_z = E_i \left(\frac{\mathrm{d}w_i}{\mathrm{d}z} - y\frac{\mathrm{d}^2 v}{\mathrm{d}z^2} \right), \qquad (x,y,z) \in B_i, \quad (i = 1,2). \tag{2.6}$$

The analysis is restricted to the case of absent axial forces [1, 9, 10, 64, 87], i.e. $N = 0$ so we get

$$N = N_1 + N_2 = \int_{A_1} \sigma_z \mathrm{d}A + \int_{A_2} \sigma_z \mathrm{d}A = 0. \tag{2.7}$$

The interlayer slip s is defined as the difference of the axial displacements of the layers along the boundary surface ∂B_{12} [10]

$$s(x,y,z) = w_1(z) - w_2(z), \qquad (x,y,z) \in \partial B_{12}. \tag{2.8}$$

The interlayer shear force can be written in the next form

$$Q = ks, \tag{2.9}$$

where k is the slip modulus which represents the stiffness of the connection [1, 9, 10, 64, 87, 88] The value of the slip modulus can alter from 0 to ∞. If the k is equal to 0 ($Q = 0$) then there is no connection between the layers in axial direction, and when $k = \infty$ ($s = 0$) the connection is perfect. The units of Q and k are

$$[Q] = \frac{\text{force}}{\text{length}}, \quad [k] = \frac{\text{force}}{(\text{length})^2}. \tag{2.10}$$

By means of Eq. (2.6) the internal forces and moments in the layers are defined as

$$N_1 = \int_{A_1} \sigma_z \mathrm{d}A = E_1 A_1 \left(\frac{\mathrm{d}w_1}{\mathrm{d}z} - c_1 \frac{\mathrm{d}^2 v}{\mathrm{d}z^2} \right), \tag{2.11}$$

$$N_2 = \int_{A_2} \sigma_z \mathrm{d}A = E_2 A_2 \left(\frac{\mathrm{d}w_2}{\mathrm{d}z} + c_2 \frac{\mathrm{d}^2 v}{\mathrm{d}z^2} \right), \tag{2.12}$$

$$M_1 = \int_{A_1} y \sigma_z \mathrm{d}A = c_1 E_1 A_1 \frac{\mathrm{d}w_1}{\mathrm{d}z} - I_1 E_1 \frac{\mathrm{d}^2 v}{\mathrm{d}z^2}, \tag{2.13}$$

$$M_2 = \int_{A_2} y \sigma_z \mathrm{d}A = -c_2 E_2 A_2 \frac{\mathrm{d}w_2}{\mathrm{d}z} - I_2 E_2 \frac{\mathrm{d}^2 v}{\mathrm{d}z^2}, \tag{2.14}$$

where

$$\int_{A_1} y \mathrm{d}A = c_1 A_1, \qquad \int_{A_2} y \mathrm{d}A = -c_2 A_2, \qquad \int_{A_i} y^2 \mathrm{d}A = I_i, \quad (i = 1, 2). \tag{2.15}$$

Eqs. (2.11–2.14) show that the normal stresses acting on cross-section A_i $(i = 1, 2)$ are equivalent a force-couple system (N_i, M_i) $(i = 1, 2)$ at C [10]. The total normal force and bending moment are as follows

$$N = N_1 + N_2 = E_1 A_1 \frac{\mathrm{d}w_1}{\mathrm{d}z} + E_2 A_2 \frac{\mathrm{d}w_2}{\mathrm{d}z}, \tag{2.16}$$

$$M = M_1 + M_2 = c_1 E_1 A_1 \frac{\mathrm{d}w_1}{\mathrm{d}z} - c_2 E_2 A_2 \frac{\mathrm{d}w_2}{\mathrm{d}z} - \{IE\} \frac{\mathrm{d}^2 v}{\mathrm{d}z^2}. \tag{2.17}$$

Here,

$$\{IE\} = I_1 E_1 + I_2 E_2. \tag{2.18}$$

Following the method applied in [10] it can be proven that if $N = 0$ then we have

$$\frac{\mathrm{d}w_1}{\mathrm{d}z} = \frac{A_2 E_2}{\langle AE \rangle} \frac{\mathrm{d}s}{\mathrm{d}z} = \frac{c_1}{c} \frac{\mathrm{d}s}{\mathrm{d}z}, \tag{2.19}$$

$$\frac{\mathrm{d}w_2}{\mathrm{d}z} = -\frac{A_1 E_1}{\langle AE \rangle} \frac{\mathrm{d}s}{\mathrm{d}z} = -\frac{c_2}{c} \frac{\mathrm{d}s}{\mathrm{d}z}. \tag{2.20}$$

Using of Eqs. (2.16), (2.19) and (2.20) we obtain

$$N_1 = -N_2 = \langle AE \rangle_{-1} \left(\frac{\mathrm{d}s}{\mathrm{d}z} - c \frac{\mathrm{d}^2 v}{\mathrm{d}z^2} \right), \tag{2.21}$$

where

$$\langle AE \rangle_{-1} = \frac{A_1 E_1 A_2 E_2}{\langle AE \rangle}. \tag{2.22}$$

Substitution of Eqs. (2.19), (2.20) into Eq. (2.17) gives

$$M = c \langle AE \rangle_{-1} \frac{\mathrm{d}s}{\mathrm{d}z} - \{IE\} \frac{\mathrm{d}^2 v}{\mathrm{d}z^2}. \tag{2.23}$$

Application of the condition of equilibrium for forces in axial direction of beam component ΔB_1 gives [10] (Fig. 2.2)

$$\frac{\mathrm{d}N_1}{\mathrm{d}z} - Q = 0. \tag{2.24}$$

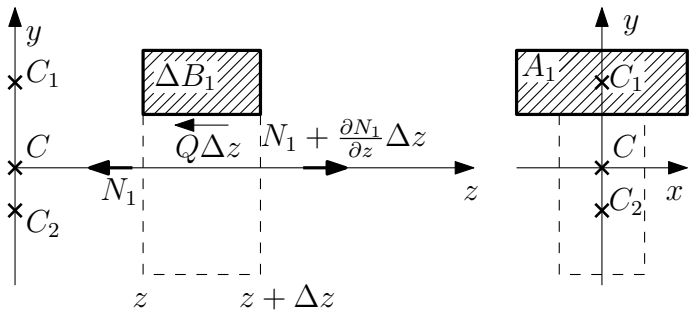

Figure 2.2. Horizontal equilibrium of a small beam element ΔB_1.

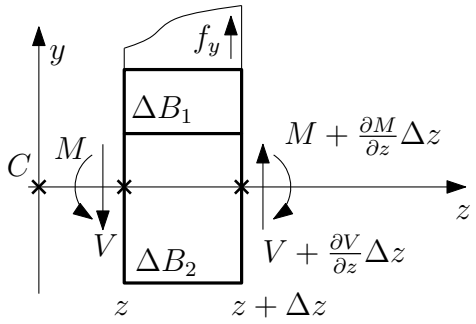

Figure 2.3. Shear force, bending moment and applied vertical load on a small beam element ΔB.

Combination of Eq. (2.24) with Eqs. (2.9) and (2.21) yields

$$\langle AE\rangle_{-1}\left(\frac{\mathrm{d}^2 s}{\mathrm{d}z^2}-c\frac{\mathrm{d}^3 v}{\mathrm{d}z^3}\right)-ks=0. \tag{2.25}$$

Analysing the vertical and rotational equilibrium condition of a small beam element ΔB we can write two another equilibrium equations [10] (Fig. 2.3) which are as follows

$$\frac{\mathrm{d}V}{\mathrm{d}z}+f_y=0, \tag{2.26}$$

$$\frac{\mathrm{d}M}{\mathrm{d}z}-V=0. \tag{2.27}$$

By means of Eqs. (2.25) and (2.27) we can formulate the governing equation in terms of the slip and the shear force function

$$\frac{\mathrm{d}^2 s}{\mathrm{d}z^2}-\Omega^2 s+\frac{c}{\langle IE\rangle}V=0, \tag{2.28}$$

where

$$\langle IE\rangle=\{IE\}-c^2\langle AE\rangle_{-1}, \qquad \Omega^2=\frac{k\{IE\}}{\langle IE\rangle\langle AE\rangle_{-1}}. \tag{2.29}$$

In order to formulate the possible boundary conditions we consider the virtual work of the section forces and section moments on a kinematically admissible displacement field

$$\tilde{\mathbf{u}}_i=\tilde{v}(z)\,\mathbf{e}_y+\left(\tilde{w}_i(z)+y\tilde{\phi}(z)\right)\mathbf{e}_z,\quad (x,y,z)\in B_i,\quad (i=1,2). \tag{2.30}$$

A detailed computation gives

$$W = \int_{A_1} \sigma_z \tilde{w}_1(z)\,\mathrm{d}A + \int_{A_2} \sigma_z \tilde{w}_2(z)\,\mathrm{d}A + \int_A y\sigma_z \tilde{\phi}(z)\,\mathrm{d}A + \int_A \tau_{yz}\tilde{v}(z)\,\mathrm{d}A = \\ = N_1\tilde{w}_1 + N_2\tilde{w}_2 + M\tilde{\phi} + V\tilde{v} = N_1\tilde{s} + M\tilde{\phi} + V\tilde{v}, \tag{2.31}$$

where

$$\tilde{s} = \tilde{w}_1(z) - \tilde{w}_2(z). \tag{2.32}$$

From equation (2.31) we obtain the possible combinations of the boundary conditions at the end cross-section

$$V \text{ or } v \text{ may be prescribed,} \tag{2.33}$$

$$N_1 \text{ or } s \text{ may be prescribed,} \tag{2.34}$$

$$M \text{ or } \phi \text{ may be prescribed.} \tag{2.35}$$

In this thesis we are going to introduce the boundary conditions according to the above mentioned formulation.

2.1.2 Fundamental solutions

Following we are going to define the fundamental solutions. The indexes EB refers to the fundamental solutions belonging to the Euler-Bernoulli beam theory. All fundamental solutions $v_j^{EB} = v_j^{EB}(z)$, $\phi_j^{EB} = \phi_j^{EB}(z)$, $s_j^{EB} = s_j^{EB}(z)$, $M_j^{EB} = M_j^{EB}(z)$, $V_j^{EB} = V_j^{EB}(z)$, $N_{1j}^{EB} = N_{1j}^{EB}(z)$, $(j = 1\ldots 7)$ satisfy Eqs. (2.5), (2.21), (2.23), (2.24), (2.26), (2.27) and (2.28) with the next initial conditions

$$v_1^{EB}(0) = 1, \qquad \phi_1^{EB}(0) = s_1^{EB}(0) = M_1^{EB}(0) = V_1^{EB}(0) = N_{11}^{EB}(0) = 0, \tag{2.36}$$

$$\phi_2^{EB}(0) = 1, \qquad v_2^{EB}(0) = s_2^{EB}(0) = M_2^{EB}(0) = V_2^{EB}(0) = N_{12}^{EB}(0) = 0, \tag{2.37}$$

$$s_3^{EB}(0) = 1, \qquad v_3^{EB}(0) = \phi_3^{EB}(0) = M_3^{EB}(0) = V_3^{EB}(0) = N_{13}^{EB}(0) = 0, \tag{2.38}$$

$$M_4^{EB}(0) = 1, \qquad v_4^{EB}(0) = \phi_4^{EB}(0) = s_4^{EB}(0) = V_4^{EB}(0) = N_{14}^{EB}(0) = 0, \tag{2.39}$$

$$V_5^{EB}(0) = 1, \qquad v_5^{EB}(0) = \phi_5^{EB}(0) = s_5^{EB}(0) = M_5^{EB}(0) = N_{15}^{EB}(0) = 0, \tag{2.40}$$

$$N_{16}^{EB}(0) = 1, \qquad v_6^{EB}(0) = \phi_6^{EB}(0) = s_6^{EB}(0) = M_6^{EB}(0) = V_6^{EB}(0) = 0, \tag{2.41}$$

From the definitions of the fundamental solution we obtain

$$v_1^{EB}(z) = 1, \quad \phi_1^{EB}(z) = s_1^{EB}(z) = M_1^{EB}(z) = V_1^{EB}(z) = N_{11}^{EB}(z) = 0, \quad 0 \le z, \tag{2.42}$$

$$v_2^{EB}(z) = -z, \quad \phi_2^{EB}(z) = 1, \quad s_2^{EB}(z) = M_2^{EB}(z) = V_2^{EB}(z) = N_{12}^{EB}(z) = 0, \quad 0 \le z, \tag{2.43}$$

$$v_3^{EB}(z) = \frac{c\langle AE\rangle_{-1}}{\{IE\}}\left(\frac{\sinh\Omega z}{\Omega} - z\right), \qquad 0 \le z, \tag{2.44a}$$

$$\phi_3^{EB}(z) = -\frac{c\langle AE\rangle_{-1}}{\{IE\}}\left(\cosh\Omega z - 1\right), \qquad 0 \le z, \tag{2.44b}$$

$$s_3^{EB}(z) = \cosh\Omega z, \qquad 0 \le z, \tag{2.44c}$$

$$M_3^{EB}(z) = 0, \qquad 0 \le z, \tag{2.44d}$$

$$V_3^{EB}(z) = 0, \qquad 0 \le z, \tag{2.44e}$$

$$N_{13}^{EB}(z) = \frac{k}{\Omega}\sinh\Omega z, \qquad 0 \le z, \tag{2.44f}$$

$$v_4^{EB}(z) = \frac{c^2 \langle AE \rangle_{-1}}{\Omega^2 \{IE\} \langle IE \rangle} (1 - \cosh \Omega z) - \frac{z^2}{2\{IE\}}, \qquad 0 \le z, \tag{2.45a}$$

$$\phi_4^{EB}(z) = \frac{c^2 \langle AE \rangle_{-1}}{\Omega \{IE\} \langle IE \rangle} \sinh \Omega z + \frac{z}{\{IE\}}, \qquad 0 \le z, \tag{2.45b}$$

$$s_4^{EB}(z) = -\frac{c}{\Omega \langle IE \rangle} \sinh \Omega z, \qquad 0 \le z, \tag{2.45c}$$

$$M_4^{EB}(z) = 1, \qquad 0 \le z, \tag{2.45d}$$

$$V_4^{EB}(z) = 0, \qquad 0 \le z, \tag{2.45e}$$

$$N_{14}^{EB}(z) = c \frac{\langle AE \rangle_{-1}}{\{IE\}} (1 - \cosh \Omega z), \qquad 0 \le z, \tag{2.45f}$$

$$v_5^{EB}(z) = \frac{c^2 \langle AE \rangle_{-1}}{\Omega^2 \{IE\} \langle IE \rangle} \left(\frac{\sinh \Omega z}{\Omega} - z \right) + \frac{z^3}{6\{IE\}}, \qquad 0 \le z, \tag{2.46a}$$

$$\phi_5^{EB}(z) = -\frac{c^2 \langle AE \rangle_{-1}}{\Omega^2 \{IE\} \langle IE \rangle} (\cosh \Omega z - 1) - \frac{z^2}{2\{IE\}}, \qquad 0 \le z, \tag{2.46b}$$

$$s_5^{EB}(z) = \frac{c}{\Omega^2 \langle IE \rangle} (\cosh \Omega z - 1), \qquad 0 \le z, \tag{2.46c}$$

$$M_5^{EB}(z) = -z, \qquad 0 \le z, \tag{2.46d}$$

$$V_5^{EB}(z) = -1, \qquad 0 \le z, \tag{2.46e}$$

$$N_{15}^{EB}(z) = \frac{c \langle AE \rangle_{-1}}{\Omega \{IE\}} (\Omega z - \sinh \Omega z), \qquad 0 \le z, \tag{2.46f}$$

$$v_6^{EB}(z) = \frac{c}{\Omega^2 \langle IE \rangle} (\cosh \Omega z - 1), \qquad 0 \le z, \tag{2.47a}$$

$$\phi_6^{EB}(z) = -\frac{c}{\Omega \langle IE \rangle} \sinh \Omega z, \qquad 0 \le z, \tag{2.47b}$$

$$s_6^{EB}(z) = \frac{\Omega}{k} \sinh \Omega z, \qquad 0 \le z, \tag{2.47c}$$

$$M_6^{EB}(z) = 0, \qquad 0 \le z, \tag{2.47d}$$

$$V_6^{EB}(z) = 0, \qquad 0 \le z, \tag{2.47e}$$

$$N_{16}^{EB}(z) = \cosh \Omega z, \qquad 0 \le z, \tag{2.47f}$$

Figure 2.4 illustrates the applied loads for the fundamental solution $M_4^{EB}(0) = 1$ and $V_5^{EB}(z) = -1$. For uniformly distributed force shown in Fig. 2.5 the definition of the fundamental solution is as follows

$$v_7^{EB}(0) = \phi_7^{EB}(0) = s_7^{EB}(0) = M_7^{EB}(0) = V_7^{EB}(0) = N_{17}^{EB}(0) = 0. \tag{2.48}$$

Under the initial conditions (2.48) the solutions of Eqs. (2.5), (2.21), (2.23), (2.24), (2.26), (2.27) and (2.28) are

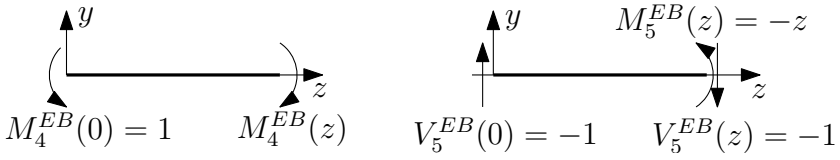

Figure 2.4. Illustration of applied load for the fundamental solutions.

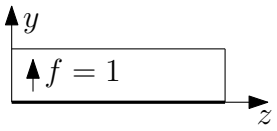

Figure 2.5. Uniformly distributed load.

$$v_7^{EB}(z)=\frac{c^2\langle AE\rangle_{-1}}{\Omega^4\{IE\}\langle IE\rangle}\left(\cosh\Omega z-\frac{\Omega^2z^2}{2}-1\right)+\frac{z^4}{24\{IE\}},\qquad 0\le z, \tag{2.49a}$$

$$\phi_7^{EB}(z)=-\frac{c^2\langle AE\rangle_{-1}}{\Omega^3\{IE\}\langle IE\rangle}\left(\sinh\Omega z-\Omega z\right)-\frac{z^3}{6\{IE\}},\qquad 0\le z, \tag{2.49b}$$

$$s_7^{EB}(z)=\frac{c}{\Omega^2\langle IE\rangle}\left(\frac{\sinh\Omega z}{\Omega}-z\right),\qquad 0\le z, \tag{2.49c}$$

$$M_7^{EB}(z)=-\frac{z^2}{2},\qquad 0\le z, \tag{2.49d}$$

$$V_7^{EB}(z)=-z,\qquad 0\le z, \tag{2.49e}$$

$$N_{17}^{EB}(z)=\frac{c\langle AE\rangle_{-1}}{\Omega^2\{IE\}}\left(\cosh\Omega z-\frac{\Omega^2z^2}{2}-1\right),\qquad 0\le z. \tag{2.49f}$$

For intermediate loads such as in the case shown in Fig. 2.6 the fundamental solutions can be expressed by the application of Heaviside functions

$$\begin{aligned}X(z)=\tilde{F}_1H(z-a_1)X_5^{EB}(z-a_1)+\tilde{M}_2H(z-a_2)X_4^{EB}(z-a_2)+\\ +f_3\left[H(z-a_3)-H(z-a_4)\right]X_7^{EB}(z-a_3),\qquad 0\le z\le L,\end{aligned} \tag{2.50}$$

where $X_j^{EB}(z)$ may be $v_j^{EB}(z)$, $\phi_j^{EB}(z)$, $s_j^{EB}(z)$, $M_j^{EB}(z)$, $V_j^{EB}(z)$ and $N_{1j}^{EB}(z)$, $(j=4,5,7)$ and

$$H(z-a)=\begin{cases}0, & \text{if } 0\le z<a,\\ 1, & \text{if } a<z<\infty.\end{cases} \tag{2.51}$$

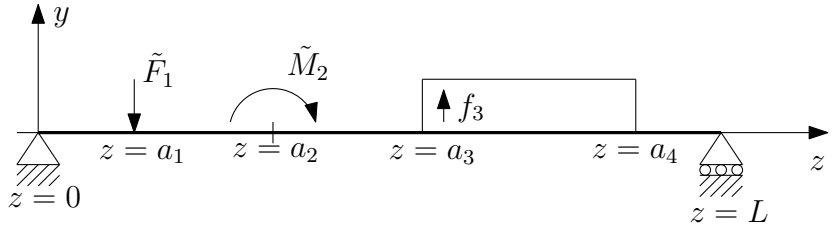

Figure 2.6. Intermediate applied loads.

2.2 Fundamental solutions for a Timoshenko composite beam

In this section we provide the fundamental solutions for composite beams with weak shear connection based on the Timoshenko beam theory.

2.2.1 Governing equations

The considered beam is shown in Fig. 2.1. The basic assumptions are the same as in section 2.1, viz. the cross-section of the beam component B_i is A_i $(i = 1, 2)$ and the common boundary surface of B_1 and B_2 is $\partial B_{12} = \partial A_{12} \times (0, L)$ as illustrated in Fig. 2.1. Here, L is the length of the two-layered beam and ∂A_{12} is the common boundary of A_1 and A_2. The axis z is located in the E-weighted centre line of the whole composite beam [10]. The plane yz is the plane of symmetry for the geometrical and material properties and loading conditions. The centre of A_i is C_i $(i = 1, 2)$ and C denotes the E-weighted centre of the whole cross-section $A = A_1 \cup A_2$ (Fig. 2.1). In this case Eqs. (2.1) and (2.2) are valid as well. It is assumed that both beam components follow the requirements of the Timoshenko beam theory with a common cross-sectional rotation $\phi = \phi(z)$. According to this assumption the deformed configuration of the two-layered shear deformable composite beam with imperfect shear connection can be described by the next displacement field

$$\mathbf{u} = u\mathbf{e}_x + v\mathbf{e}_y + w\mathbf{e}_z, \qquad (x, y, z) \in B, \tag{2.52}$$

$$u = 0, \qquad v = v(z), \qquad w = w_i(z) + y\phi(z), \qquad (x, y, z) \in B_i, \qquad (i = 1, 2). \tag{2.53}$$

In Eq. (2.52) $\mathbf{e}_x$, $\mathbf{e}_y$ and $\mathbf{e}_z$ are the unit vectors of the coordinate system $Oxyz$. The interlayer slip is defined by Eq. (2.8) and Eq. (2.9) represents the interlayer shear force in this case, too. Application of the strain-displacement relationship of the linearised theory of elasticity gives [89, 90]

$$\varepsilon_x = \varepsilon_y = \gamma_{xy} = \gamma_{xz} = 0, \qquad (x, y, z) \in B, \tag{2.54}$$

$$\varepsilon_z = \frac{\mathrm{d}w_i}{\mathrm{d}z} + y\frac{\mathrm{d}\phi}{\mathrm{d}z}, \qquad \gamma_{yz} = \frac{\mathrm{d}v}{\mathrm{d}z} + \phi, \qquad (x, y, z) \in B_i, \qquad (i = 1, 2), \tag{2.55}$$

where ε_x, ε_y, ε_z are the normal strains, γ_{xy}, γ_{xz}, γ_{yz} are the shearing strains. From the Hooke's law for the normal stress σ_z we get

$$\sigma_z = E_i\left(\frac{\mathrm{d}w_i}{\mathrm{d}z} + y\frac{\mathrm{d}\phi}{\mathrm{d}z}\right), \qquad (x, y, z) \in B_i, \qquad (i = 1, 2). \tag{2.56}$$

The following internal forces and moments are defined

$$N_1 = \int_{A_1} \sigma_z \mathrm{d}A = E_1 A_1\left(\frac{\mathrm{d}w_1}{\mathrm{d}z} + c_1\frac{\mathrm{d}\phi}{\mathrm{d}z}\right), \tag{2.57}$$

$$N_2 = \int_{A_2} \sigma_z \mathrm{d}A = E_2 A_2\left(\frac{\mathrm{d}w_2}{\mathrm{d}z} - c_2\frac{\mathrm{d}\phi}{\mathrm{d}z}\right), \tag{2.58}$$

$$M_1 = \int_{A_1} y\sigma_z \mathrm{d}A = c_1 E_1 A_1\frac{\mathrm{d}w_1}{\mathrm{d}z} + E_1 I_1\frac{\mathrm{d}\phi}{\mathrm{d}z}, \tag{2.59}$$

$$M_2 = \int_{A_2} y\sigma_z \mathrm{d}A = -c_2 E_2 A_2 \frac{\mathrm{d}w_2}{\mathrm{d}z} + E_2 I_2 \frac{\mathrm{d}\phi}{\mathrm{d}z}, \tag{2.60}$$

Here,

$$\int_{A_1} y\mathrm{d}A = c_1 A_1, \qquad \int_{A_2} y\mathrm{d}A = -c_2 A_2, \qquad \int_{A_i} y^2 \mathrm{d}A = I_i, \quad (i = 1, 2). \tag{2.61}$$

The cross-sectional shear force V_i is obtained as

$$V_i = \kappa_i G_i A_i \gamma_{yz} = \kappa_i G_i A_i \left(\frac{\mathrm{d}v}{\mathrm{d}z} + \phi \right), \qquad (i = 1, 2), \tag{2.62}$$

where G_i is the shear modulus of beam component B_i and κ_i is the shear factor of cross-section A_i $(i = 1, 2)$. Eqs. (2.57–2.60) show that the normal stresses acting on cross-section A_i $(i = 1, 2)$ are equivalent a force-couple system (N_i, M_i) $(i = 1, 2)$ at C [10]. The total normal force and bending moment are as follows

$$N = N_1 + N_2 = E_1 A_1 \frac{\mathrm{d}w_1}{\mathrm{d}z} + E_2 A_2 \frac{\mathrm{d}w_2}{\mathrm{d}z}, \tag{2.63}$$

$$M = M_1 + M_2 = c_1 E_1 A_1 \frac{\mathrm{d}w_1}{\mathrm{d}z} - c_2 E_2 A_2 \frac{\mathrm{d}w_2}{\mathrm{d}z} + \{IE\} \frac{\mathrm{d}\phi}{\mathrm{d}z}. \tag{2.64}$$

The meaning of $\{IE\}$ is defined by Eq. (2.18). The analysis of the shear deformable composite beam with interlayer slip is restricted to the case of absent axial force, i.e. $N = 0$. Following the method applied in [10] it can be proven that if $N = 0$ then we have

$$\frac{\mathrm{d}w_1}{\mathrm{d}z} = \frac{A_2 E_2}{\langle AE \rangle} \frac{\mathrm{d}s}{\mathrm{d}z} = \frac{c_1}{c} \frac{\mathrm{d}s}{\mathrm{d}z}, \tag{2.65}$$

$$\frac{\mathrm{d}w_2}{\mathrm{d}z} = -\frac{A_1 E_1}{\langle AE \rangle} \frac{\mathrm{d}s}{\mathrm{d}z} = -\frac{c_2}{c} \frac{\mathrm{d}s}{\mathrm{d}z}, \tag{2.66}$$

Utilizing of Eqs. (2.57), (2.58) and (2.64–2.66) we obtain

$$N_1 = -N_2 = \langle AE \rangle_{-1} \left(\frac{\mathrm{d}s}{\mathrm{d}z} + c \frac{\mathrm{d}\phi}{\mathrm{d}z} \right). \tag{2.67}$$

The definition of $\langle AE \rangle_{-1}$ is represented in Eq. (2.22). Substitution of Eqs. (2.65), (2.66) into Eq. (2.64) gives

$$M = c \langle AE \rangle_{-1} \frac{\mathrm{d}s}{\mathrm{d}z} + \{IE\} \frac{\mathrm{d}\phi}{\mathrm{d}z}. \tag{2.68}$$

Application of the condition of equilibrium for forces in axial direction of beam component B_1 provides [10] (Fig. 2.2)

$$\frac{\mathrm{d}N_1}{\mathrm{d}z} - Q = \frac{\mathrm{d}N_1}{\mathrm{d}z} - ks = \langle AE \rangle_{-1} \left(\frac{\mathrm{d}^2 s}{\mathrm{d}z^2} + c \frac{\mathrm{d}^2 \phi}{\mathrm{d}z^2} \right) - ks = 0. \tag{2.69}$$

According to the vertical and rotational equilibrium condition of a small beam element ΔB we can write two another equilibrium equations [10] (Fig. 2.3) which are the same as in Eqs. (2.26) and (2.27). The total cross-sectional shear force can be described as

$$V = V_1 + V_2 = \langle \kappa GA \rangle \left(\frac{\mathrm{d}v}{\mathrm{d}z} + \phi \right), \tag{2.70}$$

where

$$\langle \kappa GA \rangle = \kappa_1 G_1 A_1 + \kappa_2 G_2 A_2. \tag{2.71}$$

From Eqs. (2.26), (2.27) and (2.68) it follows that

$$V(z) = c \langle AE \rangle_{-1} \frac{\mathrm{d}^2 s}{\mathrm{d}z^2} + \{IE\} \frac{\mathrm{d}^2 \phi}{\mathrm{d}z^2}. \tag{2.72}$$

Application of Eqs. (2.29), (2.69) and (2.72) the governing equation can be written in the next form

$$\frac{\mathrm{d}^2 s}{\mathrm{d}z^2} - \Omega^2 s + c \frac{V}{\langle IE \rangle} = 0. \tag{2.73}$$

2.2.2 Fundamental solutions

Here, we provide the fundamental solutions for the case of using Timoshenko beam theory which is denoted by the indexes T. All fundamental solutions $v_j^T = v_j^T(z)$, $\phi_j^T = \phi_j^T(z)$, $s_j^T = s_j^T(z)$, $M_j^T = M_j^T(z)$, $V_j^T = V_j^T(z)$ and $N_{1j}^T = N_{1j}^T(z)$ $(j = 1 \dots 7)$ satisfy Eqs. (2.26), (2.27), (2.67), (2.68), (2.70) and (2.73) with the next initial conditions

$$v_1^T(0) = 1, \qquad \phi_1^T(0) = s_1^T(0) = M_1^T(0) = V_1^T(0) = N_{11}^T(0) = 0, \tag{2.74}$$

$$\phi_2^T(0) = 1, \qquad v_2^T(0) = s_2^T(0) = M_2^T(0) = V_2^T(0) = N_{12}^T(0) = 0, \tag{2.75}$$

$$s_3^T(0) = 1, \qquad v_3^T(0) = \phi_3^T(0) = M_3^T(0) = V_3^T(0) = N_{13}^T(0) = 0, \tag{2.76}$$

$$M_4^T(0) = 1, \qquad v_4^T(0) = \phi_4^T(0) = s_4^T(0) = V_4^T(0) = N_{14}^T(0) = 0, \tag{2.77}$$

$$V_5^T(0) = 1, \qquad v_5^T(0) = \phi_5^T(0) = s_5^T(0) = M_5^T(0) = N_{15}^T(0) = 0, \tag{2.78}$$

$$N_{16}^T(0) = 1, \qquad v_6^T(0) = \phi_6^T(0) = s_6^T(0) = M_6^T(0) = V_6^T(0) = 0, \tag{2.79}$$

From the derivation of fundamental solutions we can determine that the majority of the fundamental solutions obtained by using the Euler-Bernoulli and Timoshenko beam theory are identical except few functions. The fundamental solutions are as follows

$$\begin{aligned} v_1^T(z) = v_1^{EB}(z), \quad \phi_1^T(z) = \phi_1^{EB}(z), \quad s_1^T(z) = s_1^{EB}(z), \\ M_1^T(z) = M_1^{EB}(z), \quad V_1^T(z) = V_1^{EB}(z), \quad N_{11}^T(z) = N_{11}^{EB}(z), \quad 0 \le z, \end{aligned} \tag{2.80}$$

$$\begin{aligned} v_2^T(z) = v_2^{EB}(z), \quad \phi_2^T(z) = \phi_2^{EB}(z), \quad s_2^T(z) = s_2^{EB}(z), \\ M_2^T(z) = M_2^{EB}(z), \quad V_2^T(z) = V_2^{EB}(z), \quad N_{12}^T(z) = N_{12}^{EB}(z), \quad 0 \le z, \end{aligned} \tag{2.81}$$

$$\begin{aligned} v_3^T(z) = v_3^{EB}(z), \quad \phi_3^T(z) = \phi_3^{EB}(z), \quad s_3^T(z) = s_3^{EB}(z), \\ M_3^T(z) = M_3^{EB}(z), \quad V_3^T(z) = V_3^{EB}(z), \quad N_{13}^T(z) = N_{13}^{EB}(z), \quad 0 \le z, \end{aligned} \tag{2.82}$$

$$\begin{aligned} v_4^T(z) = v_4^{EB}(z), \quad \phi_4^T(z) = \phi_4^{EB}(z), \quad s_4^T(z) = s_4^{EB}(z), \\ M_4^T(z) = M_4^{EB}(z), \quad V_4^T(z) = V_4^{EB}(z), \quad N_{14}^T(z) = N_{14}^{EB}(z), \quad 0 \le z, \end{aligned} \tag{2.83}$$

$$\begin{aligned} v_5^T(z) = v_5^{EB}(z) - \frac{z}{\langle \kappa GA \rangle}, \quad \phi_5^T(z) = \phi_5^{EB}(z), \quad s_5^T(z) = s_5^{EB}(z), \\ M_5^T(z) = M_5^{EB}(z), \quad V_5^T(z) = V_5^{EB}(z), \quad N_{15}^T(z) = N_{15}^{EB}(z), \quad 0 \le z, \end{aligned} \tag{2.84}$$

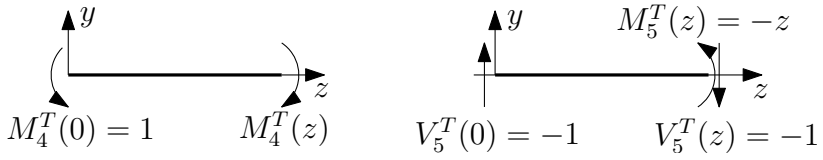

Figure 2.7. Illustration of applied load for the fundamental solutions.

$$v_6^T(z)=v_6^{EB}(z),\quad \phi_6^T(z)=\phi_6^{EB}(z),\quad s_6^T(z)=s_6^{EB}(z),$$
$$M_6^T(z)=M_6^{EB}(z),\quad V_6^T(z)=V_6^{EB}(z),\quad N_{16}^T(z)=N_{16}^{EB}(z),\quad 0\le z. \tag{2.85}$$

Figure 2.7 illustrate the applied loads for the fundamental solution $M_4^T(z)=1$ and $V_5^T(z)=-1$ which are assigned as in the case using the Euler-Bernoulli beam theory. For uniformly distributed force shown in Fig. 2.5 the definition of the fundamental solution is as follows

$$v_7^T(0)=\phi_7^T(0)=s_7^T(0)=M_7^T(0)=V_7^T(0)=N_{17}^T(0)=0. \tag{2.86}$$

Under the initial conditions (2.86) the fundamental solutions are

$$v_7^T(z)=v_7^{EB}(z)-\frac{z^2}{2\langle\kappa GA\rangle},\quad \phi_7^T(z)=\phi_7^{EB}(z),\quad s_7^T(z)=s_7^{EB}(z),$$
$$M_7^T(z)=M_7^{EB}(z),\quad V_7^T(z)=V_7^{EB}(z),\quad N_{17}^T(z)=N_{17}^{EB}(z),\quad 0\le z. \tag{2.87}$$

For intermediate loads such as in the case shown in Fig. 2.6 the fundamental solutions can be expressed by the application of Heaviside functions similarly to the case of employing the Euler-Bernoulli beam theory

$$X(z)=\tilde{F}_1H(z-a_1)X_5^T(z-a_1)+\tilde{M}_2H(z-a_2)X_4^T(z-a_2)+$$
$$+f_3\left[H(z-a_3)-H(z-a_4)\right]X_7^T(z-a_3),\qquad 0\le z\le L, \tag{2.88}$$

where $X_j^T(z)$ may be $v_j^T(z)$, $\phi_j^T(z)$, $s_j^T(z)$, $M_j^T(z)$, $V_j^T(z)$ and $N_{1j}^T(z)$, $(j=4,5,7)$ and Eq. (2.51) represents the Heaviside function.

Here we note that we have investigated a Timoshenko composite beam **(5)** of which layers have different cross-sectional rotations ($\phi_1\neq\phi_2$).

2.3 Numerical examples

2.3.1 Simply supported composite beam

This example is taken from the paper by Schnabl et al. [69]. The simply supported two-layered beam with imperfect shear connection and its cross-section are shown in Fig. 2.8. The following data are used: $h_1=0.2\,\mathrm{m}$, $h_2=0.3\,\mathrm{m}$, $b=0.3\,\mathrm{m}$, $L=2.5\,\mathrm{m}$, $E_1=1.2\times10^{10}\,\mathrm{Pa}$, $E_2=1.2\times10^{10}\,\mathrm{Pa}$, $G_1=8\times10^8\,\mathrm{Pa}$, $G_2=1.2\times10^9\,\mathrm{Pa}$, $k=2.43\times10^6\,\mathrm{Pa}$, $\kappa_1=\kappa_2=\frac{5}{6}$, $f_y(z)=-f=-50000\,\mathrm{N/m}$. In this case the boundary conditions are as follows

$$v(0)=M(0)=N_1(0)=0, \tag{2.89}$$
$$v(L)=M(L)=N_1(L)=0, \tag{2.90}$$

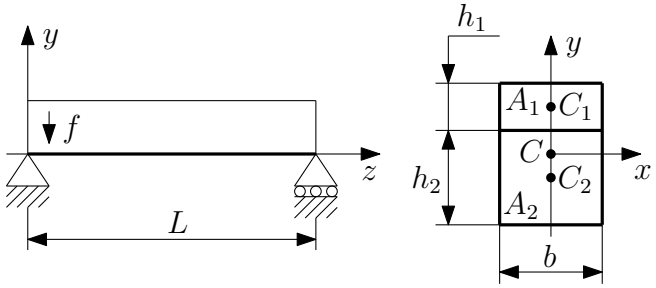

Figure 2.8. Simply supported composite beam.

It is evident that

$$V(0) = -\frac{fL}{2}, \tag{2.91}$$

and $\phi(0)$, $s(0)$ are obtained from Eq. (2.90). Using the Euler-Bernoulli beam theory the following equations can be derived from the boundary conditions

$$v(L) = \phi_{EB}(0)v_2^{EB}(L) + s_{EB}(0)v_3^{EB}(L) + \frac{fL}{2}v_5^{EB}(L) + fv_7^{EB}(L) = 0, \tag{2.92}$$

$$N_1(L) = s_{EB}(0)N_{13}^{EB}(L) + \frac{fL}{2}N_{15}^{EB}(L) + fN_{17}^{EB}(L) = 0. \tag{2.93}$$

By means of the Timoshenko beam theory we obtain similar equations

$$v(L) = \phi_T(0)v_2^T(L) + s_T(0)v_3^T(L) + \frac{fL}{2}v_5^T(L) + fv_7^T(L) = 0, \tag{2.94}$$

$$N_1(L) = s_T(0)N_{13}^T(L) + \frac{fL}{2}N_{15}^T(L) + fN_{17}^T(L) = 0. \tag{2.95}$$

Substituting the data into Eqs. (2.93) and (2.95) yields a linear equation with one unknown parameter which is $s_{EB}(0)$ and $s_T(0)$. A simple computation gives

$$s_{EB}(0) = s_T(0) = s(0) = -0.00076544\,\mathrm{m} \tag{2.96}$$

since the N_{1j}^{EB} $(j = 2, 3, 5, 7)$ functions are the same as N_{1j}^T $(j = 2, 3, 5, 7)$. From the Eqs. (2.92) and (2.94) the value of $\phi_{EB}(0)$ and $\phi_T(0)$ can be received by means of $s(0)$. However, the functions v_j^{EB} and v_j^T $(j = 2, 3, 5, 7)$ differ from each other we get

$$\phi_{EB}(0) = \phi_T(0) = \phi(0) = 0.00307252. \tag{2.97}$$

The solution of the considered boundary value problem can be represented in terms of fundamental solutions as

$$\begin{gathered} X(z) = \phi(0)X_2(z) + s(0)X_3(z) - \frac{fL}{2}X_5(z) + fX_7(z), \\ (X = v^{EB}, \phi^{EB}, s^{EB}, M^{EB}, V^{EB}, N_1^{EB} \text{ or } v^T, \phi^T, s^T, M^T, V^T, N_1^T). \end{gathered} \tag{2.98}$$

Figures 2.9, 2.10, 2.11, 2.12, 2.13 and 2.14 illustrate the graphs of deflection, cross-sectional rotation, slip, bending moment, shear force and axial force in the layer B_1, respectively. We also investigated the considered simply supported beam by means of FEM to validate our results. For this analysis we used the FEM software Abaqus. The

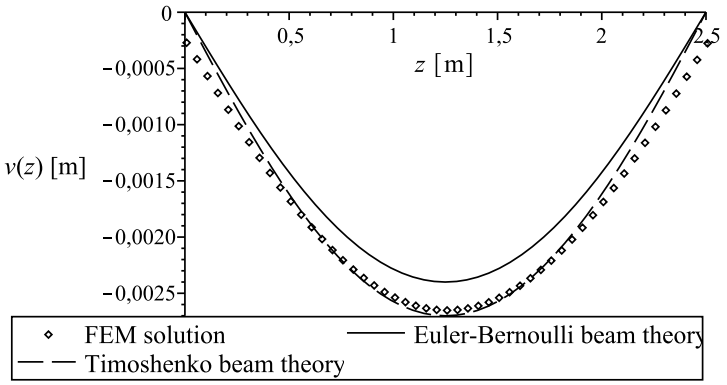

Figure 2.9. The deflection functions.

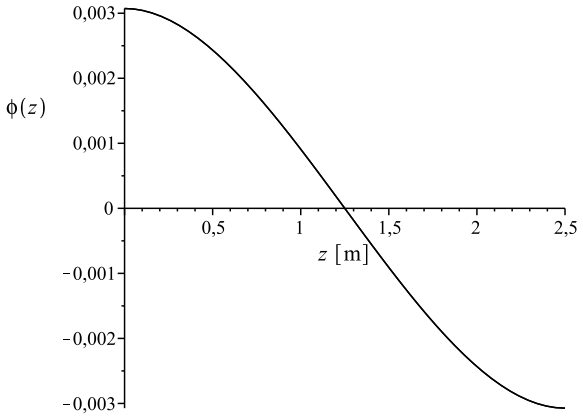

Figure 2.10. The rotation function.

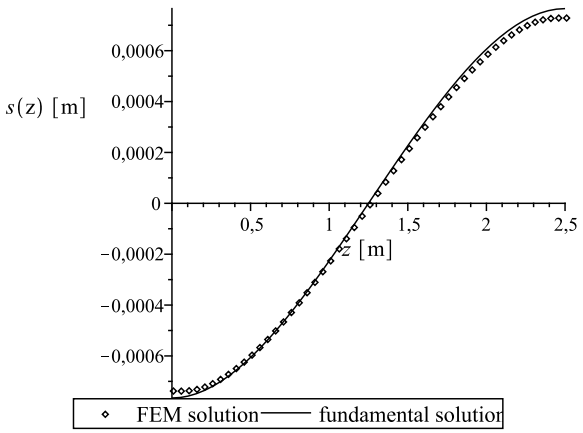

Figure 2.11. The slip functions.

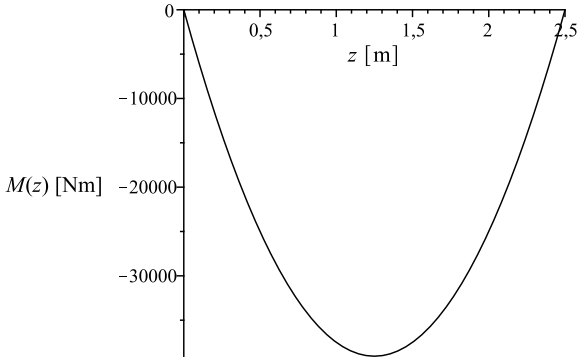

Figure 2.12. The bending moment function.

Table 2.1. Comparison of deflection and slip.

	Paper [69] (FEM)	Euler-Bernoulli beam	Timoshenko beam	FEM (Abaqus)
$v\left(\frac{L}{2}\right)$	-0.00271026	-0.00240005	-0.00270053	-0.00263727
$s(0)$	-0.00077293	-0.00076544	-0.00076544	-0.0007321886

beam was modelled as a plane stress problem with 50000 elements which were 4-node bilinear plane stress quadrilateral elements (their code is CPS4R in Abaqus). The solution was convergent, more elements did not provide more accurate results. The deflection function and the slip function from this FEM analysis are also shown in Fig. 2.9 and 2.11, respectively. Because of the equivalence of the coefficients $\phi_{EB}(0) = \phi_T(0)$ and $s_{EB}(0) = s_T(0)$ only the deflection functions are different for the Euler-Bernoulli and for the Timoshenko beam, the other functions are the same in both cases. Comparison of deflection $v(\frac{L}{2})$ and slip $s(0)$ obtained by Schnabl et al. from FEM solution [69], derived from the fundamental solutions and gained from our FEM analysis is given in Table 2.1

2.3.2 Propped cantilever with concentrated force

The considered two-layered beam with the applied load is shown in Fig. 2.15. The numerical data are as follows: $E_1 = 2 \times 10^{11}$ Pa, $E_2 = 6.9 \times 10^{10}$ Pa, $G_1 = 7.6923 \times 10^{10}$ Pa, $G_2 = 2.5862 \times 10^{10}$ Pa, $f = 0$, $F = 5 \times 10^5$ N. The other data are the same as in Example 2.3.1. In this case the boundary conditions are as follows

$$v(0) = \phi(0) = s(0) = 0, \tag{2.99}$$

$$v(L) = M(L) = N_1(L) = 0. \tag{2.100}$$

The unknown initial values $M_{EB}(0)$, $V_{EB}(0)$, $N_{1EB}(0)$ for an Euler-Bernoulli beam and $M_T(0)$, $V_T(0)$, $N_{1T}(0)$ for a Timoshenko beam can be computed from boundary conditions (2.100). By dint of the Euler-Bernoulli beam theory we can formulate the next system of equation

$$M(L) = M_{EB}(0)M_4^{EB}(L) + V_{EB}(0)M_5^{EB}(L) + N_{1EB}(0)M_6^{EB}(L) + 0.5FM_5^{EB}(L/2) = 0, \tag{2.101}$$

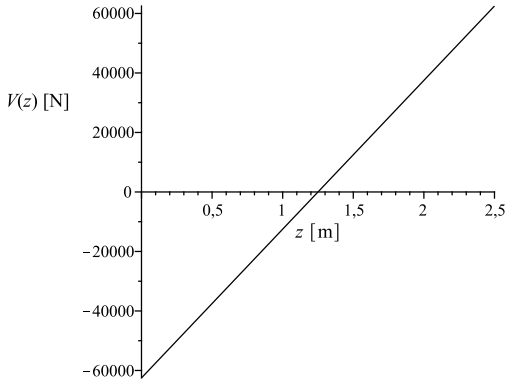

Figure 2.13. The shear force function.

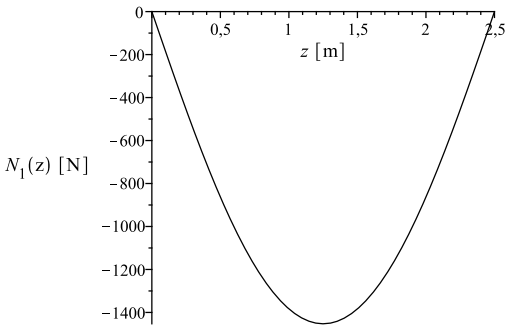

Figure 2.14. The axial force function in layer B_1.

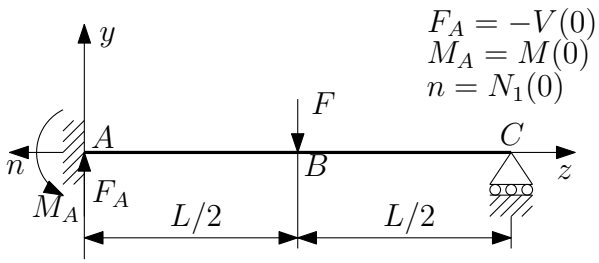

Figure 2.15. Propped cantilever with concentrated force.

$$v(L) = M_{EB}(0)v_4^{EB}(L) + V_{EB}(0)v_5^{EB}(L)+ \\ +N_{1EB}(0)v_6^{EB}(L) + Fv_5^{EB}(L/2) = 0, \tag{2.102}$$

$$N_1(L) = M_{EB}(0)N_{14}^{EB}(L) + V_{EB}(0)N_{15}^{EB}(L)+ \\ +N_{1EB}(0)N_{16}^{EB}(L) + FN_{15}^{EB}(L/2) = 0. \tag{2.103}$$

According to the Timoshenko beam theory the next system of equation is provided

$$M(L) = M_T(0)M_4^T(L) + V_T(0)M_5^T(L) + N_{1T}(0)M_6^T(L) + 0.5FM_5^T(L/2) = 0, \tag{2.104}$$

$$v(L) = M_T(0)v_4^T(L) + V_T(0)v_5^T(L)+ \\ +N_{1T}(0)v_6^T(L) + Fv_5^T(L/2) = 0, \tag{2.105}$$

$$N_1(L) = M_T(0)N_{14}^T(L) + V_T(0)N_{15}^T(L)+ \\ +N_{1T}(0)N_{16}^T(L) + FN_{15}^T(L/2) = 0. \tag{2.106}$$

Inserting the data into Eqs. (2.101–2.103) and Eqs. (2.104–2.106) we get the following results

$$M_{EB}(0) = 23427.883463\,\mathrm{Nm}, \tag{2.107}$$

$$V_{EB}(0) = 34371.115339\,\mathrm{N}, \tag{2.108}$$

$$N_{1EB}(0) = 0.475863\,\mathrm{N}, \tag{2.109}$$

$$M_T(0) = 23260.088641\,\mathrm{Nm}, \tag{2.110}$$

$$V_T(0) = 34304.035457\,\mathrm{N}, \tag{2.111}$$

$$N_{1T}(0) = -23.91063\,\mathrm{N}, \tag{2.112}$$

With the help of these results the sought functions can be determined

$$X(z) = M_{EB}(0)X_4(z) + V_{EB}(0)X_5(z) + N_{1EB}(0)X_6(z) + FH\left(z - \frac{L}{2}\right)X_5\left(z - \frac{L}{2}\right), \\ (X = v^{EB}, \phi^{EB}, s^{EB}, M^{EB}, V^{EB}, N_1^{EB}), \tag{2.113}$$

$$X(z) = M_T(0)X_4(z) + V_T(0)X_5(z) + N_{1T}(0)X_6(z) + FH\left(z - \frac{L}{2}\right)X_5\left(z - \frac{L}{2}\right), \\ (X = v^T, \phi^T, s^T, M^T, V^T, N_1^T). \tag{2.114}$$

Figures 2.16, 2.17, 2.18, 2.19, 2.20 and 2.21 represent the deflection, cross-sectional rotation, slip, bending moment, shear force and axial force function in layer B_1, respectively. We investigated this example by means of FEM software Abaqus as well. The parameters of the analysis were the same as in Example 2.3.1 except the boundary conditions and the loading. We used the same elements for this case. The deflection and slip functions are gained from the FEM analysis which are also illustrated in Fig. 2.16 and 2.18. In this case the functions obtained from the Euler-Bernoulli beam theory are different as the functions won from Timoshenko beam theory. The deflection function from the FEM solution is in good agreement with the one from the Euler-Bernoulli beam theory. Between the slip function from FEM and from the fundamental solutions a difference can be observed which is caused by the elastic deformation of the layers.

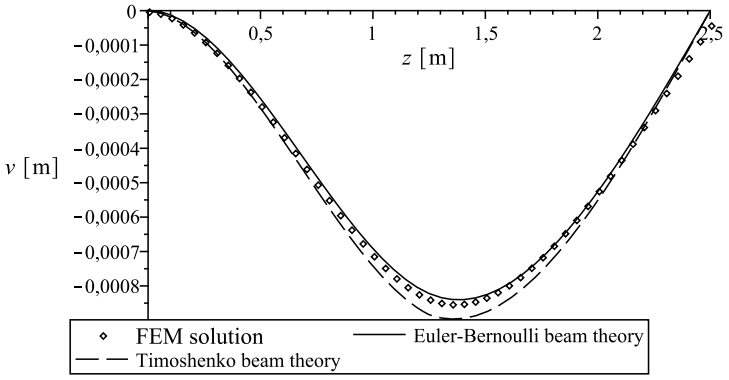

Figure 2.16. The deflection functions.

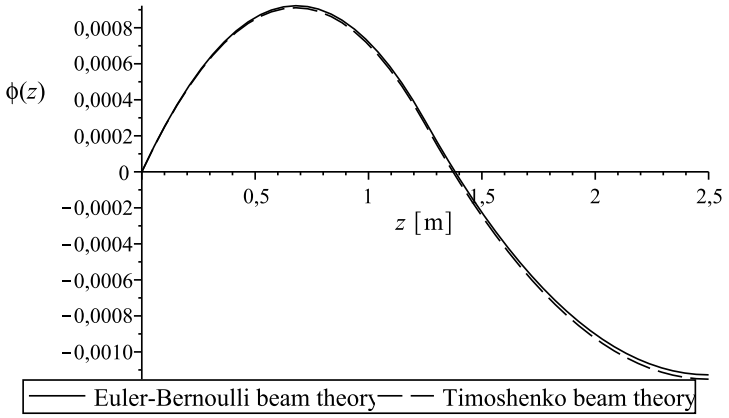

Figure 2.17. The rotation functions.

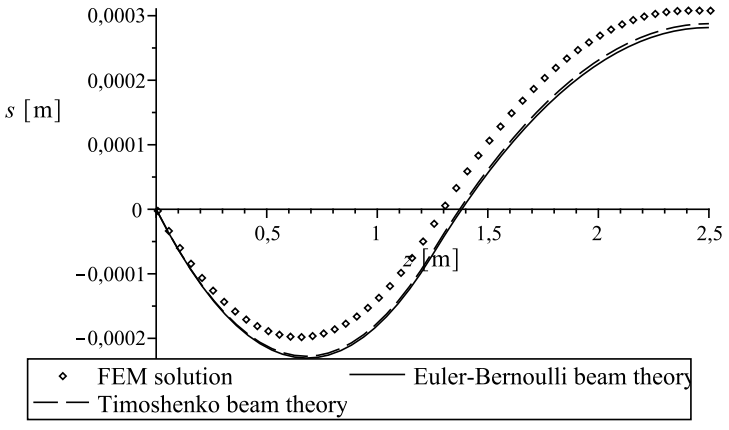

Figure 2.18. The slip functions.

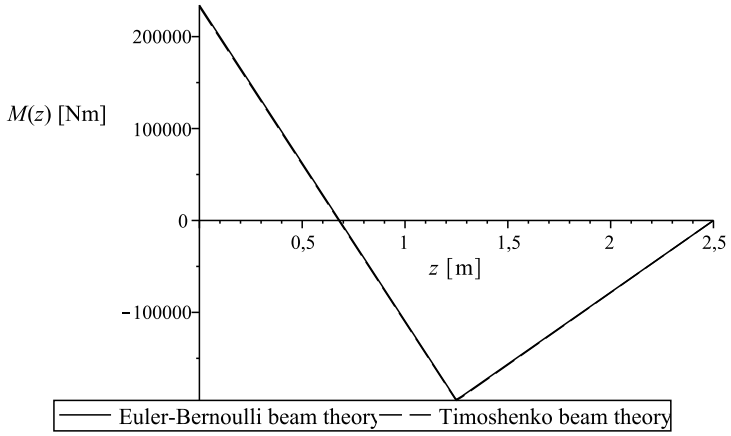

Figure 2.19. The bending moment functions.

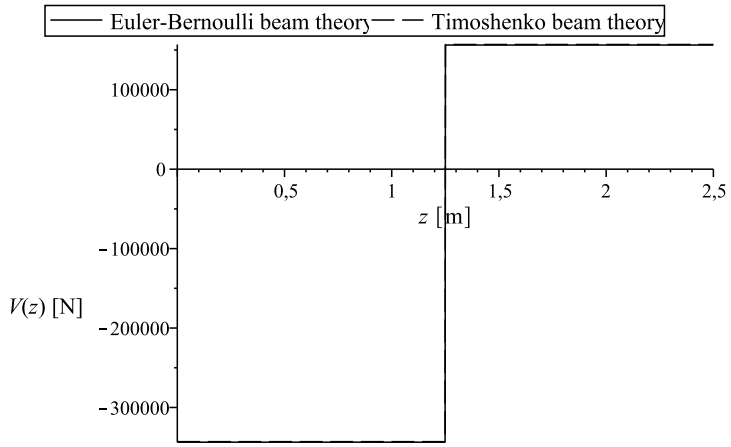

Figure 2.20. The shear force functions.

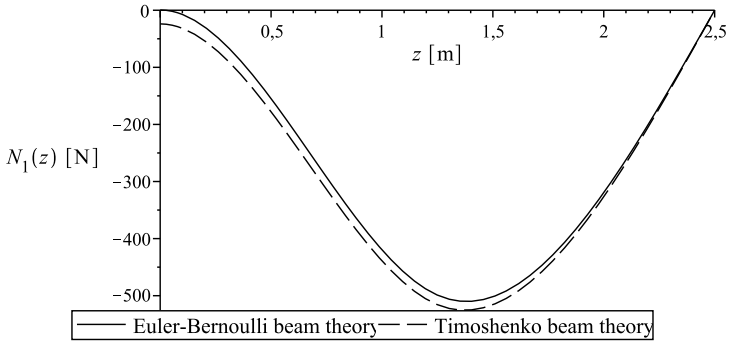

Figure 2.21. The axial force functions in layer B_1.

Chapter 3

The influence of thermal load on the behaviour of composite beams with weak shear connection

In this chapter we introduce a novel analytical method for two-layered composite beams with interlayer slip in order to investigate the behaviour of the considered composite beam subjected to thermal load. Our aim is to determine the deflection, the rotation, the slip, the bending moment, the axial force and the shear force function of the beam. Knowing these functions the normal and shear stresses can be computed as well. The present analytical method is based on the Euler-Bernoulli beam theory and on the one-dimensional version of the constitutive equation of linear thermoelasticity (Duhamel-Neumann's law). At the end of the chapter two numerical examples illustrate the application of the method. Some equations which have already appeared in the previous chapter are also written in the following for the ease of reference.

3.1 Governing equations

The considered two-layered beam configuration is shown in Fig. 3.1. The beam component B_i has the rectangular cross-section A_i whose dimensions are h_i and b $(i = 1, 2)$. The modulus of elasticity for beam component B_i is E_i and the coefficients of linear thermal expansion is α_i $(i = 1, 2)$. The length of the composite beam is L. The origin O of the rectangular Cartesian coordinate system $Oxyz$ is the E-weighted centre of the left end cross-section, so that axis z is the E-weighted centreline of the considered beam. The mechanical load is represented by f (distributed line load), $\tilde{F}$ (concentrated force) and $\tilde{M}$ (concentrated moment). A point P in $B = B_1 \cup B_2$ is indicated by the position vector $\overrightarrow{OP} = \mathbf{r} = \mathbf{R} + z\mathbf{e}_z = x\mathbf{e}_x + y\mathbf{e}_y + z\mathbf{e}_z$, where $\mathbf{e}_x$, $\mathbf{e}_y$ and $\mathbf{e}_z$ are the unit vectors of the coordinate system $Oxyz$. It is known that the position of E-weighted centre of the cross-section $A = A_1 \cup A_2$ is obtained from next equation [10]

$$E_1 \int_{A_1} \mathbf{R} \mathrm{d}A + E_2 \int_{A_2} \mathbf{R} \mathrm{d}A = \mathbf{0}. \tag{3.1}$$

For cross-section shown in Fig. 3.1 we have

$$c_1 = \left|\overrightarrow{CC_1}\right| = \frac{A_2 E_2}{\langle AE \rangle} c, \quad c_2 = -\left|\overrightarrow{CC_2}\right| = -\frac{A_1 E_1}{\langle AE \rangle} c, \tag{3.2}$$

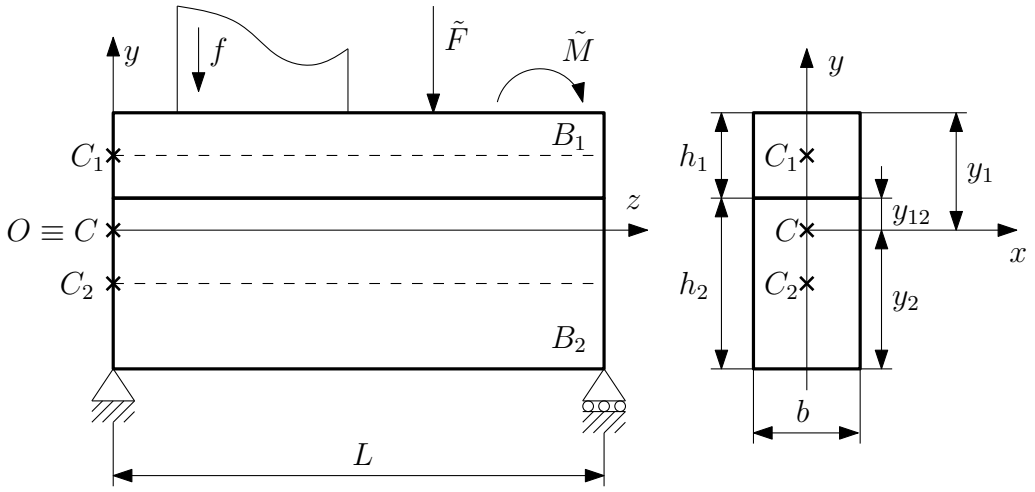

Figure 3.1. The considered two-layered beam.

$$c = \left|\overrightarrow{C_2C_1}\right| = c_1 - c_2 = \frac{1}{2}\left(h_1 + h_2\right), \tag{3.3}$$

$$\langle AE \rangle = A_1E_1 + A_2E_2, \tag{3.4}$$

$$y_1 = c_1 + \frac{1}{2}h_1, \quad y_2 = c_2 - \frac{1}{2}h_2, \quad y_{12} = c_1 - \frac{1}{2}h_1. \tag{3.5}$$

In Eqs. (3.2), (3.4) A_i denotes the cross-sectional area of beam component B_i $(i = 1, 2)$ and the position of the common boundary of A_1 and A_2 is indicated by y_{12} (Fig. 3.1). According to the Euler-Bernoulli hypothesis (kinematic assumption) which is valid for each homogeneous beam components the deformed configuration is described by the displacement field [10]

$$\mathbf{u} = \mathbf{u}\left(x, y, z\right) = v(z)\mathbf{e}_y + \left(w_i(z) - y\frac{\mathrm{d}v}{\mathrm{d}z}\right)\mathbf{e}_z, \tag{3.6}$$

where $(x, y, z) \in B_i$, $(i = 1, 2)$. Eq. (3.6) shows that the axial displacement of beam component B_i $(i = 1, 2)$ is separated into two parts: $w_i(z)$ $(i = 1, 2)$ describes the rigid translation of the cross-section A_i $(i = 1, 2)$ at z and the second part of the axial displacement of A_i $(i = 1, 2)$ derived from the deflection of cross-section [10]. On the common boundary of B_1 and B_2 the axial displacement has jump which is called the interlayer slip. According to Eq. (3.6) the interlayer slip $s = s(z)$ can be computed as

$$s(z) = w_1(z) - w_2(z). \tag{3.7}$$

Application of the strain-displacement relationships of the linearised theory of elasticity gives

$$\varepsilon_x = \varepsilon_y = \gamma_{xy} = \gamma_{xz} = \gamma_{yz} = 0, \quad (x, y, z) \in B_1 \cup B_2, \tag{3.8}$$

$$\varepsilon_z = \frac{\mathrm{d}w_i}{\mathrm{d}z} - y\frac{\mathrm{d}^2v}{\mathrm{d}z^2}, \quad (x, y, z) \in B_i\,(i = 1, 2). \tag{3.9}$$

In Eqs. (3.8), (3.9) ε_x, ε_y, ε_z are the normal strains and γ_{xy}, γ_{xz}, γ_{yz} are the shearing strains. The normal stress σ_z is computed from the one-dimensional version of Duhamel-Neumann's law [91–93]

$$\sigma_z = E_i\left(\frac{\mathrm{d}w_i}{\mathrm{d}z} - y\frac{\mathrm{d}^2v}{\mathrm{d}z^2} - \alpha_i T\right), \quad (x, y, z) \in B_1 \cup B_2. \tag{3.10}$$

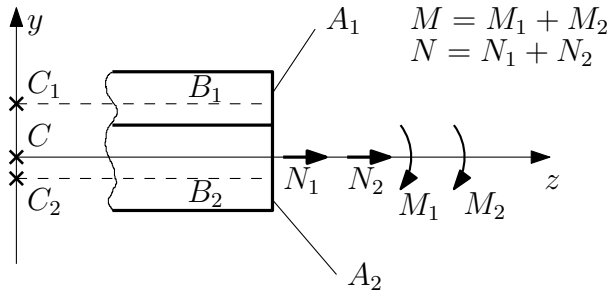

Figure 3.2. Normal forces and bending moments.

In Eq. (3.10) T denotes the temperature change. The temperature of the two-layered composite beam initially is the reference temperature ϑ_0. Its temperature is slowly raised to a constant uniform temperature $\vartheta = \vartheta_0 + T$, so that the temperature change is T. According to the linear thermo-elasticity it is assumed that $|T| \leq 200$ K so the material properties can be considered constant. Following we define the next section forces and moments [10]

$$N_1 = \int_{A_1} \sigma_z \mathrm{d}A = A_1 E_1 \left(\frac{\mathrm{d}w_1}{\mathrm{d}z} - c_1 \frac{\mathrm{d}^2 v}{\mathrm{d}z^2} - \alpha_1 T \right), \tag{3.11}$$

$$N_2 = \int_{A_2} \sigma_z \mathrm{d}A = A_2 E_2 \left(\frac{\mathrm{d}w_2}{\mathrm{d}z} - c_2 \frac{\mathrm{d}^2 v}{\mathrm{d}z^2} - \alpha_2 T \right), \tag{3.12}$$

$$M_1 = \int_{A_1} y \sigma_z \mathrm{d}A = A_1 E_1 c_1 \left(\frac{\mathrm{d}w_1}{\mathrm{d}z} - \alpha_1 T \right) - E_1 I_1 \frac{\mathrm{d}^2 v}{\mathrm{d}z^2}, \tag{3.13}$$

$$M_2 = \int_{A_2} y \sigma_z \mathrm{d}A = A_2 E_2 c_2 \left(\frac{\mathrm{d}w_2}{\mathrm{d}z} - \alpha_2 T \right) - E_2 I_2 \frac{\mathrm{d}^2 v}{\mathrm{d}z^2}, \tag{3.14}$$

where

$$I_i = \int_{A_i} y^2 \mathrm{d}A, \quad (i = 1, 2). \tag{3.15}$$

Eqs. (3.11–3.14) show that the normal stresses acting on cross-section A_i $(i = 1, 2)$ are equivalent to a force-couple system (N_i, M_i) $(i = 1, 2)$ at C. This force-couple system (N_i, M_i) $(i = 1, 2)$ is illustrated in Fig. 3.2. The interlayer slip s is assumed to be a linear function of shear force Q transmitted between the two beam components, that is we have [9]

$$Q = ks, \tag{3.16}$$

where k is the slip modulus. In present problem there is no axial force $N = N_1 + N_2$, that is

$$N = N_1 + N_2 = A_1 E_1 \frac{\mathrm{d}w_1}{\mathrm{d}z} + A_2 E_2 \frac{\mathrm{d}w_2}{\mathrm{d}z} - \langle AE\alpha \rangle T = 0. \tag{3.17}$$

Here,

$$\langle AE\alpha \rangle = \alpha_1 E_1 A_1 + \alpha_2 E_2 A_2. \tag{3.18}$$

From Eqs. (3.7) and (3.17) it follows that

$$\frac{\mathrm{d}w_1}{\mathrm{d}z} = \frac{A_2 E_2}{\langle AE \rangle} \frac{\mathrm{d}s}{\mathrm{d}z} + \frac{\langle AE\alpha \rangle}{\langle AE \rangle} T, \tag{3.19}$$

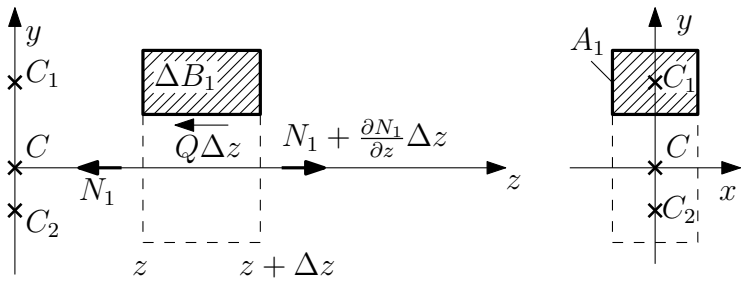

Figure 3.3. Equilibrium condition in z direction for a small beam element ΔB_1.

$$\frac{\mathrm{d}w_2}{\mathrm{d}z} = -\frac{A_1 E_1}{\langle AE \rangle}\frac{\mathrm{d}s}{\mathrm{d}z} + \frac{\langle AE\alpha \rangle}{\langle AE \rangle} T. \tag{3.20}$$

A simple computation based on Eqs. (3.11), (3.12) and Eqs. (3.19), (3.20) gives

$$N_1 = \langle AE \rangle_{-1} \left[\frac{\mathrm{d}s}{\mathrm{d}z} - c\frac{\mathrm{d}^2 v}{\mathrm{d}z^2} + (\alpha_2 - \alpha_1)\, T \right], \tag{3.21}$$

$$N_2 = \langle AE \rangle_{-1} \left[-\frac{\mathrm{d}s}{\mathrm{d}z} + c\frac{\mathrm{d}^2 v}{\mathrm{d}z^2} + (\alpha_1 - \alpha_2)\, T \right], \tag{3.22}$$

where

$$\langle AE \rangle_{-1} = \frac{A_1 E_1 A_2 E_2}{A_1 E_1 + A_2 E_2}. \tag{3.23}$$

Application of the condition of equilibrium for forces in axial direction to beam component ΔB_1 gives (Fig. 3.3)

$$\frac{\mathrm{d}N_1}{\mathrm{d}z} - Q = \frac{\mathrm{d}N_1}{\mathrm{d}z} - ks = 0. \tag{3.24}$$

Substitution of Eq. (3.21) into Eq. (3.24) yields

$$\frac{\mathrm{d}^2 s}{\mathrm{d}z^2} - c\frac{\mathrm{d}^3 v}{\mathrm{d}z^3} - \frac{k}{\langle AE \rangle_{-1}} s = 0. \tag{3.25}$$

It is evident that the bending moment acting on the whole cross-section $A = A_1 \cup A_2$ is as follows

$$M = M_1 + M_2 = c\,\langle AE \rangle_{-1} \left[\frac{\mathrm{d}s}{\mathrm{d}z} + (\alpha_2 - \alpha_1)\, T \right] - \{IE\}\, \frac{\mathrm{d}^2 v}{\mathrm{d}z^2}. \tag{3.26}$$

Here,

$$\{IE\} = I_1 E_1 + I_2 E_2. \tag{3.27}$$

According to Eq. (3.26) we can obtain

$$V(z) = \frac{\mathrm{d}M}{\mathrm{d}z} = c\,\langle AE \rangle_{-1} \frac{\mathrm{d}^2 s}{\mathrm{d}z^2} - \{IE\}\, \frac{\mathrm{d}^3 v}{\mathrm{d}z^3}. \tag{3.28}$$

Further manipulation of Eq. (3.28) provides

$$\frac{\mathrm{d}^3 v}{\mathrm{d}z^3} = \frac{c\,\langle AE \rangle_{-1}}{\{IE\}} \frac{\mathrm{d}^2 s}{\mathrm{d}z^2} - V(z). \tag{3.29}$$

Substitution of Eq. (3.29) into Eq. (3.25) we gain

$$\frac{\mathrm{d}^2 s}{\mathrm{d}z^2} - \Omega^2 s + \frac{c}{\langle IE \rangle} V(z) = 0, \tag{3.30}$$

where

$$\Omega^2 = k \frac{\{IE\}}{\langle AE \rangle_{-1} \langle IE \rangle}, \quad \langle IE \rangle = \{IE\} - c^2 \langle AE \rangle_{-1}. \tag{3.31}$$

Taking into account the boundary conditions one can solve the governing differential equations (3.30) and the slip function can be determined. Substituting the slip function into the function of bending moment (3.26) the deflection function can be computed as well.

3.2 Computations of thermal stresses

We assume that the state of stresses of the two-layered composite beam under the action of thermal load can be characterized by the following stresses $\sigma_z = \sigma_z(y,z)$, $\tau_{yz} = \tau_{yz}(y,z)$, $\sigma_y = \sigma_y(y,z)$. The normal stress σ_z is obtained from Eqs. (3.10), (3.19) and (3.20) as

$$\sigma_z = E_1 \left[\frac{c_1}{c} \frac{\mathrm{d}s}{\mathrm{d}z} - y \frac{\mathrm{d}^2 v}{\mathrm{d}z^2} + \frac{c_1}{c} (\alpha_2 - \alpha_1) T \right], \quad (x,y,z) \in B_1, \tag{3.32}$$

$$\sigma_z = E_2 \left[\frac{c_2}{c} \frac{\mathrm{d}s}{\mathrm{d}z} - y \frac{\mathrm{d}^2 v}{\mathrm{d}z^2} + \frac{c_2}{c} (\alpha_2 - \alpha_1) T \right], \quad (x,y,z) \in B_2. \tag{3.33}$$

The shearing stress $\tau_{yz} = \tau_{yz}(y,z)$ is computed by the use of equation of equilibrium

$$\frac{\partial \tau_{yz}}{\partial y} + \frac{\partial \sigma_z}{\partial z} = 0, \quad (x,y,z) \in B_1 \cup B_2. \tag{3.34}$$

A detailed computation yields the next result

$$\tau_{yz} = -E_2 \left[(y - y_2) \frac{c_2}{c} \frac{\mathrm{d}^2 s}{\mathrm{d}z^2} - \frac{1}{2} \left(y^2 - y_2^2 \right) \frac{\mathrm{d}^3 v}{\mathrm{d}z^3} \right], \quad (x,y,z) \in B_2, \tag{3.35}$$

$$\begin{aligned} \tau_{yz} = &-E_2 \left[(y_{12} - y_2) \frac{c_2}{c} \frac{\mathrm{d}^2 s}{\mathrm{d}z^2} - \frac{1}{2} \left(y_{12}^2 - y_2^2 \right) \frac{\mathrm{d}^3 v}{\mathrm{d}z^3} \right] - \\ &-E_1 \left[(y - y_{12}) \frac{c_1}{c} \frac{\mathrm{d}^2 s}{\mathrm{d}z^2} - \frac{1}{2} \left(y^2 - y_{12}^2 \right) \frac{\mathrm{d}^3 v}{\mathrm{d}z^3} \right], \quad (x,y,z) \in B_1. \end{aligned} \tag{3.36}$$

Here, the stress boundary condition

$$\tau_{yz}(y_2, z) = 0 \tag{3.37}$$

and the continuity condition of τ_{yz} at $y = y_{12}$

$$\lim_{\varepsilon \to 0} \left[\tau_{yz}(y_{12} - \varepsilon, z) - \tau_{yz}(y_{12} + \varepsilon, z) \right] = 0 \tag{3.38}$$

are used. To obtain the normal stress $\sigma_y = \sigma_y(y,z)$ we consider the next equation of mechanical equilibrium

$$\frac{\partial \sigma_y}{\partial y} + \frac{\partial \tau_{yz}}{\partial z} = 0. \tag{3.39}$$

Integration of Eq. (3.39) gives

$$\sigma_y = E_2 \left[\left(\frac{y^2 + y_2^2}{2} - y y_2 \right) \frac{c_2}{c} \frac{\mathrm{d}^3 s}{\mathrm{d}z^3} - \frac{1}{2} \left(\frac{y^3 + 2y_2^3}{3} - y_2^2 y \right) \frac{\mathrm{d}^4 v}{\mathrm{d}z^4} \right], \quad (x, y, z) \in B_2, \tag{3.40}$$

$$\begin{aligned} \sigma_y = E_2 & \left[\left(\frac{y_{12}^2 + y_2^2}{2} - y_{12} y_2 \right) \frac{c_2}{c} \frac{\mathrm{d}^3 s}{\mathrm{d}z^3} - \frac{1}{2} \left(\frac{y_{12}^3 + 2y_2^3}{3} - y_2^2 y_{12} \right) \frac{\mathrm{d}^4 v}{\mathrm{d}z^4} \right] + \\ & + E_1 \left[\left(\frac{y^2 + y_{12}^2}{2} - y y_{12} \right) \frac{c_1}{c} \frac{\mathrm{d}^3 s}{\mathrm{d}z^3} - \frac{1}{2} \left(\frac{y^3 + 2y_{12}^3}{3} - y_{12}^2 y \right) \frac{\mathrm{d}^4 v}{\mathrm{d}z^4} \right] - \\ & - (y - y_{12}) \left(\frac{\partial \tau_{yz}}{\partial z} \right)_{y = y_{12}} \qquad (x, y, z) \in B_1. \end{aligned} \tag{3.41}$$

Here, we use the stress boundary condition

$$\sigma_y (y_2, z) = 0, \tag{3.42}$$

and stress continuity condition of σ_y at $y = y_{12}$

$$\lim_{\varepsilon \to 0} \left[\sigma_y (y_{12} - \varepsilon, z) - \sigma_y (y_{12} + \varepsilon, z) \right] = 0. \tag{3.43}$$

Integration of Eq. (3.34) leads to next equation

$$\tau_{yz} (y_1, z) - \tau_{yz} (y_2, z) + \frac{\partial}{\partial z} \int_{y_2}^{y_1} \sigma_z \mathrm{d}y = 0, \tag{3.44}$$

that is

$$\tau_{yz} (y_1, z) = -\frac{1}{b} \frac{\partial N}{\partial z} = 0. \tag{3.45}$$

By the same method from Eq. (3.39) we obtain

$$\sigma_y (y_1, z) - \sigma_y (y_2, z) + \frac{\partial}{\partial z} \int_{y_2}^{y_1} \tau_{yz} \mathrm{d}y = 0, \tag{3.46}$$

that is

$$\sigma_y (y_1, z) = -\frac{1}{b} \frac{\partial V}{\partial z}. \tag{3.47}$$

Eqs. (3.45) and (3.47) show that the stress boundary conditions for τ_{yz} and σ_y at $y = y_1$ are satisfied. In the following we prove that

$$\tau_{yz} (y_{12}, z) = \frac{Q(z)}{b} = \frac{k s(z)}{b}. \tag{3.48}$$

Starting from Eq. (3.35) we can write

$$\begin{aligned} \tau_{yz} (y_{12}, z) &= -E_2 \left[(y_{12} - y_2) \frac{c_2}{c} \frac{\mathrm{d}^2 s}{\mathrm{d}z^2} - \frac{1}{2} \left(y_{12}^2 - y_2^2 \right) \frac{\mathrm{d}^3 v}{\mathrm{d}z^3} \right] = \\ &= -E_2 \left[\frac{c_2 h_2}{c} \frac{\mathrm{d}^2 s}{\mathrm{d}z^2} - c_2 h_2 \frac{\mathrm{d}^3 v}{\mathrm{d}z^3} \right] = -\frac{E_2 A_2}{b} \frac{c_2}{c} \left[\frac{\mathrm{d}^2 s}{\mathrm{d}z^2} - c \frac{\mathrm{d}^3 v}{\mathrm{d}z^3} \right] = \\ &= -\frac{E_2 A_2}{b} \frac{c_2}{c} \frac{k}{\langle AE \rangle_{-1}} s(z) = \frac{E_1 A_1 E_2 A_2}{\langle AE \rangle \langle AE \rangle_{-1}} \frac{Q(z)}{b} = \frac{Q(z)}{b} \end{aligned} \tag{3.49}$$

Here, Eqs. (3.2–3.5) and Eqs. (3.25), (3.35) have been used to prove the validity of Eq. (3.49).

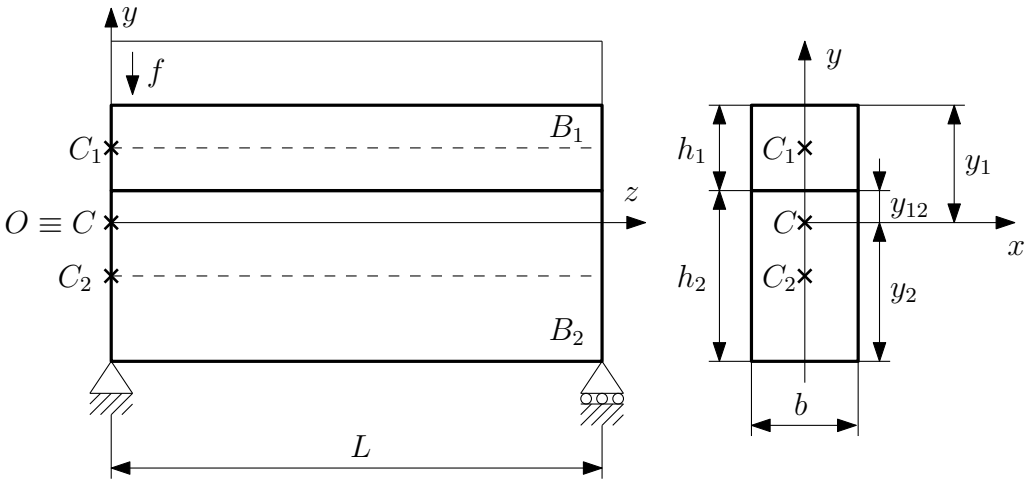

Figure 3.4. Simply supported two-layered beam with thermal load and distributed line load.

3.3 Numerical examples

3.3.1 Simply supported two-layered beam

In this example we consider a simply supported two-layered beam (Fig. 3.4) on which only a thermal load and a distributed line load act. The following data are used for the computations: $b = 0.03\,\mathrm{m}$, $h_1 = 0.01\,\mathrm{m}$, $h_2 = 0.03\,\mathrm{m}$, $E_1 = 1.22{\times}10^{11}\,\mathrm{Pa}$, $E_2 = 8{\times}10^{10}\,\mathrm{Pa}$, $L = 1.5\,\mathrm{m}$, $\alpha_1 = 2.8 \times 10^{-6}\,{}^1\!/_{\mathrm{K}}$, $\alpha_2 = 1.43 \times 10^{-5}\,{}^1\!/_{\mathrm{K}}$, $T = 200\,\mathrm{K}$, $k = 60 \times 10^6\,\mathrm{Pa}$, $f = 1000\,{}^{\mathrm{N}}\!/_{\mathrm{m}}$. First of all we are going to determine the slip and the deflection function of the beam. For the simply supported two-layered beam shown in Fig. 3.4 the following boundary conditions are valid

$$v(0) = 0, \quad v(L) = 0, \tag{3.50}$$

$$N_1(0) = 0, \quad N_1(L) = 0, \tag{3.51}$$

$$M(0) = 0, \quad M(L) = 0 \tag{3.52}$$

By the application of the equation of statics we gain

$$V(z) = fz - \frac{fL}{2}, \tag{3.53}$$

$$M(z) = \frac{fz^2}{2} - \frac{fLz}{2}. \tag{3.54}$$

The function of the bending moment satisfies the boundary conditions (3.52). By means of Eq. (3.53) the general solution of the differential equation (3.30) can be represented as

$$s(z) = K_1 \cosh \Omega z + K_2 \sinh \Omega z - \frac{c}{\langle IE \rangle \Omega^2} \left(\frac{fL}{2} - fz \right), \tag{3.55}$$

where K_1 and K_2 are constants of integration. Using Eqs. (3.26) and (3.54) we can write

$$\frac{\mathrm{d}^2 v}{\mathrm{d}z^2} = \frac{c \langle AE \rangle_{-1}}{\{IE\}} \left[K_1 \Omega \sinh \Omega z + K_2 \Omega \cosh \Omega z + \frac{cf}{\langle IE \rangle \Omega^2} + (\alpha_2 - \alpha_1) T \right] + \\ + \frac{f}{2\{IE\}} \left(Lz - z^2 \right). \tag{3.56}$$

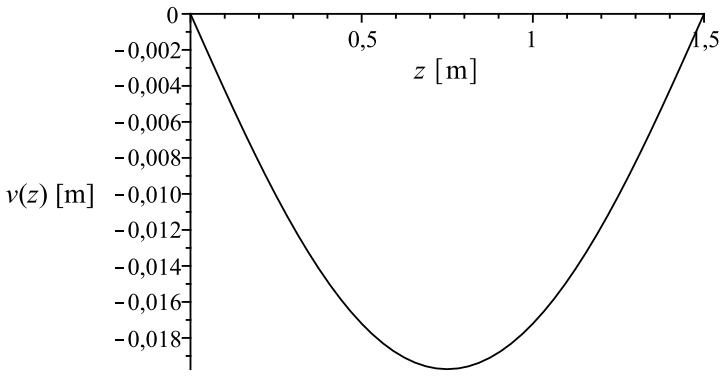

Figure 3.5. The deflection function.

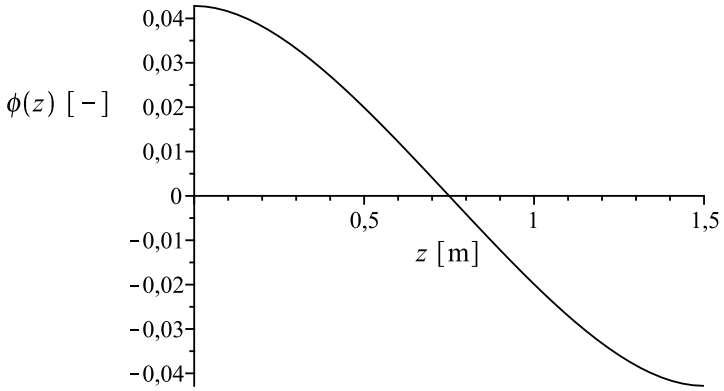

Figure 3.6. The cross-sectional rotation function.

Integration of Eq. (3.56) with respect to z we get the rotation function according to the Euler-Bernoulli hypothesis, i.e.

$$\phi(z) = -\frac{\mathrm{d}v}{\mathrm{d}z}. \tag{3.57}$$

Integration of the rotation function with respect to z provides the deflection function. So we have two further integration constants. By means of the boundary conditions (3.50), (3.51) and the axial force function (3.21) the integration constants can be obtained. In this case we get the following functions

$$v(z) = -\frac{c\,\langle AE\rangle_{-1}}{\{IE\}\,\Omega^2}\left[\frac{cf}{\langle IE\rangle\,\Omega^2} + (\alpha_2-\alpha_1)\,T\right]\left[\cosh\Omega z - 1 - \tanh\frac{\Omega L}{2}\sinh\Omega z + \right.$$
$$\left. + \frac{\Omega^2}{2}\left(Lz - z^2\right)\right] + \frac{f}{24\,\{IE\}}\left(2Lz^3 - z^4 - L^3 z\right), \tag{3.58}$$

$$\phi(z) = \frac{c\,\langle AE\rangle_{-1}}{\{IE\}\,\Omega}\left[\frac{cf}{\langle IE\rangle\,\Omega^2} + (\alpha_2-\alpha_1)\,T\right]\left[\sinh\Omega z - \Omega z - \tanh\frac{\Omega L}{2}\cosh\Omega z + \right.$$
$$\left. + \frac{\Omega L}{2}\right] - \frac{f}{24\,\{IE\}}\left(6Lz^2 - 4z^3 - L^3\right), \tag{3.59}$$

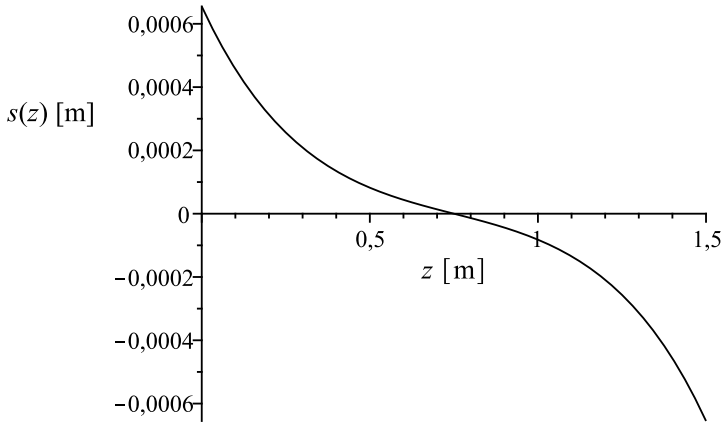

Figure 3.7. The slip function.

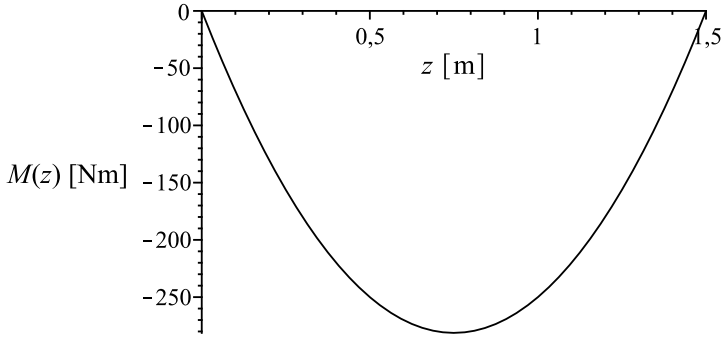

Figure 3.8. The bending moment function.

$$s(z) = \frac{1}{\Omega}\left[\frac{cf}{\langle IE\rangle \Omega^2} + (\alpha_2 - \alpha_1)\, T\right]\left(\tanh\frac{\Omega L}{2}\cosh\Omega z - \sinh\Omega z\right) - \frac{cf}{\langle IE\rangle \Omega^2}\left(\frac{1}{2}L - z\right), \tag{3.60}$$

$$N_1(z) = -\frac{k}{\Omega^2}\left[\frac{cf}{\langle IE\rangle \Omega^2} + (\alpha_2 - \alpha_1)\, T\right]\left[\cosh\Omega z - 1 - \tanh\frac{\Omega L}{2}\sinh\Omega z\right] + \\ + \frac{c\,\langle AE\rangle_{-1}}{\{IE\}}\frac{f}{2}\left(z^2 - Lz\right). \tag{3.61}$$

The deflection function is shown in Fig. 3.5, the rotation function is illustrated in Fig. 3.6 and in Fig. 3.7 the slip function can be seen. Furthermore Figs. 3.8, 3.9 and 3.10 represent de bending moment, the cross-sectional shear force and the axial force in the first layer, respectively. We computed the stresses as well according to Eqs. (3.32), (3.33), (3.35), (3.36), (3.40) and (3.41) at three cross-sections $\left(z = \frac{L}{2}; z = \frac{L}{3}; z = \frac{L}{4}\right)$. The results are shown in Figs. 3.11, 3.12 and 3.13. If the thermal load is equal to zero ($T = 0$), this method provides the exact solution of the problem when only the distributed line load acts on the beam. We computed the functions for this case by means of the fundamental solutions mentioned in the previous chapter, and we gain exactly the same functions from each method. The deflection functions and the slip functions are illustrated in Figs. 3.14 and 3.15 in this case.

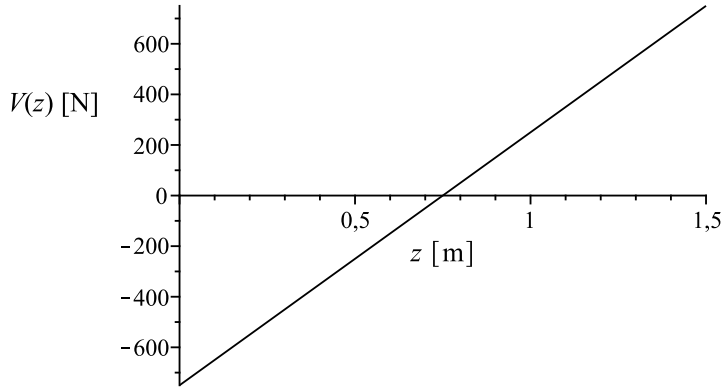

Figure 3.9. The shear force function.

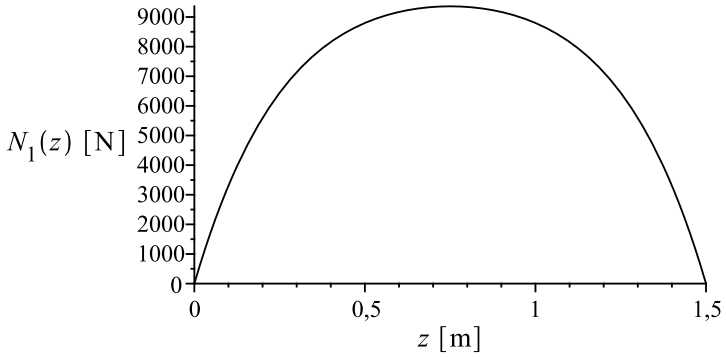

Figure 3.10. The axial force function.

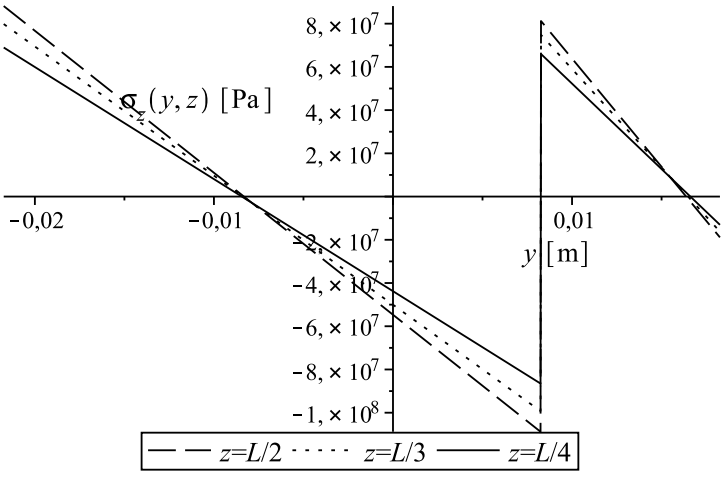

Figure 3.11. The function of σ_z.

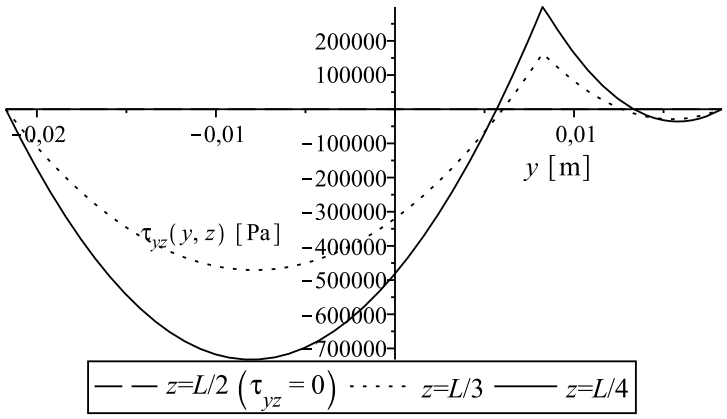

Figure 3.12. The function of τ_{yz}.

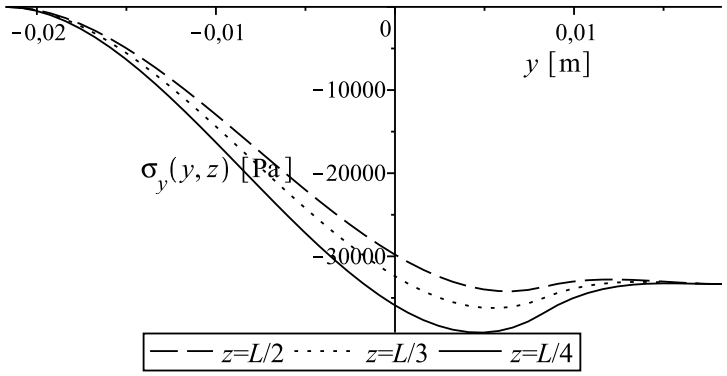

Figure 3.13. The function of σ_y.

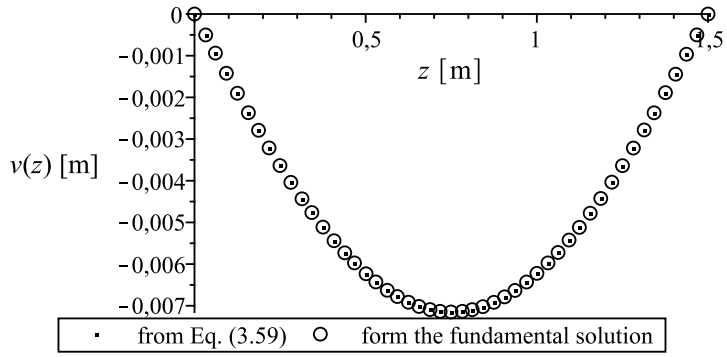

Figure 3.14. The deflection functions in case of $T = 0$.

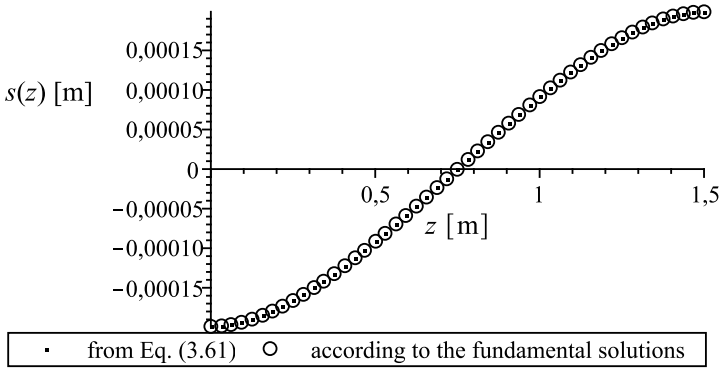

Figure 3.15. The slip functions in case of $T = 0$.

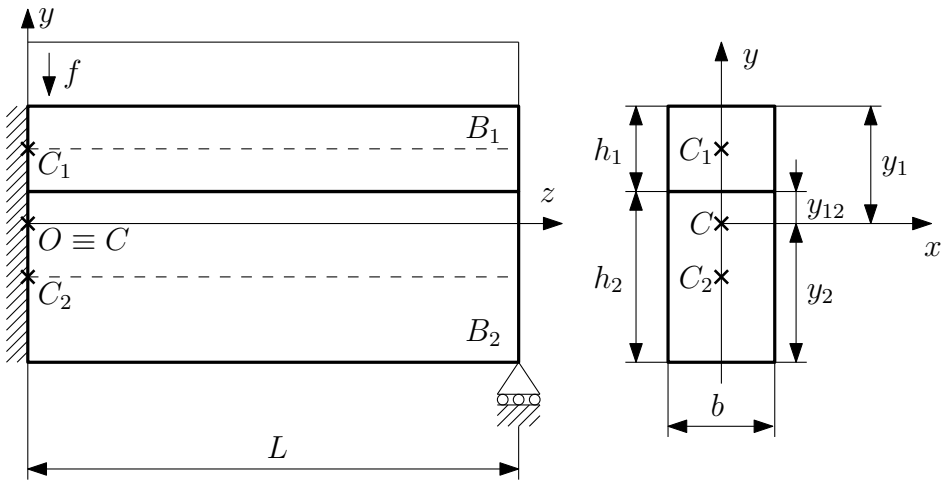

Figure 3.16. Two-layered propped cantilever with thermal load and distributed line load.

3.3.2 Two-layered propped cantilever

In this example we consider a two-layered propped cantilever (Fig. 3.16) on which only a thermal load and a distributed line load act. The following data are used for the computations: $b = 0.01\,\mathrm{m}$, $h_1 = 0.03\,\mathrm{m}$, $h_2 = 0.06\,\mathrm{m}$, $E_1 = 1.22{\times}10^{11}\,\mathrm{Pa}$, $E_2 = 8{\times}10^{10}\,\mathrm{Pa}$, $L = 1.5\,\mathrm{m}$, $\alpha_1 = 2.8 \times 10^{-6}\,{}^1\!/_{\mathrm{K}}$, $\alpha_2 = 1.43 \times 10^{-5}\,{}^1\!/_{\mathrm{K}}$, $T = 250\,\mathrm{K}$, $k = 60 \times 10^6\,\mathrm{Pa}$, $f = 1000\,{}^{\mathrm{N}}\!/_{\mathrm{m}}$. The solution method are the same as in the example 3.3.1. For the propped cantilever we have the following boundary conditions

$$v(0) = 0, \quad v(L) = 0, \tag{3.62}$$

$$\phi(0) = 0, \quad s(0) = 0, \tag{3.63}$$

$$N_1(L) = 0, \quad M(L) = 0, \tag{3.64}$$

From the equation of statics the shear force function and the bending moment function can be determined

$$V(z) = F + f(z - L), \tag{3.65}$$

$$M(z) = F(z - L) + \frac{f}{2}(z - L)^2, \tag{3.66}$$

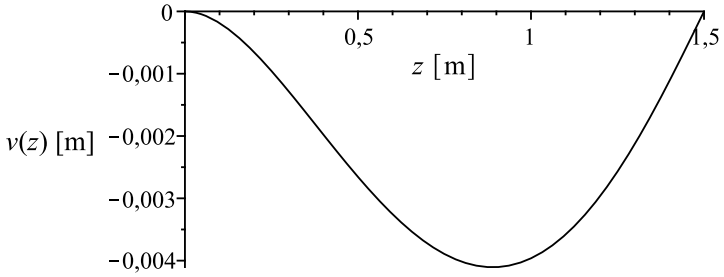

Figure 3.17. The function of the deflection.

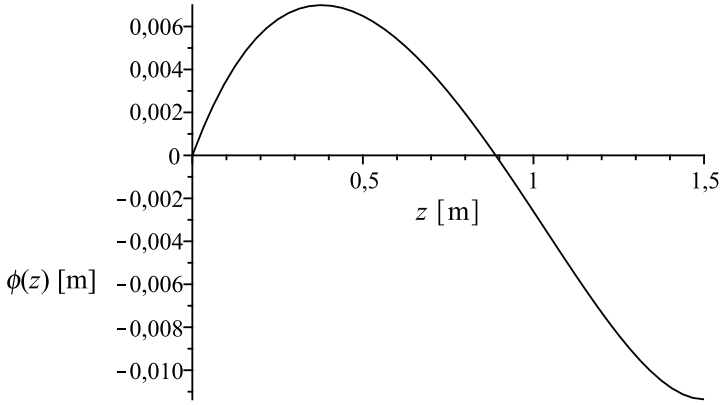

Figure 3.18. The function of the cross-sectional rotation.

where F is the unknown reaction force at the roller. The bending moment function satisfies the boundary condition $(3.64)_2$. Knowing the shear force function we can solve the governing equation (3.30) to create the slip function

$$s(z) = K_1 \sinh \Omega z + K_2 \cosh \Omega z + \frac{c}{\langle IE \rangle \Omega^2} \left(F + fz - fL \right). \tag{3.67}$$

Here, K_1 and K_2 are constants of integration. Writing Eq. (3.67) into Eq. (3.26) and using Eq. (3.54) we win

$$\begin{aligned} \frac{\mathrm{d}^2 v}{\mathrm{d}z^2} = \frac{c \langle AE \rangle_{-1}}{\{IE\}} \left[K_1 \Omega \cosh \Omega z + K_2 \Omega \sinh \Omega z + \frac{cf}{\langle IE \rangle \Omega^2} + (\alpha_2 - \alpha_1) T \right] - \\ - \frac{F}{\{IE\}} (z - L) - \frac{f}{2 \{IE\}} \left(z^2 - 2Lz + L^2 \right). \end{aligned} \tag{3.68}$$

Integration of Eq. (3.68) with respect to z leads to the rotation function according to Eq. (3.57)

$$\begin{aligned} \phi(z) = -\frac{c \langle AE \rangle_{-1}}{\{IE\}} \left[K_1 \sinh \Omega z + K_2 \cosh \Omega z + \left(\frac{cf}{\langle IE \rangle \Omega^2} + (\alpha_2 - \alpha_1) T \right) z \right] + \\ + \frac{F}{\{IE\}} \left(\frac{z^2}{2} - Lz \right) + \frac{f}{2 \{IE\}} \left(\frac{z^3}{3} - Lz^2 + L^2 z \right) + K_3. \end{aligned} \tag{3.69}$$

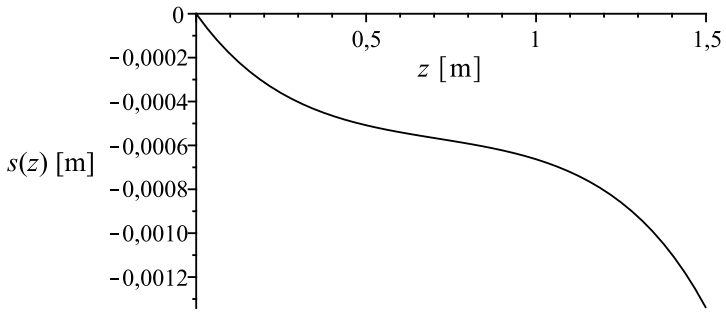

Figure 3.19. The function of the slip.

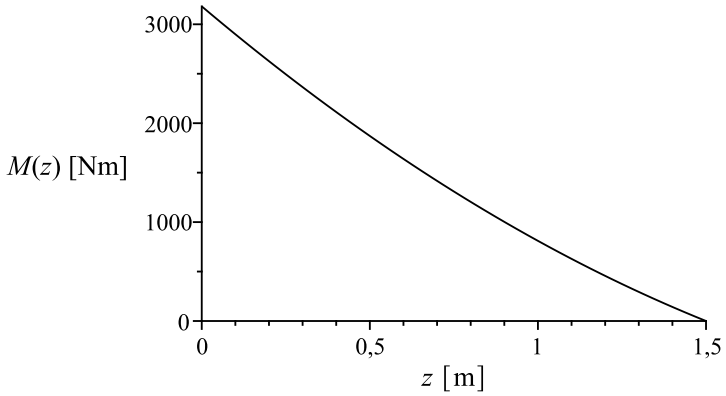

Figure 3.20. The function of the bending moment.

Further integration provides the deflection function

$$v(z) = \frac{c\,\langle AE\rangle_{-1}}{\{IE\}}\left[\frac{K_1}{\Omega}\cosh\Omega z + \frac{K_2}{\Omega}\sinh\Omega z + \left(\frac{cf}{\langle IE\rangle\,\Omega^2} + (\alpha_2-\alpha_1)\,T\right)\frac{z^2}{2}\right] - \\ - \frac{F}{\{IE\}}\left(\frac{z^3}{6} - \frac{Lz^2}{2}\right) - \frac{f}{2\,\{IE\}}\left(\frac{z^4}{12} - \frac{Lz^3}{3} + \frac{L^2z^2}{2}\right) - K_3z + K_4. \tag{3.70}$$

By the application of Eq. (3.21) the axial force function can be computed

$$N_1(z) = \frac{\langle AE\rangle_{-1}}{\{IE\}}\left\{\langle IE\rangle\left[K_1\Omega\cosh\Omega z + K_2\Omega\sinh\Omega z + \frac{cf}{\langle IE\rangle\,\Omega^2} + (\alpha_2-\alpha_1)\,T\right] - \right. \\ \left. - cF(z-L) - \frac{cf}{2}\left(z^2 - 2Lz - L^2\right)\right\}. \tag{3.71}$$

During the computations of these functions we obtain four unknown constants of integration $(K_1; K_2; K_3; K_4)$ and the unknown reaction (F) at the roller. Application of the boundary conditions (3.62), (3.63) and $(3.64)_1$ these unknown can be formulated.

$$F = \frac{K_5}{K_6}, \tag{3.72}$$

where

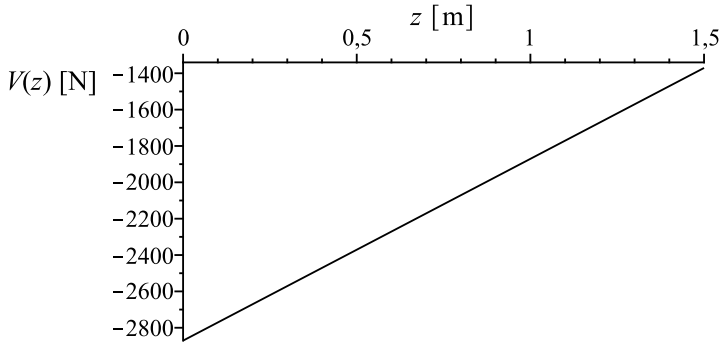

Figure 3.21. The function of the shear force.

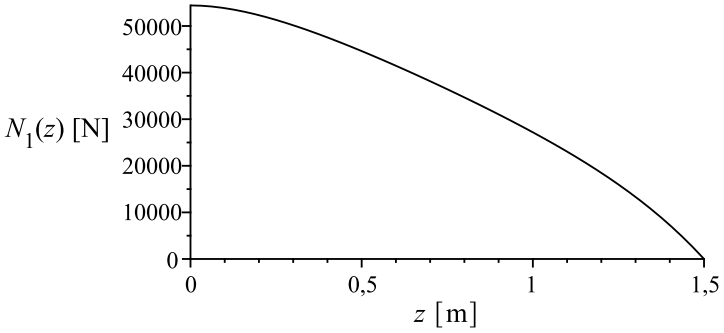

Figure 3.22. The function of the axial force in the first layer.

$$K_5 = f\left(\frac{L^4\Omega^3\langle IE\rangle}{8c^2\langle AE\rangle_{-1}} + \frac{\Omega L^2}{2} - L\tanh\Omega L + \frac{1}{\Omega} - \frac{1}{\Omega\cosh\Omega L}\right) + \\ + (\alpha_2-\alpha_1)\,T\frac{\Omega\langle IE\rangle}{c}\left(1 - \frac{1}{\cosh\Omega L} - \frac{\Omega^2L^2}{2}\right), \tag{3.73}$$

$$K_6 = \frac{L^3\Omega^3\langle IE\rangle}{3c^2\langle AE\rangle_{-1}} + \Omega L - \tanh\Omega L. \tag{3.74}$$

Substituting the given data into Eqs. (3.73), (3.74) and (3.72) the reaction force at the roller is

$$F = -1370.772652\,\mathrm{N} \tag{3.75}$$

By dint of the reaction force the further constants of integration can be formulated as

$$K_1 = -\frac{1}{\cosh\Omega L}\left[\frac{c}{\langle IE\rangle\Omega^2}(fL-F)\sinh\Omega L + \frac{cf}{\langle IE\rangle\Omega^3} + (\alpha_2-\alpha_1)\frac{T}{\Omega}\right], \tag{3.76}$$

$$K_2 = \frac{c}{\langle IE\rangle\Omega^2}(fL-F), \tag{3.77}$$

$$K_3 = \frac{c^2\langle AE\rangle_{-1}}{\{IE\}\langle IE\rangle\Omega^2}(fL-F), \tag{3.78}$$

$$K_4 = -\frac{c\langle AE\rangle_{-1}}{\{IE\}}\frac{K_1}{\Omega}. \tag{3.79}$$

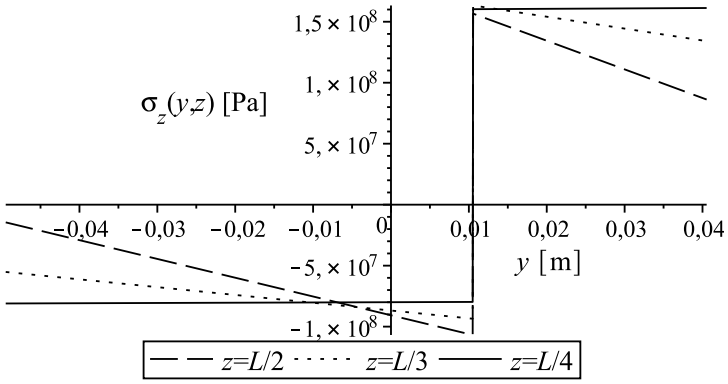

Figure 3.23. The function of σ_z.

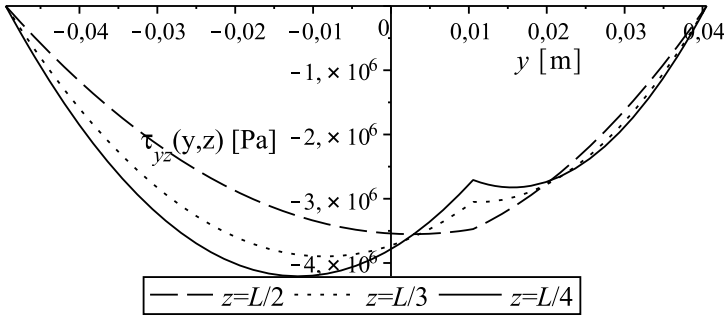

Figure 3.24. The function of τ_{yz}.

According to these results the functions belonging to the propped cantilever are shown in Figs. 3.17, 3.18, 3.19, 3.20, 3.21 and 3.22. Knowing the deflection function and the slip function the stress functions can be computed. Figures 3.23, 3.24 and 3.25 illustrate the normal stress σ_z, the shear stress τ_{yz} and the normal stress σ_y, respectively, at three cross-sections $\left(z = \frac{L}{2}; z = \frac{L}{3}; z = \frac{L}{4}\right)$. We consider the case of $T = 0$ similarly to Example 3.3.1. The results were derived from the present method and from the fundamental solutions for Euler-Bernoulli beam according to chapter 2. The results are exactly the same both cases which are shown in Figs. 3.26 and 3.27.

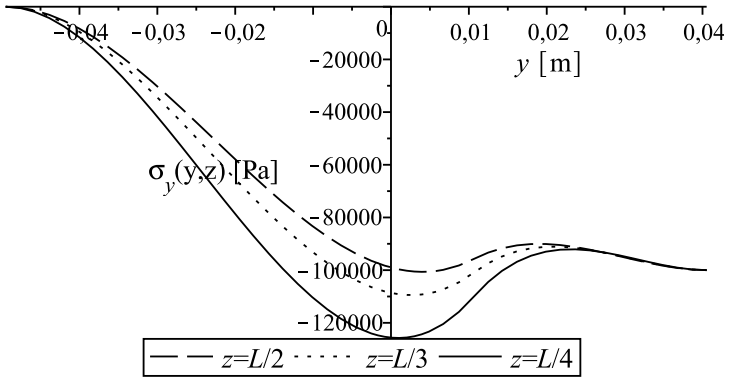

Figure 3.25. The function of σ_y.

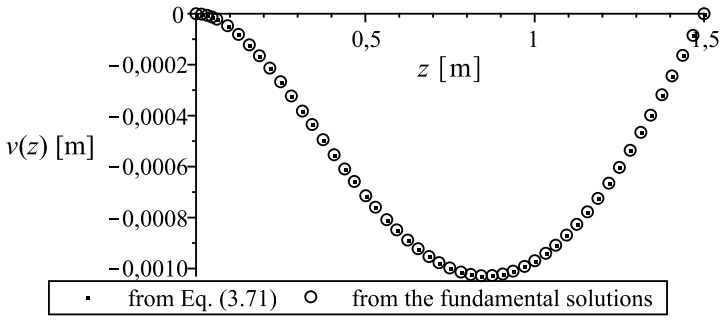

Figure 3.26. The function of the deflection in case of $T = 0$.

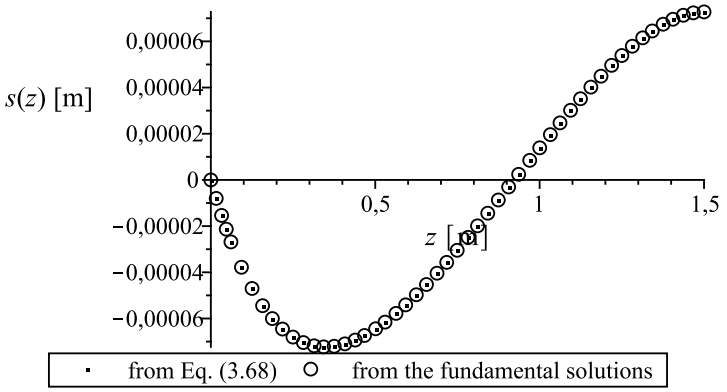

Figure 3.27. The function of the slip in case of $T = 0$.

Chapter 4

Elastic stability of composite beams and columns with weak shear connection

In this chapter we are going to introduce two new analytical methods for the stability analysis of composite beams and columns with weak shear connection. Each method is based on the Euler-Bernoulli beam theory. At the end of the chapter two examples illustrate the application of the methods. Some equations which were mentioned the previous chapters are repeated in this chapter for the ease of reference.

4.1 Stability analysis by a variational method

An elastic two-layered beam with partial shear interaction is considered. It is assumed that each layer separately follows the Euler-Bernoulli hypothesis and the load-slip relation for the flexible shear connection is a linear relationship. In the reference configuration, the composite beam occupies the 3D region $B = A \times [0, L]$ generated by translating its symmetrical cross-section A along a rectilinear axis, orthogonal to the cross-section. The cross-section A is divided into two parts A_1 and A_2, that is $A = A_1 \cup A_2$ and the common boundary A_1 and A_2 is denoted by ∂A_{12}. The components B_1 and B_2 are defined as $B_i = A_i \times [0, L]$, $\partial B_i = \partial A_i \times [0, L]$, $\partial A_i = \partial A_{0i} \cup \partial A_{12}$, $(i = 1, 2)$ (Fig. 4.1). Here L is the length of the beam and ∂A_{0i} is the 'outer' boundary curve of the cross-section A_i $(i = 1, 2)$. A point P in $\overline{B} = B \cup \partial B$ $(\partial B = (\partial A_{01} \cup \partial A_{02}) \times [0, L])$ is determined by the position vector $\mathbf{r} = x\mathbf{e}_x + y\mathbf{e}_y + z\mathbf{e}_z$, where x, y, z and $\mathbf{e}_x$, $\mathbf{e}_y$, $\mathbf{e}_z$ are referred to the rectangular coordinate system $Oxyz$ shown in Fig. 4.1. The axis z is located in the E-weighted centreline of the whole composite beam and the plane yz is the plane of symmetry for the geometrical and support conditions. The centre of A_i is C_i $(i = 1, 2)$ and C is the E-weighted centre of the whole cross-section $A = A_1 \cup A_2$ (Fig. 4.1). According to the Euler-Bernoulli beam theory the displacement field $\mathbf{u} = u\mathbf{e}_x + v\mathbf{e}_y + w\mathbf{e}_z$ has the form [10]

$$u = 0, \quad v = v(z), \quad w = w_i(z) - y\frac{\mathrm{d}v}{\mathrm{d}z}, \quad (x, y, z) \in B_i, \quad (i = 1, 2). \tag{4.1}$$

By the application of the strain-displacement relationship of elasticity and the Hooke's law we get

$$\sigma_z = E_i \left(\frac{\mathrm{d}w_i}{\mathrm{d}z} - y\frac{\mathrm{d}^2 v}{\mathrm{d}z^2} \right), \quad (x, y, z) \in B_i, \quad (i = 1, 2). \tag{4.2}$$

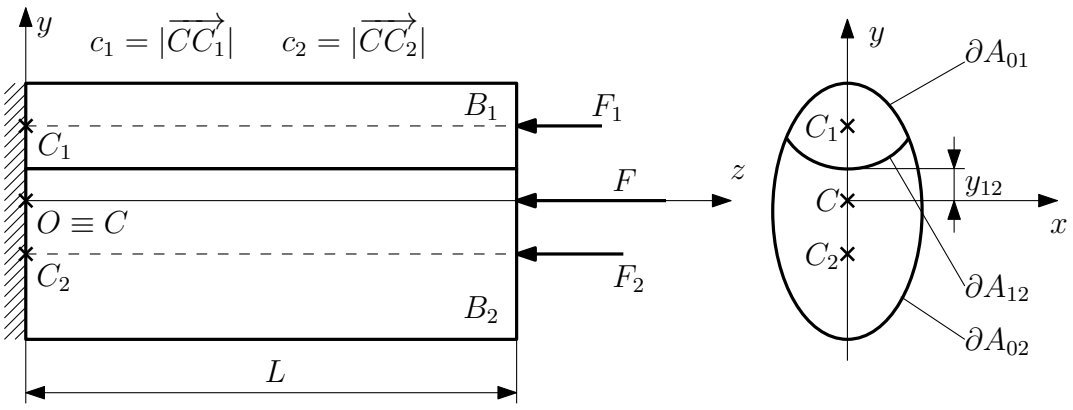

Figure 4.1. Two-layered beam with weak shear connection.

The other stress components are equal to zero. The interlayer slip in axial direction is defined on the common boundary of beam components B_1 and B_2 as the difference of the axial displacement components [10, 11]

$$s(z) = w_1(z) - w_2(z), \quad (x, y, z) \in \partial A_{12} \times [0, L]. \tag{4.3}$$

The interlayer shear force Q is a linear function of the slip s:

$$Q = ks. \tag{4.4}$$

Here k is the slip modulus [10, 11]. Our analysis of the composite beam is restricted to the case of absent axial forces from deflection and slip which means

$$N = N_1 + N_2 = 0, \quad N_i = \int_{A_i} \sigma_z \mathrm{d}A, \quad (i = 1, 2). \tag{4.5}$$

A detailed computation for N_1 gives the next result [10]

$$N_1 = \langle AE \rangle_{-1} \left(\frac{\mathrm{d}s}{\mathrm{d}z} - c \frac{\mathrm{d}^2 v}{\mathrm{d}z^2} \right), \tag{4.6}$$

where

$$\langle AE \rangle_{-1} = \frac{A_1 E_1 A_2 E_2}{A_1 E_1 + A_2 E_2}, \quad c = c_1 + c_2 \text{ (Fig. 4.1)}. \tag{4.7}$$

The expression of the bending moment is as follows [10]

$$M = \int_A y \sigma_z \mathrm{d}A = -\{IE\} \frac{\mathrm{d}^2 v}{\mathrm{d}z^2} + c \langle AE \rangle_{-1} \frac{\mathrm{d}s}{\mathrm{d}z}, \tag{4.8}$$

where

$$\{IE\} = I_1 E_1 + I_2 E_2, \quad I_i = \int_{A_i} y^2 \mathrm{d}A, \quad (i = 1, 2). \tag{4.9}$$

The cross-sectional shear force $V = V(z)$ is obtained as [10, 11]

$$V(z) = \frac{\mathrm{d}M}{\mathrm{d}z} = -\{IE\} \frac{\mathrm{d}^3 v}{\mathrm{d}z^3} + c \langle AE \rangle_{-1} \frac{\mathrm{d}^2 s}{\mathrm{d}z^2} \tag{4.10}$$

Denote U the strain energy of the whole composite beam. Starting from the next formulas [94]

$$U = \frac{1}{2}\int_0^L \left(\int_A \sigma_z \varepsilon_z \mathrm{d}A\right)\mathrm{d}z + \frac{k}{2}\int_0^L s^2 \mathrm{d}z, \tag{4.11}$$

and Eq. (4.2) we obtain

$$U = \frac{1}{2}\int_0^L \left[\{IE\}\left(\frac{\mathrm{d}^2 v}{\mathrm{d}z^2}\right)^2 + 2c\left\langle AE\right\rangle_{-1}\frac{\mathrm{d}^2 v}{\mathrm{d}z^2}\frac{\mathrm{d}s}{\mathrm{d}z} + \left\langle AE\right\rangle_{-1}\left(\frac{\mathrm{d}s}{\mathrm{d}z}\right)^2 + ks^2\right]\mathrm{d}z, \tag{4.12}$$

and the potential energy of the applied axial force is

$$W = -\frac{F}{2}\int_0^L \left(\frac{\mathrm{d}v}{\mathrm{d}z}\right)^2 \mathrm{d}z. \tag{4.13}$$

The total potential energy of the composite beam can be written as the sum of the strain energy and the potential energy of the applied axial force

$$\Pi = U + W. \tag{4.14}$$

The first variation of the total potential energy must be equal to zero according to the principal of minimum total potential energy

$$\delta\Pi = 0, \tag{4.15}$$

so we gain the next form for the considered composite beam

$$\begin{aligned}\delta\Pi = \int_0^L \Bigg[\{IE\}\frac{\mathrm{d}^2 v}{\mathrm{d}z^2}\delta\frac{\mathrm{d}^2 v}{\mathrm{d}z^2} + c\left\langle AE\right\rangle_{-1}\frac{\mathrm{d}s}{\mathrm{d}z}\delta\frac{\mathrm{d}^2 v}{\mathrm{d}z^2} + c\left\langle AE\right\rangle_{-1}\frac{\mathrm{d}^2 v}{\mathrm{d}z^2}\delta\frac{\mathrm{d}s}{\mathrm{d}z} + \\ + \left\langle AE\right\rangle_{-1}\frac{\mathrm{d}s}{\mathrm{d}z}\delta\frac{\mathrm{d}s}{\mathrm{d}z} + ks\delta s\Bigg]\mathrm{d}z - F\int_0^L \frac{\mathrm{d}v}{\mathrm{d}z}\delta\frac{\mathrm{d}v}{\mathrm{d}z}\mathrm{d}z = 0.\end{aligned} \tag{4.16}$$

From this equation the dynamic boundary conditions and the system of the equilibrium equations can be determined. This latter system of equations is the next

$$\{IE\}\frac{\mathrm{d}^4 v}{\mathrm{d}z^4} + c\left\langle AE\right\rangle_{-1}\frac{\mathrm{d}^3 s}{\mathrm{d}z^3} + F\frac{\mathrm{d}^2 v}{\mathrm{d}z^2} = 0, \tag{4.17}$$

$$-c\left\langle AE\right\rangle_{-1}\frac{\mathrm{d}^3 v}{\mathrm{d}z^3} - \left\langle AE\right\rangle_{-1}\frac{\mathrm{d}^2 s}{\mathrm{d}z^2} + ks = 0, \tag{4.18}$$

because the variation of the deflection and slip are arbitrary in $(0, L)$.

4.2 Equilibrium method

According to the Euler-Bernoulli beam theory the displacement field can be written in the next form

$$u = 0, \quad v = v(z), \quad \tilde{w}_i(y,z) = -\frac{F}{\left\langle AE\right\rangle}z + w_i(z) - y\frac{\mathrm{d}v}{\mathrm{d}z}, \quad (x,y,z) \in B_i, \quad (i = 1,2), \tag{4.19}$$

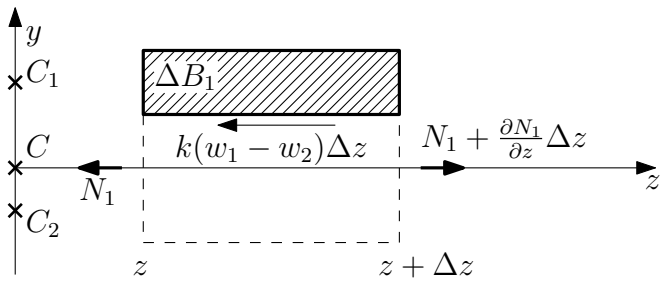

Figure 4.2. Free body diagram for axial forces.

where $\langle AE\rangle = A_1E_1 + A_2E_2$. Application of the strain-displacement relationship of elasticity and the Hooke's law gives

$$\sigma_{zi} = E_i\varepsilon_i = E_i\frac{\mathrm{d}\tilde{w}_i}{\mathrm{d}z} = E_i\left(-\frac{F}{\langle AE\rangle} + \frac{\mathrm{d}w_i}{\mathrm{d}z} - y\frac{\mathrm{d}^2v}{\mathrm{d}z^2}\right), \quad (i = 1, 2). \tag{4.20}$$

The definition of section axial forces provides

$$\tilde{N}_i = \int_{A_i}\sigma_{zi}\mathrm{d}A = -F\frac{A_iE_i}{\langle AE\rangle} + A_iE_i\frac{\mathrm{d}w_i}{\mathrm{d}z} - c_iA_iE_i\frac{\mathrm{d}^2v}{\mathrm{d}z^2}, \quad (i = 1, 2). \tag{4.21}$$

The mechanical meaning of the first term in the expression of $\tilde{N}_i$ is as follows (Fig. 4.1)

$$F_i = \frac{A_iE_i}{\langle AE\rangle}F, \quad (i = 1, 2), \quad F = F_1 + F_2. \tag{4.22}$$

According to this we have

$$N_1 + N_2 = A_1E_1\left(\frac{\mathrm{d}w_1}{\mathrm{d}z} - c_1\frac{\mathrm{d}^2v}{\mathrm{d}z^2}\right) + A_2E_2\left(\frac{\mathrm{d}w_2}{\mathrm{d}z} + c_2\frac{\mathrm{d}^2v}{\mathrm{d}z^2}\right) = 0. \tag{4.23}$$

The moment of normal stress σ_z about axis x is expressed as

$$M = E_1A_1c_1\frac{\mathrm{d}w_1}{\mathrm{d}z} + E_2A_2c_2\frac{\mathrm{d}w_2}{\mathrm{d}z} - \{IE\}\frac{\mathrm{d}^2v}{\mathrm{d}z^2}, \tag{4.24}$$

where $\{IE\}$ is defined by Eq. (4.9). Condition of equilibrium for forces acting in axial direction on column components B_1 and B_2 leads to equations (Fig. 4.2)

$$\frac{\mathrm{d}\tilde{N}_1}{\mathrm{d}z} - k(w_1 - w_2) = 0, \tag{4.25}$$

$$\frac{\mathrm{d}\tilde{N}_2}{\mathrm{d}z} - k(w_2 - w_1) = 0, \tag{4.26}$$

where k is the slip modulus. Eqs. (4.25) and (4.26) can be reformulated by the use of Eq. (4.21)

$$A_1E_1\frac{\mathrm{d}^2w_1}{\mathrm{d}z^2} - c_1A_1E_1\frac{\mathrm{d}^3v}{\mathrm{d}z^3} - k(w_1 - w_2) = 0, \tag{4.27}$$

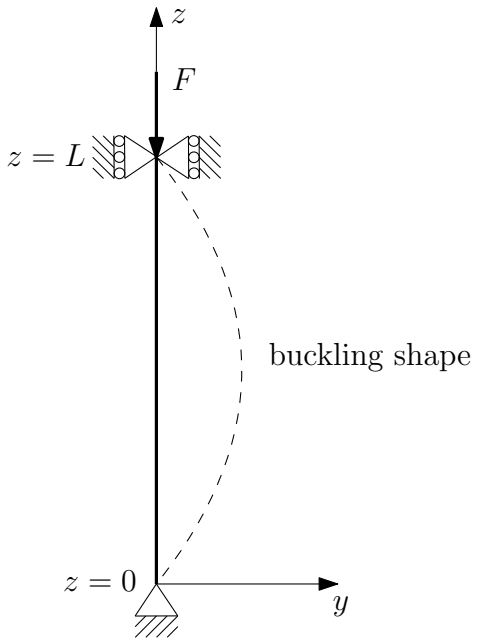

Figure 4.3. Simply supported composite column with axial load.

$$A_2E_2\frac{\mathrm{d}^2w_2}{\mathrm{d}z^2} + c_2A_2E_2\frac{\mathrm{d}^3v}{\mathrm{d}z^3} - k(w_2 - w_1) = 0. \tag{4.28}$$

In the following we are going to investigate two cases using the variational and the equilibrium method. The same composite beam is considered with different boundary conditions in both cases. At the end of each case numerical examples illustrate the application of both methods.

4.3 Simply supported beam

4.3.1 Buckling load

In the first case a simply supported column was analysed (Fig. 4.3). First we use the variational method. Hence we have the next kinematically admissible deflection and slip function

$$v_j(z) = V_j \sin j\frac{\pi}{L}z, \quad s_j(z) = S_j \cos j\frac{\pi}{L}z, \tag{4.29}$$

which satisfy the boundary conditions $[v(0) = 0,\, v(L) = 0]$. The constant j denotes the number of the buckling load and L is the length of the beam. Substituting these functions into the Eqs. (4.17) and (4.18) we obtain the following system of equations

$$\begin{bmatrix} \{IE\}\left(j\frac{\pi}{L}\right)^2 - F & c\,\langle AE\rangle_{-1}\left(j\frac{\pi}{L}\right) \\ c\,\langle AE\rangle_{-1}\left(j\frac{\pi}{L}\right)^3 & \langle AE\rangle_{-1}\left(j\frac{\pi}{L}\right)^2 + k \end{bmatrix} \begin{bmatrix} V_j \\ S_j \end{bmatrix} = \begin{bmatrix} 0 \\ 0 \end{bmatrix}. \tag{4.30}$$

The non trivial solution gives the buckling load, that means the determinant of the coefficients must be equal to zero. Thus we have a closed form for the critical load

$$F_j^{cr} = \frac{\langle IE\rangle\,\langle AE\rangle_{-1}\left(j\frac{\pi}{L}\right)^4 + k\{IE\}\left(j\frac{\pi}{L}\right)^2}{\langle AE\rangle_{-1}\left(j\frac{\pi}{L}\right)^2 + k}, \quad (j = 1, 2, \ldots), \tag{4.31}$$

where $\langle IE\rangle = \{IE\} - c^2 \langle AE\rangle_{-1}$.

Let us consider the equilibrium method for the simply supported beam. We have the same boundary conditions $[v(0) = 0,\, v(L) = 0]$. For simply supported column we have

$$M(z) = Fv(z). \tag{4.32}$$

Combination of Eq. (4.8) with Eq. (4.32) provides

$$E_1 A_1 c_1 \frac{\mathrm{d}w_1}{\mathrm{d}z} + E_2 A_2 c_2 \frac{\mathrm{d}w_2}{\mathrm{d}z} - \{IE\}\frac{\mathrm{d}^2 v}{\mathrm{d}z^2} - Fv(z) = 0. \tag{4.33}$$

We look for the solution of the system of equations (4.27), (4.28), (4.33) which satisfy the boundary conditions in the form

$$w_1(z) = \sum_{j=1}^{\infty} W_{1j} \cos j\frac{\pi}{L}z, \quad w_2(z) = \sum_{j=1}^{\infty} W_{2j} \cos j\frac{\pi}{L}z, \quad v(z) = \sum_{j=1}^{\infty} V_j \sin j\frac{\pi}{L}z. \tag{4.34}$$

Substitution of Eq. (4.34) into Eqs. (4.27), (4.28) and (4.33) yields the eigenvalue problem

$$\mathbf{A}_j \mathbf{X}_j = \begin{bmatrix} a_{11j} & a_{12j} & a_{13j} \\ a_{21j} & a_{22j} & a_{23j} \\ a_{31j} & a_{32j} & a_{33j} \end{bmatrix} \begin{bmatrix} W_{1j} \\ W_{2j} \\ V_j \end{bmatrix} = \begin{bmatrix} 0 \\ 0 \\ 0 \end{bmatrix}, \tag{4.35}$$

where

$$a_{11j} = \left(j\frac{\pi}{L}\right)^2 A_1 E_1 + k, \quad a_{12j} = -k, \quad a_{13j} = -c_1 A_1 E_1 \left(j\frac{\pi}{L}\right)^3, \tag{4.36}$$

$$a_{21j} = j\frac{\pi}{L} A_1 E_1, \quad a_{22j} = j\frac{\pi}{L} A_2 E_2, \quad a_{23j} = 0, \tag{4.37}$$

$$a_{31j} = j\frac{\pi}{L} A_1 E_1 c_1, \quad a_{32j} = j\frac{\pi}{L} A_2 E_2 c_2, \quad a_{33j} = F - \{IE\}\left(j\frac{\pi}{L}\right)^2, \tag{4.38}$$

The critical loads depend on the value of j, the buckling load belongs to $j = 1$ in this case as well. The following closed formula can be derived from

$$\det \mathbf{A}_j(F) = 0 \tag{4.39}$$

for the critical loads

$$F_j^{cr} = \frac{\langle IE\rangle \langle AE\rangle_{-1} \left(j\frac{\pi}{L}\right)^4 + k\{IE\}\left(j\frac{\pi}{L}\right)^2}{\langle AE\rangle_{-1}\left(j\frac{\pi}{L}\right)^2 + k}, \quad (j = 1, 2, \ldots). \tag{4.40}$$

We obtain the same closed formula from the equilibrium method as from the variational method.

4.3.2 Numerical example

We consider the simply supported beam shown in Fig. 4.3. The cross-section of the beam is illustrated in Fig. 4.4 and the following data are used for the computations. $L = 4\,\mathrm{m}$; $E_1 = 12 \times 10^9\,\mathrm{Pa}$; $E_2 = 8 \times 10^9\,\mathrm{Pa}$; $k = 5 \times 10^7\,\mathrm{Pa}$; $h_1 = 0.05\,\mathrm{m}$; $h_2 = 0.15\,\mathrm{m}$; $b_1 = 0.3\,\mathrm{m}$; $b_2 = 0.05\,\mathrm{m}$. Substituting these data into the formula (4.31) or (4.40) the buckling load is

$$F_1^{cr} = 271.018\,\mathrm{kN}. \tag{4.41}$$

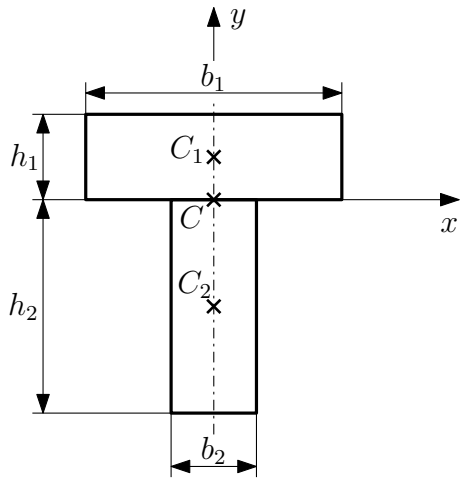

Figure 4.4. The cross-section of the simply supported column.

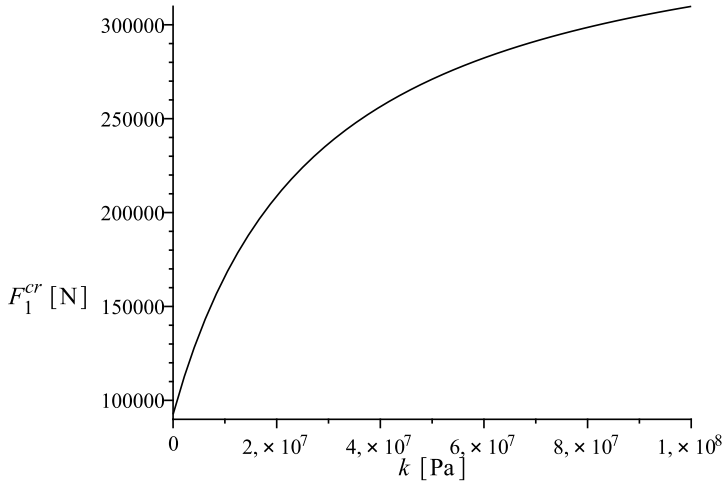

Figure 4.5. The buckling load in terms of the slip modulus ($0 \leq k \leq 10^8$).

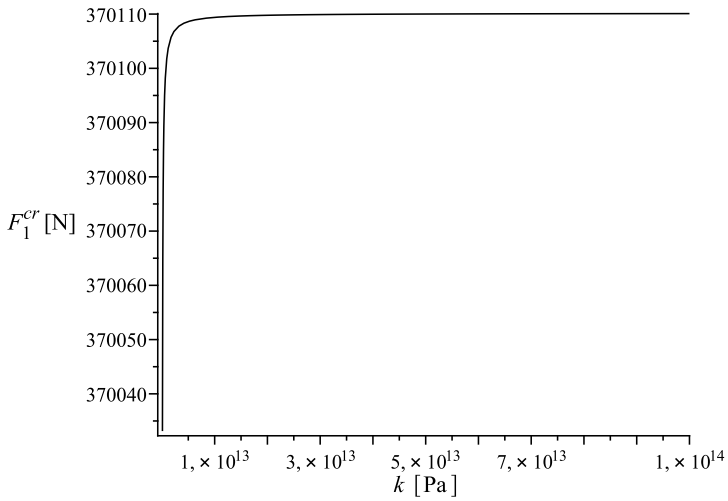

Figure 4.6. The buckling load in terms of the slip modulus ($10^{11} \leq k \leq 10^{14}$).

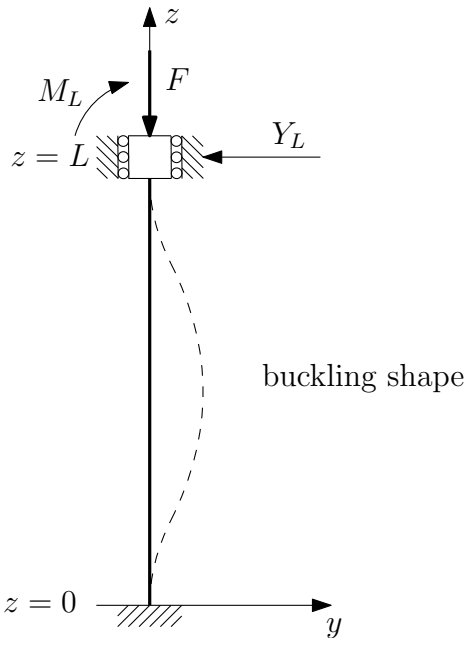

Figure 4.7. Column with fixed ends.

In an early study Girhammar and Gopu [9] proposed an approximate solution for the determination of buckling load. They investigated a column with the same cross-section, data and boundary conditions. Their analysis led to the next result for the first buckling load

$$F_1^{cr} = 270.3\,\text{kN}. \tag{4.42}$$

It can be determined that the results are in good agreement. The buckling load in terms of the slip modulus is shown in Figs. 4.5 and 4.6. If the slip modulus is equal to zero (there is no connection between the layers), then the buckling load $F_1^{cr} = 92527.54\,\text{N}$. The functions illustrate as well that while the slip modulus converges to infinity (perfect connection between the layers) the buckling load approaches the value of the composite beam having perfect connection.

4.4 Column with fixed ends

4.4.1 Buckling load

In this case a column is analysed which has fixed ends (Fig. 4.7). First we used the variational method as section 4.3. We must write new kinematically admissible deflection and slip functions to content the new kinematical boundary conditions. The functions are as follows

$$v_j(z) = V_j \left(1 - \cos j\frac{2\pi}{L}z\right), \quad s_j(z) = S_j \sin j\frac{2\pi}{L}z. \tag{4.43}$$

Taking these functions into the Eqs. (4.17), (4.18) a newer system of equation is won

$$\begin{bmatrix} -\{IE\}\left(j\frac{2\pi}{L}\right)^2 + F & -c\,\langle AE\rangle_{-1}\, j\frac{2\pi}{L} \\ c\,\langle AE\rangle_{-1}\left(j\frac{2\pi}{L}\right)^3 & \langle AE\rangle_{-1}\left(j\frac{2\pi}{L}\right)^2 + k \end{bmatrix} \begin{bmatrix} V_j \\ S_j \end{bmatrix} = \begin{bmatrix} 0 \\ 0 \end{bmatrix}. \tag{4.44}$$

From this system we can gain another closed form for the buckling load

$$F_j^{cr} = \frac{\langle IE\rangle \langle AE\rangle_{-1} \left(j\frac{2\pi}{L}\right)^4 + k\{IE\}\left(j\frac{2\pi}{L}\right)^2}{\langle AE\rangle_{-1}\left(j\frac{2\pi}{L}\right)^2 + k}, \quad (j = 1, 2, \ldots). \tag{4.45}$$

Let us consider the equilibrium method. It is evident that the bending moment $M = M(z)$ in terms of the reactions Y_L, M_L can be expressed as (Fig. 4.7)

$$M(z) = M_L - Y_L(L - z) + Fv(z). \tag{4.46}$$

From this equation we get

$$\frac{\mathrm{d}^2 M}{\mathrm{d}z^2} = F\frac{\mathrm{d}^2 v}{\mathrm{d}z^2}. \tag{4.47}$$

Combination of Eq. (4.24) with Eq. (4.47) provides

$$E_1A_1c_1\frac{\mathrm{d}^3 w_1}{\mathrm{d}z^3} + E_2A_2c_2\frac{\mathrm{d}^3 w_2}{\mathrm{d}z^3} - \{IE\}\frac{\mathrm{d}^4 v}{\mathrm{d}z^4} - F\frac{\mathrm{d}^2 v}{\mathrm{d}z^2} = 0. \tag{4.48}$$

Eqs. (4.27), (4.28) and (4.48) generate a system of linear differential equations for $w_1 = w_1(z)$, $w_2 = w_2(z)$, $v = v(z)$. The associated boundary conditions to Eqs. (4.27), (4.28) and (4.48) are as follows:

$$v(0) = v(L) = w_1(0) = w_2(0) = 0, \quad \frac{\mathrm{d}v}{\mathrm{d}z} = 0 \text{ for } z = 0 \text{ and } z = L. \tag{4.49}$$

We search the solution of boundary value problem formulated by Eqs. (4.27), (4.28), (4.48) and (4.49) as

$$w_1(z) = \sum_{j=1}^{\infty} W_{1j}\sin\frac{2j\pi}{L}z, \quad w_2(z) = \sum_{j=1}^{\infty} W_{2j}\sin\frac{2j\pi}{L}z, \quad v(z) = \sum_{j=1}^{\infty} V_j\left(1 - \cos\frac{2j\pi}{L}z\right). \tag{4.50}$$

The functions given by Eq. (4.50) satisfy the boundary conditions (4.49). Substitution of Eq. (4.50) into Eqs. (4.27), (4.28) and (4.48) we get a linear eigenvalue problem from which the critical loads can be determined. The eigenvalue problem has the form

$$\mathbf{A}_j\mathbf{X}_j = \begin{bmatrix} a_{11j} & a_{12j} & a_{13j} \\ a_{21j} & a_{22j} & a_{23j} \\ a_{31j} & a_{32j} & a_{33j} \end{bmatrix} \begin{bmatrix} W_{1j} \\ W_{2j} \\ V_j \end{bmatrix} = \begin{bmatrix} 0 \\ 0 \\ 0 \end{bmatrix}, \tag{4.51}$$

where

$$a_{11j} = \left(\frac{2j\pi}{L}\right)^2 A_1E_1 + k, \quad a_{12j} = -k, \quad a_{13j} = -c_1A_1E_1\left(\frac{2j\pi}{L}\right)^3, \tag{4.52}$$

$$a_{21j} = \frac{2j\pi}{L}A_1E_1, \quad a_{22j} = \frac{2j\pi}{L}A_2E_2, \quad a_{23j} = 0, \tag{4.53}$$

$$a_{31j} = \frac{2j\pi}{L}A_1E_1c_1, \quad a_{32j} = \frac{2j\pi}{L}A_2E_2c_2, \quad a_{33j} = F - \{IE\}\left(\frac{2j\pi}{L}\right)^2. \tag{4.54}$$

The following closed formula can be derived from

$$\det\mathbf{A}_j(F) = 0 \tag{4.55}$$

for the critical loads

$$F_j^{cr} = \frac{\langle IE\rangle \langle AE\rangle_{-1} \left(j\frac{2\pi}{L}\right)^4 + k\{IE\}\left(j\frac{2\pi}{L}\right)^2}{\langle AE\rangle_{-1}\left(j\frac{2\pi}{L}\right)^2 + k}, \quad (j = 1, 2, \ldots). \tag{4.56}$$

Formula (4.56) is exactly the same as Eq. (4.45) which we obtain from the variational method.

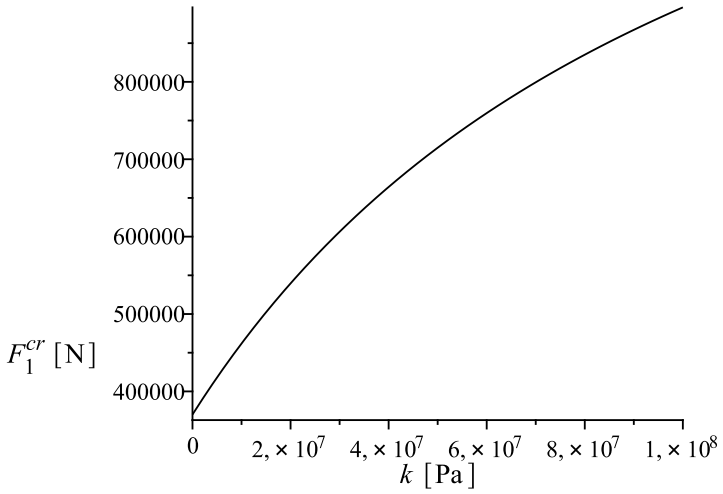

Figure 4.8. The buckling load in terms of the slip modulus ($0 \leq k \leq 10^8$).

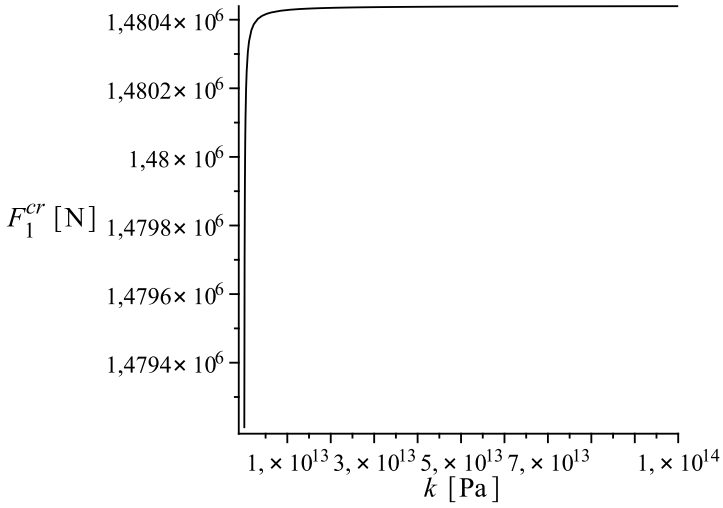

Figure 4.9. The buckling load in terms of the slip modulus ($10^{11} \leq k \leq 10^{14}$).

4.4.2 Numerical example

In this example we use the same column as in the case of the simply supported beam. I.e. we use the data from Example 4.3.2 and the cross-section shown in Fig. 4.4. Inserting the data into the formula (4.45) or (4.56) the buckling load

$$F_1^{cr} = 714.863\,\mathrm{kN} \tag{4.57}$$

for the column with fixed ends. The buckling load in terms of the slip modulus is illustrated in Figs. 4.8 and 4.9. If there is no connection between the layers the value of the buckling load is $F_1^{cr} = 370110.165\,\mathrm{N}$. We can determine the same conclusions as the Example 4.3.2.

Chapter 5

Vibration analysis of composite beams with weak shear connection

In this chapter we deal with an analytical solution for free flexural vibration of a simply supported two-layered composite beam with interlayer slip if the rotary inertia and the inertia of longitudinal motion are taken into account. A numerical example illustrates the application of the method. Some equations which have already appeared in the previous chapters are repeated as well in the following for the ease of reference.

5.1 Equation of motion and boundary conditions

The considered simply supported two-layered composite beam with interlayer slip is shown in Fig. 5.1. The beam components occupy the spatial domain $B_i = A_i \times [0, L]$ $(i = 1, 2)$ where A_i $(i = 1, 2)$ means the cross-section of the i-th layer and L is the length of the beam. The plane yz is the plane of symmetry of the beam, furthermore the plane $y = 0$, $0 \leq z \leq L$ denotes the common surfaces of the beam components B_1 and B_2. The elastic moduli of the beam components B_1 and B_2 are indicated by E_1 and E_2. It is assumed in this case as well that the beam components separately content the requirements of the Euler-Bernoulli beam theory. Accordingly the displacement components are as follows

$$u(x, y, z, t) = 0, \quad v = v(z, t), \quad (x, y, z) \in B_1 \cup B_2, \tag{5.1}$$

$$w(x, y, z, t) = w_i(z, t) - y\frac{\partial v}{\partial z}, \quad (x, y, z) \in B_i, \quad (i = 1, 2). \tag{5.2}$$

In Eqs. (5.1), (5.2) u, v, w are the coordinates of the displacement vector (Fig. 5.1) and t denotes the time. Application of the kinematic equation of linear elasticity and using Eqs. (5.1), (5.2) provides [95, 96]

$$\varepsilon_x = \varepsilon_y = \gamma_{xy} = \gamma_{xz} = \gamma_{yz} = 0, \tag{5.3}$$

$$\varepsilon_z = \frac{\partial w_i}{\partial z} - y\frac{\partial^2 v}{\partial z^2}, \quad (x, y, z) \in B_i, \quad (i = 1, 2). \tag{5.4}$$

The inner axial force N_i of beam component B_i is

$$N_i(z, t) = \int_{A_i} \sigma_z \mathrm{d}A = E_i A_i \left(\frac{\partial w_i}{\partial z} - c_i \frac{\partial^2 v}{\partial z^2} \right), \quad (i = 1, 2). \tag{5.5}$$

Here, we applied the Hooke's law and the next notation

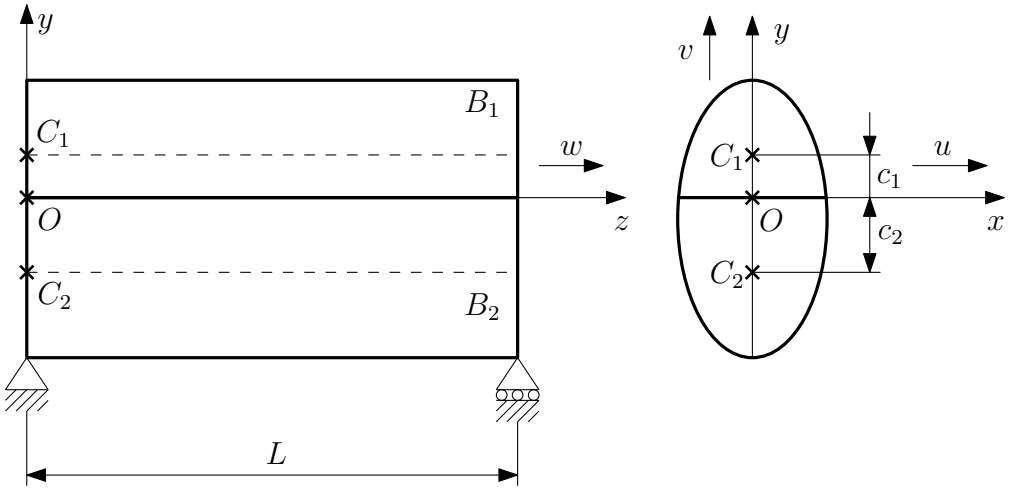

Figure 5.1. The considered simply supported two-layered composite beam.

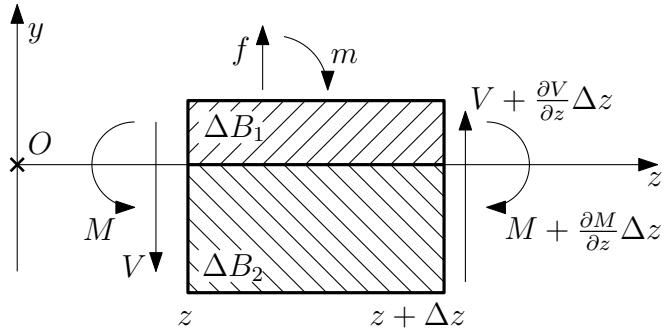

Figure 5.2. Shear force, bending moment, the applied distributed line load and distributed moment on a small beam element.

$$c_i = \frac{1}{A_i}\int_{A_i} y \mathrm{d}A, \quad (i = 1, 2), \tag{5.6}$$

and σ_z represents the normal stress. The bending moment of the whole cross-section can be formulated as

$$M = \int_{A_1} y\sigma_z \mathrm{d}A + \int_{A_2} y\sigma_z \mathrm{d}A = c_1 E_1 A_1 \frac{\partial w_1}{\partial z} + c_2 E_2 A_2 \frac{\partial w_2}{\partial z} - \{IE\}\frac{\partial^2 v}{\partial z^2}, \tag{5.7}$$

where

$$\{IE\} = E_1 \int_{A_1} y^2 \mathrm{d}A + E_2 \int_{A_2} y^2 \mathrm{d}A = E_1 I_1 + E_2 I_2. \tag{5.8}$$

A $\Delta B_1 \cup \Delta B_2$ beam element is illustrated in Fig. 5.2 without the axial forces. The cross-sectional shear force, the applied distributed line load in y direction and the applied distributed bending moment in x direction are denoted by $V = V(z,t)$, $f = f(z,t)$ and $m = m(z,t)$, respectively. According to this beam element the following equilibrium equations can be deduced

$$\frac{\partial V}{\partial z} + f = 0, \quad \frac{\partial M}{\partial z} - V + m = 0. \tag{5.9}$$

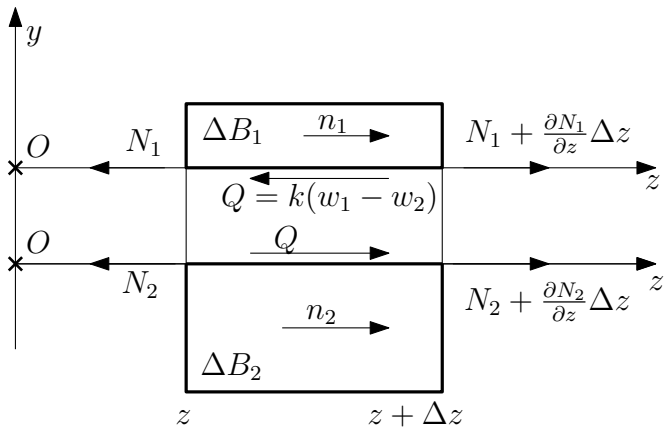

Figure 5.3. Axial forces on a small beam element.

From the Eq. (5.9) the shear force can be eliminated. In this way we obtain only one equilibrium equation instead of the two ones in Eq. (5.9)

$$\frac{\partial^2 M}{\partial z^2} + \frac{\partial m}{\partial z} + f = 0. \tag{5.10}$$

The beam elements ΔB_1 and ΔB_2 assigned by z and $z + \Delta z$ coordinates are shown in Fig. 5.3. Only the axial forces act on these beam elements. The interlayer shear force Q has the form

$$Q = k(w_1 - w_2), \tag{5.11}$$

where k is the slip modulus. The axial forces n_1 and n_2 acting on B_1 and B_2, respectively, derive from the outer loading. The equilibrium equations in axial direction for beam component ΔB_1 and ΔB_2 can be written in the next form

$$\frac{\partial N_1}{\partial z} + n_1 - k(w_1 - w_2) = 0, \tag{5.12}$$

$$\frac{\partial N_2}{\partial z} + n_2 + k(w_1 - w_2) = 0. \tag{5.13}$$

In regard to the fact that we analyse the free vibration of the considered composite beam the function of $f = f(z,t)$, $n_1 = n_1(z,t)$, $n_2 = n_2(z,t)$, $m = m(z,t)$ can be deduced from the d'Alembert inertial forces so we have

$$f(z,t) = -(\rho_1 A_1 + \rho_2 A_2)\frac{\partial^2 v}{\partial t^2}, \tag{5.14}$$

$$n_1(z,t) = -\rho_1 A_1 \frac{\partial^2 w_1}{\partial t^2} + c_1 \rho_1 A_1 \frac{\partial^3 v}{\partial z \partial t^2}, \tag{5.15}$$

$$n_2(z,t) = -\rho_2 A_2 \frac{\partial^2 w_2}{\partial t^2} + c_2 \rho_2 A_2 \frac{\partial^3 v}{\partial z \partial t^2}, \tag{5.16}$$

$$m(z,t) = -c_1 \rho_1 A_1 \frac{\partial^2 w_1}{\partial t^2} - c_2 \rho_2 A_2 \frac{\partial^2 w_2}{\partial t^2} + \{\rho I\}\frac{\partial^3 v}{\partial z \partial t^2}. \tag{5.17}$$

Here, ρ_1 and ρ_2 mean the mass density of beam component B_1 and B_2, respectively, and

$$\{\rho I\} = \rho_1 I_1 + \rho_2 I_2 = \rho_1 \int_{A_1} y^2 \mathrm{d}A + \rho_2 \int_{A_2} y^2 \mathrm{d}A. \tag{5.18}$$

Combination of Eqs. (5.10), (5.12), (5.13) with Eqs. (5.14–5.17) yields the system of motion equations for the two-layered composite beam with interlayer slip

$$E_1A_1\frac{\partial^2 w_1}{\partial z^2} - c_1E_1A_1\frac{\partial^3 v}{\partial z^3} - k(w_1 - w_2) - \rho_1A_1\frac{\partial^2 w_1}{\partial t^2} + c_1\rho_1A_1\frac{\partial^3 v}{\partial z\partial t^2} = 0, \tag{5.19}$$

$$E_2A_2\frac{\partial^2 w_2}{\partial z^2} - c_2E_2A_2\frac{\partial^3 v}{\partial z^3} + k(w_1 - w_2) - \rho_2A_2\frac{\partial^2 w_2}{\partial t^2} + c_2\rho_2A_2\frac{\partial^3 v}{\partial z\partial t^2} = 0, \tag{5.20}$$

$$\begin{aligned} c_1E_1A_1\frac{\partial^3 w_1}{\partial z^3} + c_2E_2A_2\frac{\partial^3 w_2}{\partial z^3} - \{IE\}\frac{\partial^4 v}{\partial z^4} - c_1\rho_1A_1\frac{\partial^3 w_1}{\partial z\partial t^2} - \\ - c_2\rho_2A_2\frac{\partial^3 w_2}{\partial z\partial t^2} + \{\rho I\}\frac{\partial^4 v}{\partial z^2\partial t^2} - (\rho_1A_1 + \rho_2A_2)\frac{\partial^2 v}{\partial t^2} = 0. \end{aligned} \tag{5.21}$$

For the simply supported beam the following boundary conditions can be written (Fig. 5.1)

$$N_1(0,t) = N_1(L,t) = 0, \quad t > 0, \tag{5.22}$$

$$N_2(0,t) = N_2(L,t) = 0, \quad t > 0, \tag{5.23}$$

$$M(0,t) = M(L,t) = 0, \quad t > 0, \tag{5.24}$$

$$v(0,t) = v(L,t) = 0, \quad t > 0. \tag{5.25}$$

We look for the solution of the boundary value problem (5.19–5.25) in the next form

$$w_1(z,t) = W_{1j}\cos\frac{j\pi}{L}z\cos\omega_j t, \tag{5.26}$$

$$w_2(z,t) = W_{2j}\cos\frac{j\pi}{L}z\cos\omega_j t, \tag{5.27}$$

$$v(z,t) = V_j\sin\frac{j\pi}{L}z\cos\omega_j t, \quad (j = 1,2,\ldots). \tag{5.28}$$

These functions satisfy the boundary conditions (5.22–5.25) for all values of W_{1j}, W_{2j}, V_j. Substituting the functions into Eqs. (5.19–5.21) the following linear system of equation can be deduced

$$\mathbf{C}_j\mathbf{X}_j = \omega_j^2\mathbf{M}_j\mathbf{X}_j, \tag{5.29}$$

where

$$\mathbf{X}_j = [W_{1j}, W_{2j}, V_j]^T, \tag{5.30}$$

$$\mathbf{C}_j = \begin{bmatrix} E_1A_1\left(\frac{j\pi}{L}\right)^2 + k & -k & -c_1E_1A_1\left(\frac{j\pi}{L}\right)^3 \\ -k & E_2A_2\left(\frac{j\pi}{L}\right)^2 + k & c_2E_2A_2\left(\frac{j\pi}{L}\right)^3 \\ -c_1E_1A_1\left(\frac{j\pi}{L}\right)^3 & c_2E_2A_2\left(\frac{j\pi}{L}\right)^3 & \{IE\}\left(\frac{j\pi}{L}\right)^4 \end{bmatrix}, \tag{5.31}$$

$$\mathbf{M}_j = \begin{bmatrix} \rho_1A_1 & 0 & -c_1\rho_1A_1\frac{j\pi}{L} \\ 0 & \rho_2A_2 & -c_2\rho_2A_2\frac{j\pi}{L} \\ -c_1\rho_1A_1\frac{j\pi}{L} & -c_2\rho_2A_2\frac{j\pi}{L} & \{\rho I\}\left(\frac{j\pi}{L}\right)^4 + \rho_1A_1 + \rho_2A_2 \end{bmatrix}. \tag{5.32}$$

The non trivial solution of Eqs. (5.29) is sought that means

$$\det\left(\mathbf{C}_j - \omega_j^2\mathbf{M}_j\right) = 0, \quad (j = 1,2,\ldots). \tag{5.33}$$

Table 5.1. The eigenfrequencies of the two-layered beam with axial and rotary inertia.

j	ω_{j1} $^1/_s$	ω_{j2} $^1/_s$	ω_{j3} $^1/_s$
1	135.42	2566.01	8403.41
2	539.36	5009.04	16796.21
3	1211.79	7478.84	25191.61
4	2151.61	9955.53	33587.91
5	3357.29	12434.99	41984.87
6	4826.83	14915.86	50382.46
7	6557.84	17397.51	58780.73
8	8547.52	19879.66	67179.78
9	10792.69	22362.14	75579.67
10	13289.8	24844.86	83980.52
15	29407.05	37260.3	126002.35
20	49677.13	51117.82	168062.56
25	62094.53	77704.45	210173.28
30	74512.21	108398.66	252346.16
35	86930.04	142445.76	294592.21
40	99347.98	179150.11	336921.62
45	111765.98	217901.19	379343.58
50	124184.03	258183.26	421866.11
100	248365.55	685328.22	853330.3

From Eq. (5.33) a cubic equation can be formulated for ω_j^2 $(j = 1, 2, \ldots)$ which means that we have three eigenfrequencies for each value of j. If the axial inertia is neglected the mass matrix $\mathbf{M}_j$ has the form

$$\mathbf{M}_j = \begin{bmatrix} 0 & 0 & 0 \\ 0 & 0 & 0 \\ -c_1\rho_1 A_1 \frac{j\pi}{L} & -c_2\rho_2 A_2 \frac{j\pi}{L} & \{\rho I\}\left(\frac{j\pi}{L}\right)^4 + \rho_1 A_1 + \rho_2 A_2 \end{bmatrix}. \tag{5.34}$$

In this case we can obtain a first degree equation of ω_j^2 from Eq. (5.33) i.e. one eigenfrequency is provided for each value of j. In addition when the rotary inertia is also neglected the mass matrix is simplified further

$$\mathbf{M}_j = \begin{bmatrix} 0 & 0 & 0 \\ 0 & 0 & 0 \\ 0 & 0 & \rho_1 A_1 + \rho_2 A_2 \end{bmatrix}. \tag{5.35}$$

From Eq. (5.33) a first degree equation is also given in terms of ω_j^2, in other words there is one eigenfrequency for each value of j.

Here we note that we have made a further dynamic analysis for composite beams with interlayer slip in **(5)**. In that case the considered beam satisfies the requirements of Timoshenko beam theory and the layers of the beam have different cross-sectional rotation $(\phi_1 \neq \phi_2)$.

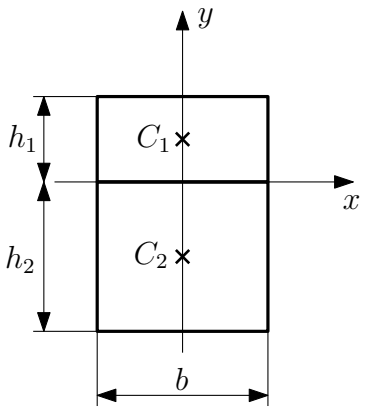

Figure 5.4. The cross-section of the composite beam.

Table 5.2. The eigenfrequencies of the two-layered beam neglecting the axial inertia (β) and neglecting the axial and the rotary inertia (δ).

	β	δ
j	ω_j $^1/_s$	ω_j $^1/_s$
1	135.42	135.44
2	539.35	539.66
3	1211.78	1213.3
4	2151.61	2156.4
5	3357.32	3368.94
6	4826.93	4850.95
7	6558.07	6602.4
8	8547.95	8623.31
9	10793.43	10913.68
10	13290.98	13473.5
15	29413.74	30314.42
20	51139.84	53891.71
25	77759.4	84205.37
30	108513.95	121255.39
35	142660.09	165041.78
40	179514.4	165041.78
45	218478.65	215564.55
50	259048.83	272823.67
100	694606.2	1347274.4

5.2 Numerical example

The cross-section of the considered beam is shown in Fig. 5.4 and the following data were applied for the computations of the eigenfrequencies: $h_1 = 0.02\,\mathrm{m}$; $h_2 = 0.04\,\mathrm{m}$; $b = 0.03\,\mathrm{m}$; $L = 2\,\mathrm{m}$; $E_1 = 10^{10}\,\mathrm{Pa}$; $E_2 = 2 \times 10^{11}\,\mathrm{Pa}$; $k = 10^6\,\mathrm{Pa}$; $\rho_1 = 4000\ {}^{\mathrm{kg}}/_{\mathrm{m}^3}$; $\rho_2 = 7000\ {}^{\mathrm{kg}}/_{\mathrm{m}^3}$. First we computed the eigenfrequencies in that case when the rotary inertia and the axial inertia was taken into account as well. In this case the mass matrix (5.32) were used in Eq. (5.33). Table 5.1 contains the eigenfrequencies for several values of j. Neglecting the axial inertia the mass matrix changes for (5.34) in Eq. (5.33). The eigenfrequencies belonging to this case are collected in the column β in Table 5.2. The column δ of Table 5.2 shows the eigenfrequencies when the axial and the rotary inertia are equally neglected, viz. the mass matrix (5.35) were used in Eq. (5.33).

Chapter 6

Analysis of curved composite beams with interlayer slip

In this chapter a Rayleigh-Betti type reciprocity relation is derived for two-layered curved composite beam with imperfect shear connection. The principle of minimum potential energy is also formulated and its applications are illustrated by numerical examples.

6.1 Governing equations

The curved two-layered composite beam and its cross-section are shown in Fig. 6.1. In the cylindrical coordinate system $Or\varphi z$ the curved layer i $(i = 1, 2)$ occupies the space domain B_i $(i = 1, 2)$

$$B_i = \{(r, \varphi, z) | (r, z) \in A_i,\ 0 \leq \varphi \leq \beta < 2\pi\}, \quad (i = 1, 2), \tag{6.1}$$

where A_i is the cross-section of beam component B_i $(i = 1, 2)$ (Fig. 6.1). The common boundary surface of B_1 and B_2 is denoted by ∂B_{12}

$$\partial B_{12} = \left\{(r, \varphi, z) | r = r_c,\ 0 \leq \varphi \leq \beta,\ |z| \leq \frac{b(r_c)}{2}\right\}. \tag{6.2}$$

Here $b = b(r)$ is the thickness of the cross-section (Fig. 6.1). The plane $z = 0$ is the plane of symmetry for the whole two-layered curved beam. The connection between the beam components B_1 and B_2 on their common boundary surface ∂B_{12} in radial direction is perfect, whilst in circumferential direction may be jump in the displacement field. The possible jump is called the interlayer slip. Denote the unit vectors of the coordinate system $Or\varphi z$ $\mathbf{e}_r$, $\mathbf{e}_\varphi$ and $\mathbf{e}_z$. The in-plane deformation of two-layered curved beam is described by the next displacement field [97]

$$\mathbf{u} = u\mathbf{e}_r + v\mathbf{e}_\varphi + w\mathbf{e}_z, \tag{6.3}$$

$$u = u(\varphi), \quad w = 0, \quad (r, \varphi, z) \in B = B_1 \cup B_2, \tag{6.4}$$

$$v(r, \varphi, z) = r\phi_i(\varphi) + \frac{\mathrm{d}u}{\mathrm{d}\varphi}, \quad (r, \varphi, z) \in B_i, \quad (i = 1, 2). \tag{6.5}$$

Application of the strain-displacement relationship of the linearised theory of elasticity gives [90]

$$\varepsilon_r = \varepsilon_z = \gamma_{r\varphi} = \gamma_{rz} = \gamma_{\varphi z} = 0, \quad (r, \varphi, z) \in B, \tag{6.6}$$

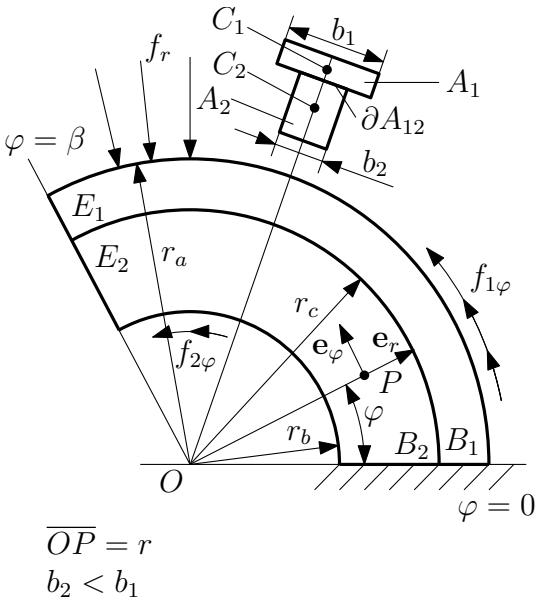

Figure 6.1. Two-layered curved beam.

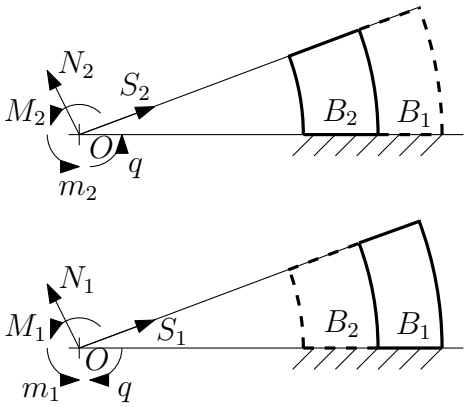

Figure 6.2. Illustration of internal forces and couples.

$$\varepsilon_\varphi = \frac{1}{r}\left(\frac{\mathrm{d}^2 u}{\mathrm{d}\varphi^2} + u\right) + \frac{\mathrm{d}\phi_i}{\mathrm{d}\varphi}, \quad (r, \varphi, z) \in B_i, \quad (i = 1, 2). \tag{6.7}$$

The strains provided by Eqs. (6.6) and (6.7) satisfy the requirements of the Euler-Bernoulli beam theory, only the one normal strain component ε_φ is different from zero and all the shearing strains vanish. From the definition of the interlayer slip $s = s(\varphi)$ it follows that (Fig. 6.1)

$$s(\varphi) = r_c(\phi_1(\varphi) - \phi_2(\varphi)). \tag{6.8}$$

Denote $\hat{Q} = \hat{Q}(\varphi)$ the interlayer shear force acting on unit area of the common boundary surface of B_1 and B_2 which is $r_c b_2 \mathrm{d}\varphi$, since $b_1 > b_2$ (Fig. 6.1). Here, we assume that

$$\hat{Q}(\varphi) = ks(\varphi) = kr_c(\phi_1(\varphi) - \phi_2(\varphi)), \tag{6.9}$$

where k is the slip modulus and its unit is force/(length)^3. The value of the interlayer shear force on this surface element is

$$Q(\varphi)\mathrm{d}\varphi = \hat{Q}(\varphi) r_c b_2 \mathrm{d}\varphi = k r_c^2 b_2 \left(\phi_1(\varphi) - \phi_2(\varphi)\right) \mathrm{d}\varphi, \tag{6.10}$$

that is

$$Q(\varphi) = kr_c^2 b_2 \left(\phi_1(\varphi) - \phi_2(\varphi)\right). \tag{6.11}$$

According to paper [97] we define the stress resultants, i.e. the normal force, the shearing force and the stress couple resultant as (Fig. 6.2)

$$N_i = \int_{A_i} \sigma_\varphi \mathrm{d}A, \quad S_i = \int_{A_i} \tau_{r\varphi} \mathrm{d}A, \quad M_i = \int_{A_i} r\sigma_\varphi \mathrm{d}A, \quad (i = 1, 2). \tag{6.12}$$

In Eqs. (6.12) σ_φ is the normal stress and $\tau_{r\varphi}$ denotes the shearing stress. The virtual work W of the section forces and moment on a kinematically admissible displacement field

$$\hat{u} = \hat{u}(\varphi), \quad \hat{w} = 0, \quad \hat{v} = r\hat{\phi}_i + \frac{\mathrm{d}\hat{u}}{\mathrm{d}\varphi}, \quad (i = 1, 2) \tag{6.13}$$

can be computed as

$$\begin{gathered} W = \int_A \sigma_\varphi \hat{v} \mathrm{d}A + \int_A \tau_{r\varphi} \hat{u} \mathrm{d}A = M_1\hat{\phi}_1 + M_2\hat{\phi}_2 + N\frac{\mathrm{d}\hat{u}}{\mathrm{d}\varphi} + S\hat{u}, \\ N = N_1 + N_2, \quad S = S_1 + S_2. \end{gathered} \tag{6.14}$$

From Eq. (6.14) we obtain the possible combinations of the boundary conditions at the end cross sections

$$S = S_1 + S_2 \text{ or } u \text{ may be prescribed,} \tag{6.15}$$

$$N = N_1 + N_2 \text{ or } \frac{\mathrm{d}u}{\mathrm{d}\varphi} \text{ may be prescribed,} \tag{6.16}$$

$$M_1 \text{ or } \phi_1 \text{ may be prescribed,} \tag{6.17}$$

$$M_2 \text{ or } \phi_2 \text{ may be prescribed.} \tag{6.18}$$

The virtual work of the distributed forces f_r, $f_{1\varphi}$ and $f_{2\varphi}$ on a small beam element (Fig. 6.3) can be computed as

$$\mathrm{d}\widetilde{W} = \left[f_r\widetilde{u} + f_\varphi\frac{\mathrm{d}\widetilde{u}}{\mathrm{d}\varphi} + m_1\widetilde{\phi}_1 + m_2\widetilde{\phi}_2 \right] \mathrm{d}\varphi, \tag{6.19}$$

where

$$\widetilde{\mathbf{u}} = \widetilde{u}\mathbf{e}_r + \left(r\widetilde{\phi}_i + \frac{\mathrm{d}\widetilde{u}}{\mathrm{d}\varphi} \right) \mathbf{e}_\varphi, \ (r, \varphi, z) \in B_i, \ (i = 1, 2) \tag{6.20}$$

is the virtual displacement field and (Fig. 6.3)

$$f_\varphi = f_{1\varphi} + f_{2\varphi}, \ m_1 = r_a f_{1\varphi}, \ m_2 = r_b f_{2\varphi}. \tag{6.21}$$

Equations of equilibrium can be formulated as [97]

$$\frac{\mathrm{d}N}{\mathrm{d}\varphi} + S + f_\varphi = 0, \tag{6.22}$$

$$-N + \frac{\mathrm{d}S}{\mathrm{d}\varphi} + f_r = 0, \tag{6.23}$$

$$\frac{\mathrm{d}M_1}{\mathrm{d}\varphi} + m_1 - q = 0, \tag{6.24}$$

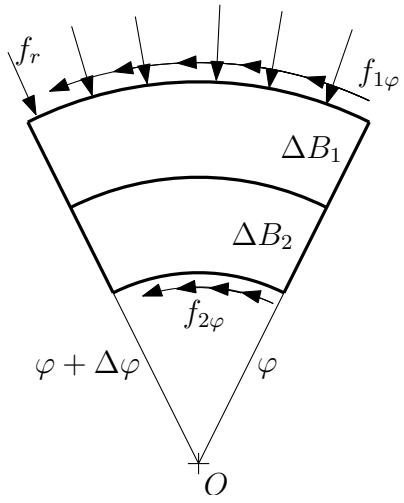

Figure 6.3. Virtual work of applied forces acting on a small beam element.

$$\frac{\mathrm{d}M_2}{\mathrm{d}\varphi} + m_2 + q = 0. \tag{6.25}$$

In Eqs. (6.24–6.25) (Fig. 6.2)

$$q = K\left(\phi_1 - \phi_2\right), \quad K = kr_c^3 b_2, \quad (b_2 < b_1), \tag{6.26}$$

and we have

$$N = N_1 + N_2, \;\; S = S_1 + S_2. \tag{6.27}$$

6.2 Rayleigh-Betti type reciprocity relation

Let us consider two equilibrium states of a two-layered curved beam with imperfect shear connection. These equilibrium states are denoted by upper one comma and upper two comma, respectively. Starting from Eqs. (6.22), (6.23) we can write

$$\left(\frac{\mathrm{d}N'}{\mathrm{d}\varphi} + S' + f'_\varphi\right)\frac{\mathrm{d}u''}{\mathrm{d}\varphi} + \left(-N' + \frac{\mathrm{d}S'}{\mathrm{d}\varphi} + f'_r\right)u'' = 0. \tag{6.28}$$

Integration of Eq. (6.28) gives

$$\left\{N'\frac{\mathrm{d}u''}{\mathrm{d}\varphi} + S'u''\right\}_0^\beta + \int_0^\beta \left(f'_\varphi\frac{\mathrm{d}u''}{\mathrm{d}\varphi} + f'_r u''\right)\mathrm{d}\varphi - \int_0^\beta N'\left(\frac{\mathrm{d}^2u''}{\mathrm{d}\varphi^2} + u''\right)\mathrm{d}\varphi = 0, \tag{6.29}$$

where the next designation

$$\left\{F\left(\varphi\right)\right\}_0^\beta = F\left(\beta\right) - F\left(0\right) \tag{6.30}$$

is introduced. From Eqs. (6.24), (6.25) it follows that

$$\begin{aligned}\int_0^\beta \left(\frac{\mathrm{d}M'_1}{\mathrm{d}\varphi}\phi''_1 + m'_1\phi''_1 - q'\phi''_1 + \frac{\mathrm{d}M'_2}{\mathrm{d}\varphi}\phi''_2 + m'_2\phi''_2 + q'\phi''_2\right)\mathrm{d}\varphi = \\ \left\{M'_1\phi''_1 + M'_2\phi''_2\right\}_0^\beta + \int_0^\beta \left(m'_1\phi''_1 + m'_2\phi''_2\right)\mathrm{d}\varphi - \\ - \int_0^\beta \left[M'_1\frac{\mathrm{d}\phi''_1}{\mathrm{d}\varphi} + M'_2\frac{\mathrm{d}\phi''_2}{\mathrm{d}\varphi} + q'\left(\phi''_1 - \phi''_2\right)\right]\mathrm{d}\varphi = 0.\end{aligned} \tag{6.31}$$

Let

$$W_{12} = \left\{ N' \frac{\mathrm{d}u''}{\mathrm{d}\varphi} + S'u'' + M_1'\phi_1'' + M_2'\phi_2'' \right\}_0^\beta + \int_0^\beta \left(f_r' u'' + f_\varphi' \frac{\mathrm{d}u''}{\mathrm{d}\varphi} + m_1'\phi_1'' + m_2'\phi_2'' \right) \mathrm{d}\varphi \tag{6.32}$$

be. The mechanical meaning of W_{12} is obvious, the work done by the applied forces and reactions of the first equilibrium state on the displacement field caused by the forces applied in second equilibrium state. We define the mixed strain energy U_{12} for the states 1 and 2 as

$$U_{12} = \int_0^\beta \left[N' \left(\frac{\mathrm{d}^2 u''}{\mathrm{d}\varphi^2} + u'' \right) + M_1' \frac{\mathrm{d}\phi_1''}{\mathrm{d}\varphi} + M_2' \frac{\mathrm{d}\phi_2''}{\mathrm{d}\varphi} + q' \left(\phi_1'' - \phi_2'' \right) \right] \mathrm{d}\varphi. \tag{6.33}$$

The combination of Eq. (6.29) with Eq. (6.31) gives

$$W_{12} = U_{12}. \tag{6.34}$$

Application of the Hooke's law and Eq. (6.7) yields the formula of normal stress σ_φ

$$\sigma_\varphi = E_i \left[\frac{1}{r} \left(\frac{\mathrm{d}^2 u}{\mathrm{d}\varphi^2} + u \right) + \frac{\mathrm{d}\phi_i}{\mathrm{d}\varphi} \right], \quad (r, \varphi, z) \in B_i, \quad (i = 1, 2), \tag{6.35}$$

where E_i is the modulus of elasticity for curved layer B_i $(i = 1, 2)$. Combination of Eqs. $(6.12)_{1,2,3}$ with Eq. (6.35) gives

$$N_i = \frac{A_i E_i}{R_i} \left(\frac{\mathrm{d}^2 u}{\mathrm{d}\varphi^2} + u \right) + A_i E_i \frac{\mathrm{d}\phi_i}{\mathrm{d}\varphi}, \quad (i = 1, 2), \tag{6.36}$$

$$M_i = A_i E_i \left(\frac{\mathrm{d}^2 u}{\mathrm{d}\varphi^2} + u \right) + r_i A_i E_i \frac{\mathrm{d}\phi_i}{\mathrm{d}\varphi}, \quad (i = 1, 2). \tag{6.37}$$

Here,

$$\frac{1}{R_i} = \frac{1}{A_i} \int_{A_i} \frac{\mathrm{d}A}{r}, \quad (i = 1, 2), \tag{6.38}$$

$$r_i = \frac{1}{A_i} \int_{A_i} r \mathrm{d}A, \quad \overline{OC_i} = r_i, \quad (i = 1, 2), \quad \text{(Fig. 6.1)}. \tag{6.39}$$

The connection between the normal force N and shear force S is as follows [97]

$$S = -\frac{\mathrm{d}N}{\mathrm{d}\varphi}. \tag{6.40}$$

Combination of Eqs. $(6.27)_1$, (6.36), (6.37) and (6.40) we obtain

$$N = \frac{AE_0}{R} \left(\frac{\mathrm{d}^2 u}{\mathrm{d}\varphi^2} + u \right) + A_1 E_1 \frac{\mathrm{d}\phi_1}{\mathrm{d}\varphi} + A_2 E_2 \frac{\mathrm{d}\phi_2}{\mathrm{d}\varphi}, \tag{6.41}$$

$$M = M_1 + M_2 = AE_0 \left(\frac{\mathrm{d}^2 u}{\mathrm{d}\varphi^2} + u \right) + r_1 A_1 E_1 \frac{\mathrm{d}\phi_1}{\mathrm{d}\varphi} + r_2 A_2 E_2 \frac{\mathrm{d}\phi_2}{\mathrm{d}\varphi}, \tag{6.42}$$

where (Fig. 6.1)

$$E_0 = \frac{A_1 E_1 + A_2 E_2}{A}, \quad A = A_1 + A_2, \tag{6.43}$$

$$\frac{AE_0}{R} = E_1 \int_{A_1} \frac{\mathrm{d}A}{r} + E_2 \int_{A_2} \frac{\mathrm{d}A}{r}. \tag{6.44}$$

By the use of Eq. (6.26) and Eqs. (6.37), (6.41) we can reformulate the expression of U_{12} as

$$\begin{aligned} U_{12} = \int_0^\beta \Bigg[& \frac{AE_0}{R}\left(\frac{\mathrm{d}^2u'}{\mathrm{d}\varphi^2}+u'\right)\left(\frac{\mathrm{d}^2u''}{\mathrm{d}\varphi^2}+u''\right) + A_1E_1\left(\frac{\mathrm{d}^2u''}{\mathrm{d}\varphi^2}+u''\right)\frac{\mathrm{d}\phi_1'}{\mathrm{d}\varphi} + \\ & + A_1E_1\left(\frac{\mathrm{d}^2u'}{\mathrm{d}\varphi^2}+u'\right)\frac{\mathrm{d}\phi_1''}{\mathrm{d}\varphi} + A_2E_2\left(\frac{\mathrm{d}^2u''}{\mathrm{d}\varphi^2}+u''\right)\frac{\mathrm{d}\phi_2'}{\mathrm{d}\varphi} + A_2E_2\left(\frac{\mathrm{d}^2u'}{\mathrm{d}\varphi^2}+u'\right)\frac{\mathrm{d}\phi_2''}{\mathrm{d}\varphi} + \\ & + r_1A_1E_1\frac{\mathrm{d}\phi_1'}{\mathrm{d}\varphi}\frac{\mathrm{d}\phi_1''}{\mathrm{d}\varphi} + r_2A_2E_2\frac{\mathrm{d}\phi_2'}{\mathrm{d}\varphi}\frac{\mathrm{d}\phi_2''}{\mathrm{d}\varphi} + K\left(\phi_1'-\phi_2'\right)\left(\phi_1''-\phi_2''\right)\Bigg]\mathrm{d}\varphi. \end{aligned} \tag{6.45}$$

It is evident

$$U_{12} = U_{21} \text{ and } U_{21} = W_{21}, \tag{6.46}$$

where

$$W_{21} = \left\{ N''\frac{\mathrm{d}u'}{\mathrm{d}\varphi} + S''u' + M_1''\phi_1' + M_2''\phi_2' \right\}_0^\beta + \int_0^\beta \left(f_r''u' + f_\varphi''\frac{\mathrm{d}u'}{\mathrm{d}\varphi} + m_1''\phi_1' + m_2''\phi_2' \right)\mathrm{d}\varphi. \tag{6.47}$$

Comparison of Eq. (6.34) with Eq. (6.46) yields the next Rayleigh-Betti type reciprocity relation

$$W_{12} = W_{21}. \tag{6.48}$$

If the two equilibrium states are the same, that is

$$u = u' = u'', \;\; \phi_1 = \phi_1' = \phi_1'', \;\; \phi_2 = \phi_2' = \phi_2'', \ldots, \tag{6.49}$$

then we have according to Clapeyron's theorem

$$U = W, \tag{6.50}$$

where U is the strain energy of the two-layered composite beam with imperfect shear connection

$$\begin{aligned} U = \frac{1}{2}\int_0^\beta \Bigg[& \frac{AE_0}{R}\left(\frac{\mathrm{d}^2u}{\mathrm{d}\varphi^2}+u\right)^2 + 2A_1E_1\left(\frac{\mathrm{d}^2u}{\mathrm{d}\varphi^2}+u\right)\frac{\mathrm{d}\phi_1}{\mathrm{d}\varphi} + 2A_2E_2\left(\frac{\mathrm{d}^2u}{\mathrm{d}\varphi^2}+u\right)\frac{\mathrm{d}\phi_2}{\mathrm{d}\varphi} + \\ & + r_1A_1E_1\left(\frac{\mathrm{d}\phi_1}{\mathrm{d}\varphi}\right)^2 + r_2A_2E_2\left(\frac{\mathrm{d}\phi_2}{\mathrm{d}\varphi}\right)^2 + K\left(\phi_1-\phi_2\right)^2\Bigg]\mathrm{d}\varphi \end{aligned} \tag{6.51}$$

and W is the work of the applied forces which can be written in the next form

$$W = \frac{1}{2}\left[\left\{ N\frac{\mathrm{d}u}{\mathrm{d}\varphi} + Su + M_1\phi_1 + M_2\phi_2 \right\}_0^\beta + \int_0^\beta \left(f_ru + f_\varphi\frac{\mathrm{d}u}{\mathrm{d}\varphi} + m_1\phi_1 + m_2\phi_2 \right)\mathrm{d}\varphi \right]. \tag{6.52}$$

6.3 Principle of minimum potential energy

Let $\widetilde{u} = \widetilde{u}(\varphi)$, $\widetilde{\phi}_1 = \widetilde{\phi}_1(\varphi)$ and $\widetilde{\phi}_2 = \widetilde{\phi}_2(\varphi)$ such functions which satisfy the geometric boundary conditions. The geometric boundary conditions refer to deflection and cross-sectional rotation. For this field we define the potential energy as [94, 98]

$$\Pi_L\left(\widetilde{u}, \widetilde{\phi}_1, \widetilde{\phi}_2\right) = U\left(\widetilde{u}, \widetilde{\phi}_1, \widetilde{\phi}_2\right) - \{\text{virtual work of the prescribed forces on } \widetilde{u},\ \widetilde{\phi}_1 \text{ and } \widetilde{\phi}_2\}. \tag{6.53}$$

It can be proven that according to the minimum property of potential energy [94, 98]

$$\Pi_L(u, \phi_1, \phi_2) \leq \Pi_L\left(\widetilde{u}, \widetilde{\phi}_1, \widetilde{\phi}_2\right), \tag{6.54}$$

where $u = u(\varphi)$, $\phi_1 = \phi_1(\varphi)$ and $\phi_2 = \phi_2(\varphi)$ are the solution of the considered equilibrium problem of layered composite beam with weak shear connection. Next, it will be proven that the equations of equilibrium and force boundary conditions are obtained from the principle of minimum of potential energy. Let $u = u(\varphi)$, $\phi_1 = \phi_1(\varphi)$, $\phi_2 = \phi_2(\varphi)$ be the solution of the considered equilibrium problem. The kinematically admissible radial displacement and cross-sectional rotations can be represented as

$$\widetilde{u} = u + \delta u,\ \ \widetilde{\phi}_1 = \phi_1 + \delta\phi_1,\ \ \widetilde{\phi}_2 = \phi_2 + \delta\phi_2. \tag{6.55}$$

Here, δu, $\delta\phi_1$ and $\delta\phi_2$ satisfy homogeneous kinematic boundary conditions where u, ϕ_1 or ϕ_2 are prescribed as a boundary condition. Assuming that all the boundary conditions are force boundary conditions, this means that $N(0)$, $N(\beta)$, $S(0)$, $S(\beta)$, $M_1(0)$, $M_1(\beta)$ and $M_2(0)$, $M_2(\beta)$ are prescribed. In this case

$$\begin{aligned}\Pi\left(\widetilde{u}, \widetilde{\phi}_1, \widetilde{\phi}_2\right) = \frac{1}{2}\int_0^\beta \Bigg[& \frac{AE_0}{R}\left(\frac{\mathrm{d}^2\widetilde{u}}{\mathrm{d}\varphi^2} + \widetilde{u}\right)^2 + 2A_1E_1\left(\frac{\mathrm{d}^2\widetilde{u}}{\mathrm{d}\varphi^2} + \widetilde{u}\right)\frac{\mathrm{d}\widetilde{\phi}_1}{\mathrm{d}\varphi} + \\ & + 2A_2E_2\left(\frac{\mathrm{d}^2\widetilde{u}}{\mathrm{d}\varphi^2} + \widetilde{u}\right)\frac{\mathrm{d}\widetilde{\phi}_2}{\mathrm{d}\varphi} + r_1A_1E_1\left(\frac{\mathrm{d}\widetilde{\phi}_1}{\mathrm{d}\varphi}\right)^2 + r_2A_2E_2\left(\frac{\mathrm{d}\widetilde{\phi}_2}{\mathrm{d}\varphi}\right)^2 + K\left(\widetilde{\phi}_1 - \widetilde{\phi}_2\right)^2\Bigg]\mathrm{d}\varphi - \\ & \int_0^\beta \left(f_r\widetilde{u} + f_\varphi\frac{\mathrm{d}\widetilde{u}}{\mathrm{d}\varphi} + m_1\widetilde{\phi}_1 + m_2\widetilde{\phi}_2\right)\mathrm{d}\varphi - \left\{\overline{N}\frac{\mathrm{d}\widetilde{u}}{\mathrm{d}\varphi} + \overline{S}\widetilde{u} + \overline{M}_1\widetilde{\phi}_1 + \overline{M}_2\widetilde{\phi}_2\right\}_0^\beta,\end{aligned} \tag{6.56}$$

where the quantities with over-bar are given. By a lengthy, but elementary computation which includes the application of the integration of parts for

$$\Delta\Pi_L = \Pi_L(u + \delta u, \phi_1 + \delta\phi_1, \phi_2 + \delta\phi_2) - \Pi_L(u, \phi_1, \phi_2) \tag{6.57}$$

the next result can be derived

$$\Delta\Pi_L = \delta\Pi + U(\delta u, \delta\phi_1, \delta\phi_2), \tag{6.58}$$

where

$$\begin{aligned}\delta\Pi = \int_0^\beta \Bigg[& \left(N + \frac{\mathrm{d}^2N}{\mathrm{d}\varphi^2} - f_r + \frac{\mathrm{d}f_\varphi}{\mathrm{d}\varphi}\right)\delta u - \left(\frac{\mathrm{d}M_1}{\mathrm{d}\varphi} + m_1 - q(\phi_1 - \phi_2)\right)\delta\phi_1 - \\ & - \left(\frac{\mathrm{d}M_2}{\mathrm{d}\varphi} + m_2 + q(\phi_1 - \phi_2)\right)\delta\phi_2\Bigg]\mathrm{d}\varphi + \Bigg\{\left(N - \overline{N}\right)\frac{\mathrm{d}}{\mathrm{d}\varphi}\delta u - \\ & - \left(\frac{\mathrm{d}N}{\mathrm{d}\varphi} + f_\varphi + \overline{S}\right)\delta u + \left(M_1 - \overline{M}_1\right)\delta\phi_1 + \left(M_2 - \overline{M}_2\right)\delta\phi_2\Bigg\}_0^\beta.\end{aligned} \tag{6.59}$$

For admissible variation of u, ϕ_1, ϕ_2, which are δu, $\delta\phi_1$ and $\delta\phi_2$ are arbitrary except where the kinematic boundary conditions are specified. Since with arbitrary admissible variation of u, ϕ_1, ϕ_2

$$\Delta\Pi_L \geq 0 \tag{6.60}$$

according to the principle of minimum of potential energy. From Eq. (6.58) and inequality relation (6.60) and

$$U\left(\delta u, \delta\phi_1, \delta\phi_2\right) \geq 0 \tag{6.61}$$

we obtian

$$\delta\Pi = 0. \tag{6.62}$$

A detailed form of Eq. (6.62), which can be derived by means of the fundamental lemma of calculus of variation [99] gives the equations of equilibrium

$$\frac{\mathrm{d}^2 N}{\mathrm{d}\varphi^2} + N - f_r + \frac{\mathrm{d}f_\varphi}{\mathrm{d}\varphi} = 0, \quad 0 < \varphi < \beta, \tag{6.63}$$

$$\frac{\mathrm{d}M_1}{\mathrm{d}\varphi} + m_1 - q\left(\phi_1 - \phi_2\right) = 0, \quad 0 < \varphi < \beta, \tag{6.64}$$

$$\frac{\mathrm{d}M_2}{\mathrm{d}\varphi} + m_2 + q\left(\phi_1 - \phi_2\right) = 0, \quad 0 < \varphi < \beta, \tag{6.65}$$

and boundary conditions

$$N - \overline{N} = 0 \text{ for } \varphi = 0 \text{ and } \varphi = \beta, \tag{6.66}$$

$$\frac{\mathrm{d}N}{\mathrm{d}\varphi} + f_\varphi + \overline{S} = 0 \text{ for } \varphi = 0 \text{ and } \varphi = \beta, \tag{6.67}$$

$$M_1 - \overline{M}_1 = 0 \text{ for } \varphi = 0 \text{ and } \varphi = \beta, \tag{6.68}$$

$$M_2 - \overline{M}_2 = 0 \text{ for } \varphi = 0 \text{ and } \varphi = \beta, \tag{6.69}$$

We note, Eq. (6.63) is obtained from Eqs. (6.22), (6.23) with the elimination of $S = S\left(\varphi\right)$ and the validity of boundary condition (6.67) follows from Eq. (6.22). In Eqs. (6.63–6.65) N, M_1, M_2, q are given by Eqs. (6.26), (6.37), (6.41) in terms of u, ϕ_1 and ϕ_2.

We have also investigated curved composite beams with interlayer slip in **(3)**. In that paper the curved composite beam at one of the end cross-sections is fixed and the other end cross-section is subjected by a concentrated radial load. The study gives solutions for radial displacements, slips and stresses.

6.4 Numerical examples

6.4.1 A curved composite beam with uniformly distributed radial load

Both ends of curved two-layered composite beam with flexible shear connection are radially guided and loaded by uniformly distributed radial forces as shown in Fig. 6.4. The applied radial load is expressed as

$$f_r\left(\varphi\right) = -f\left[H\left(\varphi - \frac{\beta}{2} + \frac{\Theta}{2}\right) - H\left(\varphi - \frac{\beta}{2} - \frac{\Theta}{2}\right)\right], \tag{6.70}$$

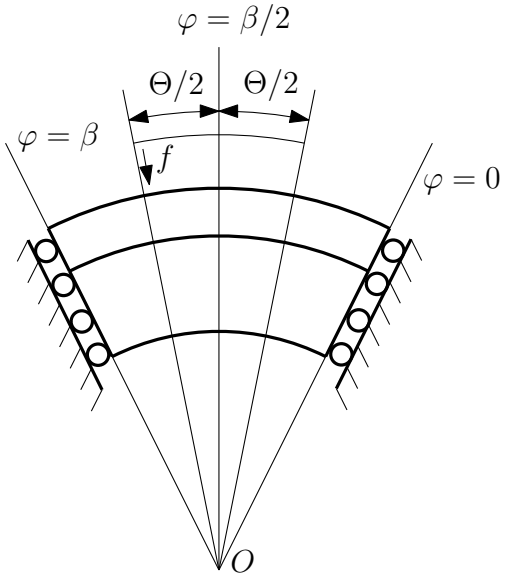

Figure 6.4. Uniformly loaded curved composite beam.

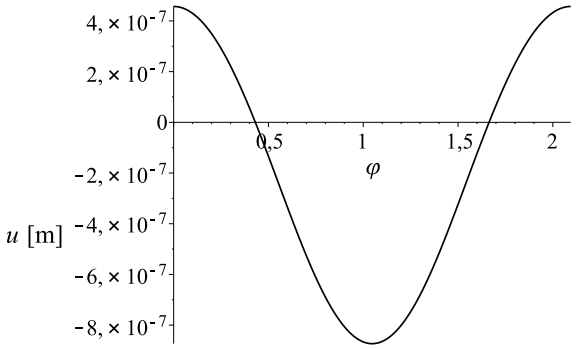

Figure 6.5. The graph of the radial displacement.

where

$$0 < \Theta \leq \beta \tag{6.71}$$

and $H = H(\varphi)$ is the Heaviside function. In this problem the boundary conditions are as follows

$$\phi_1(0) = \phi_1(\beta) = \phi_2(0) = \phi_2(\beta) = 0, \tag{6.72}$$

$$S(0) = S(\beta) = 0. \tag{6.73}$$

The minimum of the potential energy is obtained by the application of Ritz method. Assumed form of the solution is

$$u(\varphi) = u_0 + \sum_{p=1}^{\infty} u_p \cos\frac{p\pi}{\beta}\varphi, \tag{6.74}$$

$$\phi_1(\varphi) = \sum_{p=1}^{\infty} \phi_{1p} \sin\frac{p\pi}{\beta}\varphi,\ \phi_2(\varphi) = \sum_{p=1}^{\infty} \phi_{2p} \sin\frac{p\pi}{\beta}\varphi. \tag{6.75}$$

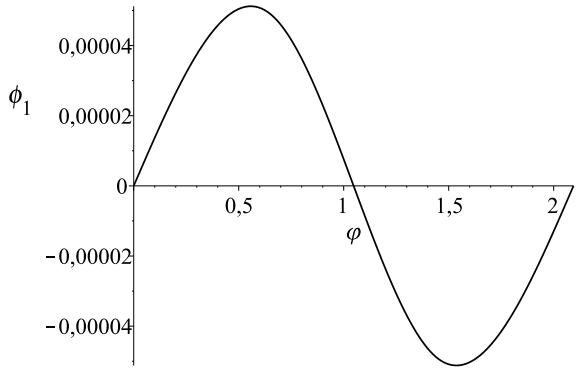

Figure 6.6. The graph of $\phi_1 = \phi_1(\varphi)$.

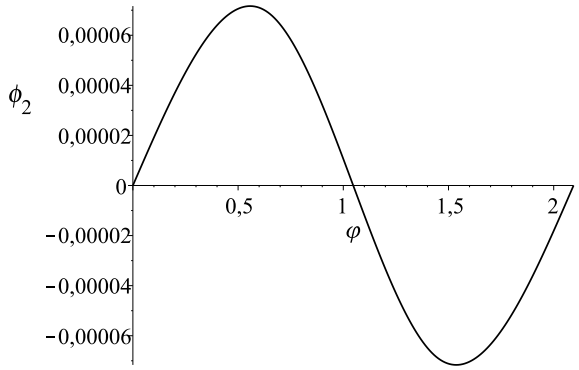

Figure 6.7. The graph of $\phi_2 = \phi_2(\varphi)$.

With arbitrary ϕ_{1p} $(i = 1, 2;\ p = 1, 2, \ldots)$ the cross-sectional rotations given by Eq. (6.75) satisfy the geometric boundary conditions formulated in Eq. (6.72). Substitution of Eqs. (6.74), (6.75) into the expression of potential energy we obtain that

$$\begin{aligned}\Pi_L(u_0, u_p, \phi_{1p}, \phi_{2p}; p = 1\ldots) = \frac{1}{2}\frac{AE_0}{R}\beta u_0^2 + \frac{\beta}{4}\sum_{p=1}^{\infty}\left\{\frac{AE_0}{R}\left(1-\left(\frac{p\pi}{\beta}\right)^2\right)^2 u_p^2 + \right.\\ +2A_1E_1\left(1-\left(\frac{p\pi}{\beta}\right)^2\right)\frac{p\pi}{\beta}u_p\phi_{1p} + 2A_2E_2\left(1-\left(\frac{p\pi}{\beta}\right)^2\right)\frac{p\pi}{\beta}u_p\phi_{2p} + \\ \left.+r_1A_1E_1\left(\frac{p\pi}{\beta}\right)^2\phi_{1p}^2 + r_2A_2E_2\left(\frac{p\pi}{\beta}\right)^2\phi_{2p}^2 + K(\phi_{1p}-\phi_{2p})^2\right\} + fu_0\Theta + \\ +\sum_{p=1}^{\infty} fu_p\frac{\beta}{p\pi}\left[\sin\frac{p\pi}{2\beta}(\beta+\Theta) - \sin\frac{p\pi}{2\beta}(\beta-\Theta)\right].\end{aligned} \tag{6.76}$$

The necessary condition of minimum of Π_L as a function of u_0, u_p, ϕ_{1p}, ϕ_{2p} $(p = 1, 2, \ldots)$ can be formulated as

$$\frac{\partial\Pi_L}{\partial u_0} = 0, \quad \frac{\partial\Pi_L}{\partial u_p} = 0, \quad \frac{\partial\Pi_L}{\partial\phi_{1p}} = 0, \quad \frac{\partial\Pi_L}{\partial\phi_{2p}} = 0, \quad (p = 1, 2\ldots). \tag{6.77}$$

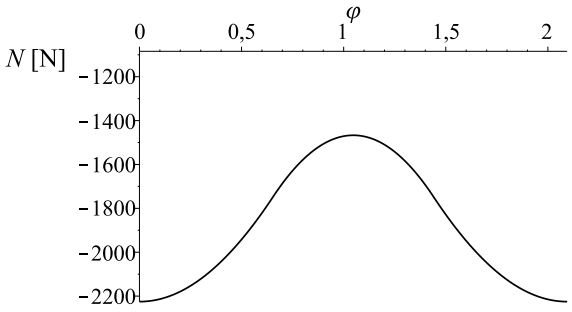

Figure 6.8. The plot of the normal force function.

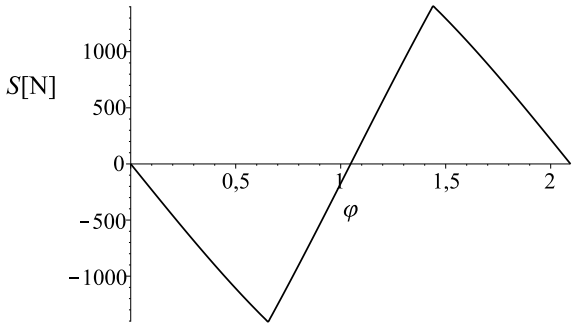

Figure 6.9. The plot of the shear force function.

From Eq. (6.77) it follows that

$$u_0 = -f\frac{R}{AE_0}\frac{\Theta}{\beta} \tag{6.78}$$

and u_p, ϕ_{1p}, ϕ_{2p} are the solution of the following system of linear equations

$$\mathbf{M}_p\mathbf{x}_p = \mathbf{b}_p, \quad \mathbf{M}_p = [m_{pij}], \quad \mathbf{x}_p = [u_p, \phi_{1p}, \phi_{2p}]^T, \tag{6.79}$$

$$\mathbf{b}_p = [b_p, 0, 0]^T, \tag{6.80}$$

where

$$\begin{gathered} m_{p11} = \frac{AE_0}{R}\left(1-\left(\frac{p\pi}{\beta}\right)^2\right)^2, \quad m_{p12} = A_1E_1\frac{p\pi}{\beta}\left(1-\left(\frac{p\pi}{\beta}\right)^2\right), \\ m_{p13} = A_2E_2\frac{p\pi}{\beta}\left(1-\left(\frac{p\pi}{\beta}\right)^2\right), \end{gathered} \tag{6.81}$$

$$m_{p21} = m_{p12}, \quad m_{p22} = r_1A_1E_1\left(\frac{p\pi}{\beta}\right)^2 + K, \quad m_{p23} = -K, \tag{6.82}$$

$$m_{p31} = m_{p13}, \quad m_{p32} = m_{p23}, \quad m_{p33} = r_2A_2E_2\left(\frac{p\pi}{\beta}\right)^2 + K, \tag{6.83}$$

$$b_p = -\frac{2f}{p\pi}\left[\sin\frac{p\pi}{2\beta}(\beta+\Theta) - \sin\frac{p\pi}{2\beta}(\beta-\Theta)\right]. \tag{6.84}$$

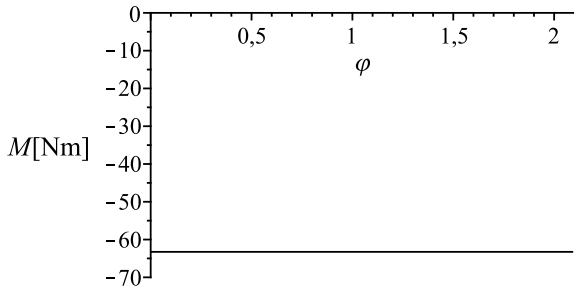

Figure 6.10. The graph of $M = M(\varphi)$.

The next data are used in Example 6.4.1: $\beta = \frac{2\pi}{3}$, $r_a = 0.04\,\mathrm{m}$, $r_b = 0.02\,\mathrm{m}$, $r_c = 0.03\,\mathrm{m}$, $b_1 = b_2 = b = 0.03\,\mathrm{m}$, $E_1 = 10^{11}\,\mathrm{Pa}$, $E_2 = 8 \times 10^{10}\,\mathrm{Pa}$, $k = 80 \times 10^{8}\,\mathrm{Pa/m^3}$, $f = 5000\,\mathrm{N}$, $\Theta = \frac{\pi}{4}$. Figs. 6.5, 6.6 and 6.7 show the graphs of deflection and cross-sectional rotation functions. The normal force as a function of φ is shown in Fig. 6.8. The graphs of shear force function $S = S(\varphi)$ and bending moment function $M = M(\varphi)$ are illustrated in Figs. 6.9 and 6.10.

6.4.2 A curved composite beam subjected to uniformly distributed radial load on its total length

In this example we consider the case $\beta = \Theta$ which is shown in Fig. 6.11. Here, the same data are used as in Example 6.4.1 except Θ $\left(\Theta = \frac{2\pi}{3}\right)$. In this case we have from Eq. (6.84)

$$b_p = 0,\ (p = 1, 2, \ldots). \tag{6.85}$$

The solution of this problem is as follows

$$u = -f\frac{R}{AE_0}, \quad \phi_1(\varphi) = 0, \quad \phi_2(\varphi) = 0, \tag{6.86}$$

$$N = -f, \quad S = 0, \quad M = -Rf. \tag{6.87}$$

6.4.3 Checking the previous examples

In this example we check the exactness of solution of Examples 6.4.1 and 6.4.2 by the application of Rayleigh-Betti reciprocity relation. The first equilibrium state of the curved composite beam with deformable shear connection is shown in Fig. 6.4 and the second equilibrium state is illustrated in Fig. 6.11. In this example

$$W_{12} = -\int_0^{\beta} f_r(\varphi)\, f\frac{R}{AE_0}\mathrm{d}\varphi, \tag{6.88}$$

where $f_r = f_r(\varphi)$ is given by Eq. (6.70), and

$$W_{21} = \int_0^{\beta} (-f)\, u(\varphi)\, \mathrm{d}\varphi, \tag{6.89}$$

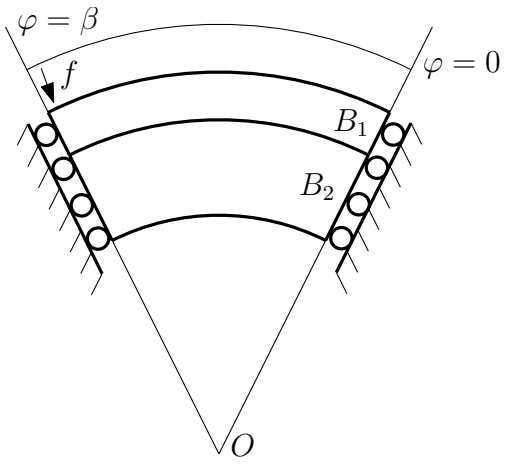

Figure 6.11. The case of $\Theta = \beta$.

where $u = u(\varphi)$ is given by Eq. (6.74). A simple computation gives

$$\begin{aligned} W_{12} &= 0.00204454608\,\mathrm{Nm}, \\ W_{21} &= 0.00204454606\,\mathrm{Nm}. \end{aligned} \tag{6.90}$$

6.4.4 A curved composite beam with concentrated radial load

This example deals with the case of concentrated radial load applied at $\varphi = \frac{\beta}{2}$ as shown in Fig. 6.12. The Ritz type solution is based on the assumed forms of radial displacement and cross-sectional rotations given by Eqs. (6.74) and (6.75). The virtual work of the concentrated radial force on the radial displacement (6.74) can be computed as

$$W_F = (-F)\left[u_0 + \sum_{p=1}^{\infty} u_p \cos\frac{p\pi}{2}\right]. \tag{6.91}$$

From the principle of minimum potential energy by the use of expression W_F we obtain that

$$u_0 = -F\frac{R}{\beta E_0 A}, \quad b_p = -\frac{2F}{\beta}\cos\frac{p\pi}{2}, \quad (p = 1, 2, \ldots). \tag{6.92}$$

Let $F = 5000\,\mathrm{N}$ be. The same geometrical and material properties are used to solve Eq. (6.79) with the new value of b_p $(p = 1, 2, \ldots)$. The results of the computations are shown in Figs. 6.13–6.18. The radial displacement and cross-sectional rotations as functions of φ are shown in Figs. 6.13 6.14 and 6.15. The graphs of normal force, shear force and bending moment are illustrated in Figs. 6.16, 6.17 and 6.18. Here we note, that the shear force function has a jump at $\varphi = \frac{\beta}{2}$ (Fig. 6.17). The small oscillation of $S = S(\varphi)$ at $\varphi = \frac{\beta}{2}$ follows from its representation by „truncated" Fourier series.

6.4.5 Checking the results of the curved beam with concentrated radial load

By the use of Rayleigh-Betti type reciprocity relation we check the accuracy of the solution obtained for concentrated radial load. The first equilibrium state of the curved composite

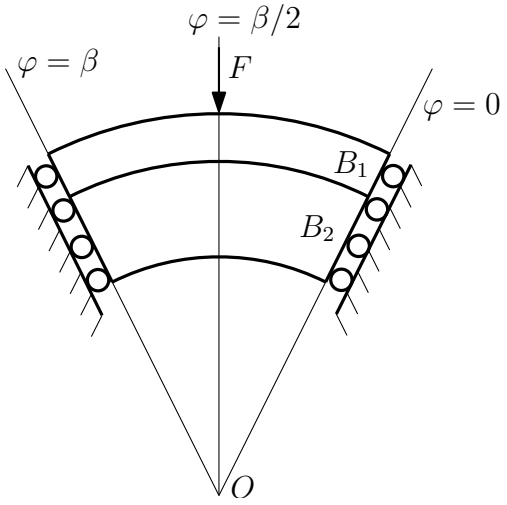

Figure 6.12. The case of concentrated radial load.

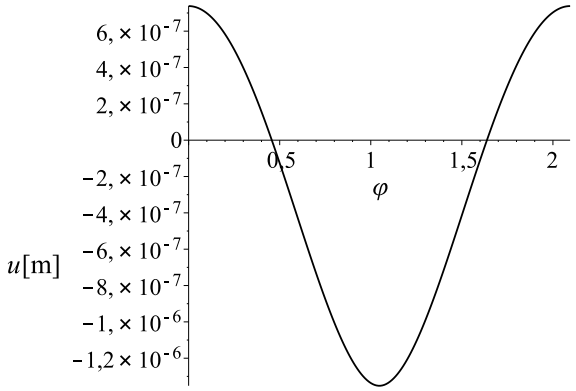

Figure 6.13. The plot of the radial displacement.

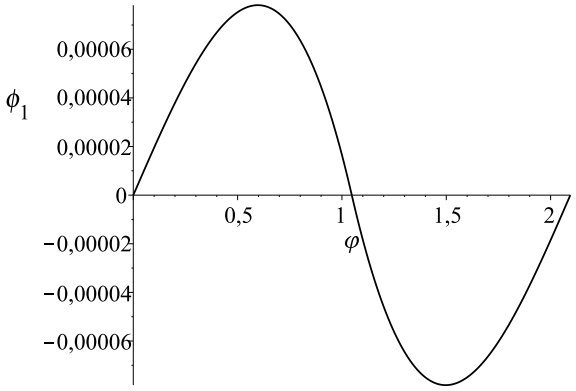

Figure 6.14. The plot of $\phi_1 = \phi_1(\varphi)$.

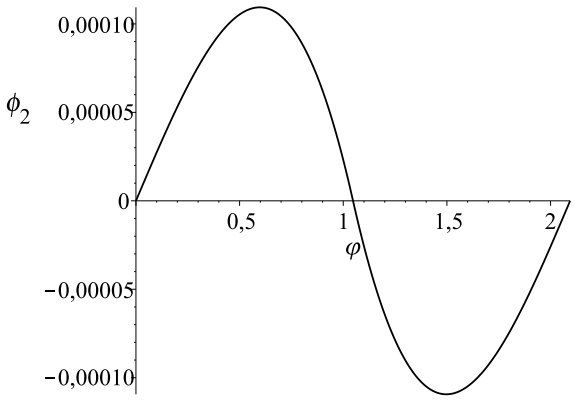

Figure 6.15. The plot of $\phi_2 = \phi_2(\varphi)$.

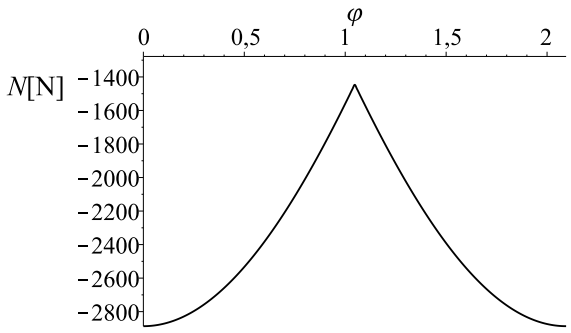

Figure 6.16. The graph of normal force function.

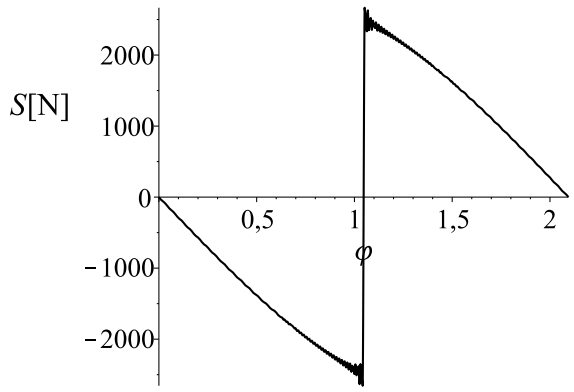

Figure 6.17. The graph of the shear force function.

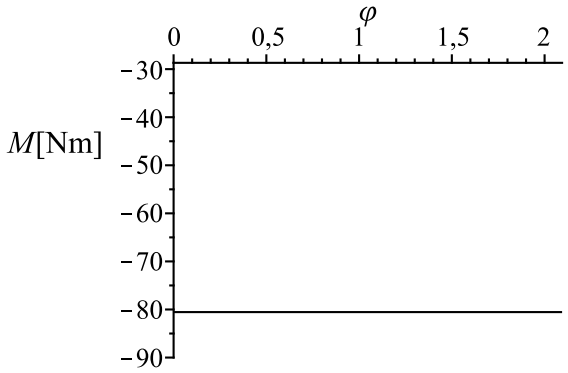

Figure 6.18. The graph of $M = M(\varphi)$.

beam is shown in Fig. 6.12 and the second equilibrium state is illustrated in Fig. 6.11. For these equilibrium states we have

$$W_{12} = (-F)(-f)\frac{R}{AE_0}, \tag{6.93}$$

$$W_{21} = (-f)\int_0^{\beta} u(\varphi)\,\mathrm{d}\varphi, \tag{6.94}$$

where $u = u(\varphi)$ is obtained in Example 6.4.4. A simple computation gives

$$\begin{aligned} W_{12} &= 0.002603196319\,\mathrm{Nm}, \\ W_{21} &= 0.002603196318\,\mathrm{Nm} \end{aligned} \tag{6.95}$$

according to the proven Rayleigh-Betti type reciprocity relation.

6.4.6 A curved composite beam uniformly loaded by tangential forces

Figure 6.19 shows a two-layered composite beam with deformable shear connection loaded by uniform tangential load on its outer cylindrical boundary. The geometrical and material properties of the considered curved beam is the same as in Example 6.4.1. In paper **(3)** the solution of two-layered composite beam with weak shear connection for radial concentrated load applied at its one of the end cross-section was derived (Fig. 6.20). The first equilibrium state of the composite curved beam is shown in Fig. 6.19 and the second equilibrium state of the same curved composite beam is given in Fig. 6.20. Our aim is to obtain the deflection of the end cross-section of curved beam loaded by uniformly distributed tangential forces (Fig. 6.19). According to the Rayleigh-Betti theorem we can write that

$$\begin{aligned} W_{12} &= f\int_0^{\beta} v''(r_a,\varphi)\,\mathrm{d}\varphi = \\ &= f\left[r_a\int_0^{\beta}\phi_1''(\varphi)\,\mathrm{d}\varphi + u''(\beta)\right], \end{aligned} \tag{6.96}$$

$$W_{21} = -Fu'(\beta). \tag{6.97}$$

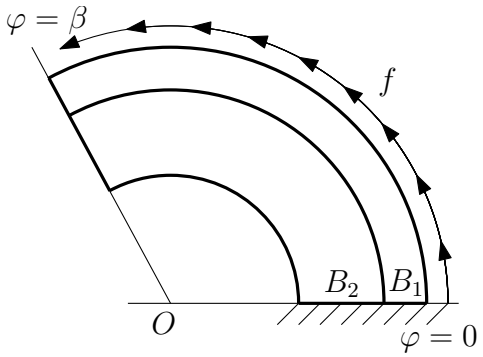

Figure 6.19. Two-layered curved composite beam uniformly loaded by tangential forces.

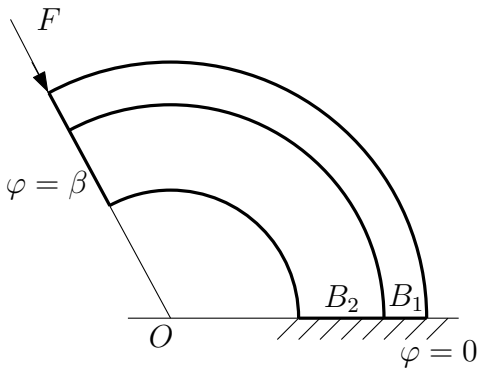

Figure 6.20. Two-layered curved composite beam with concentrated radial load.

From Eqs. (6.96) and (6.97) it follows that

$$\begin{aligned} u'(\beta) &= -\frac{f}{F}\int_0^{\beta} v''(r_a,\varphi)\,\mathrm{d}\varphi = \\ &= -\frac{f}{F}\left[r_a\int_0^{\beta}\phi_1''(\varphi)\,\mathrm{d}\varphi + u''(\beta)\right]. \end{aligned} \tag{6.98}$$

Let

$$f = 1500\,\mathrm{N}, \quad F = 1000\,\mathrm{N} \tag{6.99}$$

be in Eq. (6.98). Other data are given in Example 6.4.1. By these data using the solution presented for $\phi_1'' = \phi_1''(\varphi)$ and $u'' = u''(\varphi)$ in **(3)** we get

$$u'(\beta) = -0.0000188033149\,\mathrm{m}. \tag{6.100}$$

Summary of the novel results

In this thesis I have dealt with static and dynamic problems of layered composite beams having not perfect connection. The overview of the literature represents that a lot of investigators published their works in connection with this topic in the last 60-70 years. The importance of the topic is well illustrated by the fact that the scientists research the behaviour of the composite beams with weak shear connection nowadays as well. According to the publications available in the open literature I have been able to draw up my objectives and in the following I am going to summarize the novel results of this thesis.

Statement 1.

I have derived a novel analytical solution to describe the static behaviour of composite beams with interlayer slip. The governing equation of the problem is written in terms of the slip and the cross-sectional shear force function. The fundamental solutions for seven different initial conditions have been deduced by means of both Euler-Bernoulli and Timoshenko beam theory. With these functions the solution of the governing equation have become the solution of a linear system of equation. I have presented the methods in numerical examples with different boundary conditions in order to compare the results with ones from other publications and from my FEM analysis. The results were in good agreement.

Statement 2.

I have deduced a new analytical solution for static problem of composite beams with interlayer slip loaded by mechanical and thermal load as uniform temperature change. I have provided the governing equation of the problem and have solved it for different boundary conditions. The thermal stresses have been derived as well. In this case numerical examples also represented the developed method with and without thermal loading. The same results have been obtained from this method without thermal load as from the fundamental solutions.

Statement 3.

Two new analytical method have been formulated for the determination of the buckling load of composite beams with weak shear connection. In the first case closed form solution were derived from a variational method for two composite columns with different boundary conditions. In the second case I have obtained the same closed forms from

the equilibrium method for the same two composite columns. Two numerical examples showed the application of the forms which were in good agreement with the results come from the literature. I have also provided the function of the buckling load in terms of the slip modulus for both columns.

Statement 4.

A new analytical solution has been described in connection with the free flexural vibration of composite beams with weak shear connection. For the analysis I have introduced the d'Alembert forces. According to the obtained equations of motion three closed form solutions were provided for the eigenfrequencies of the considered composite beam. The first solution counts with the effect of the rotary and axial inertia resulting three various eigenfrequencies, whilst the second one neglected the rotary inertia, the third one eliminated all the rotary and the axial inertia. The latter two resulted one eigenfrequency.

Statement 5.

A new analytical method has been elaborated for static analysis of uniformly curved composite beams with interlayer slip. Based on the Rayleigh-Betti type reciprocity relation I have deduced the potential energy of the considered uniformly curved beam. By means of the principle of minimum potential energy I have also determined the equilibrium equations and the dynamic boundary conditions. Several numerical examples represented the applications of the potential energy combining with the Ritz method and for the checking of this method the Rayleigh-Betti type reciprocity relation were used. These results were in good agreement.

Összefoglalás

A disszertációban réteges szerkezetű, részlegesen kapcsolt kompozit rudak statikai és dinamikai problémáival foglalkoztam. Az irodalmi áttekintés is mutatja, hogy az elmúlt 60-70 évben rengeteg kutató publikálta eredményeit részlegesen kapcsolt kompozit rudakkal kapcsolatban, és a téma fontosságát jól illusztrálja, hogy napjainkban is születnek publikációk a témában. Az irodalmi áttekintés és célkitűzéseim alapján a következőkben összefoglalom az új tudományos eredményeket.

1. tézis

Új analitikus megoldást vezettem le részlegesen kapcsolt kompozit rudak statikai viselkedésének leírására. A probléma alapegyenletét a csúszás- és a nyíróerőfüggvény segítségével írtam fel. Mind az Euler-Bernoulli, mind a Timoshenko rúdmodell segítségével származtattam az ún. alapmegoldásokat hét különböző kezdeti feltételre. Az alapmegoldások segítségével az alapegyenlet megoldása egy lineáris egyenletrendszer megoldásává válik. Néhány numerikus példán keresztül bemutattam a módszer alkalmazását, az eredményeket pedig összevetettem más publikációkból, illetve az általam elvégzett végeselemes szimulációból származó eredményekkel, melyek jó egyezést mutattak.

2. tézis

Egy új analitikus módszert írtam fel részlegesen kapcsolt kompozit rudak statikai viselkedésének meghatározására, amennyiben a rúdra egyaránt hat mechanikai és hőterhelés amely egyenletes hőmérsékletváltozást jelent. Megadtam a probléma alapegyenletét és annak megoldását is különböző peremfeltételi előírásokra. A hő okozta feszültségek számítására szolgáló összefüggéseket is származtattam. Ebben az esetben is numerikus példákban mutattam be a módszer alkalmazását hőterheléssel és anélkül. A hőterhelés nélküli eset ugyanazokat a megoldásokat szolgáltatta, amelyeket az alapmegoldások módszere is.

3. tézis

Két új analitikus módszert vezettem le részlegesen kapcsolt kompozit rudak stabilitási vizsgálatával kapcsolatban. Az első esetben két különböző peremfeltételekkel rendelkező rúdra is zárt formulát állítottam elő a kritikus teher számítására, melyeket variációs módszer segítségével vezettem le. A második esetben ugyanezen rudakra ugyanazokat a zárt formulákat kaptam egyensúlyi módszer segítségével. Két számpélda illusztrálja a formulák alkalmazását, az így kapott eredmények pedig jó egyezést mutatnak az irodalomban

található eredményekkel. Mindkét rúd esetében megadtam a kritikus terhelés csúszási modulustól való függését is.

4. tézis

Egy új analitikus módszert írtam fel részlegesen kapcsolt kompozit rudak szabad rezgéseinek vizsgálatára. Bevezettem a d'Alembert féle inerciaerőket. A nyert mozgásegyenletekből három esetre is zárt formula vezethető le a tekintett kompozit rudak sajátfrekvenciáinak meghatározására. Az első esetben figyelembe vettem a forgási és az axiális inercia hatását is, mely 3 különböző sajátfrekvenciát eredményezett. A második esetben a forgási inerciát, míg a harmadik esetben mind a forgási, mind pedig az axiális inerciát elhanyagoltam. Ez utóbbi két eset egy-egy sajátfrekvenciát eredményezett.

5. tézis

Egy új analitikus módszert vezettem le körív középvonalú kompozit rudak statikai viselkedésének leírására. A Rayleigh-Betti féle felcserélhetőségi tételt felhasználva felírtam a körív középvonalú kompozit rúdra érvényes potenciális energiát. A potenciális energia minimuma elvének segítségével levezettem az egyensúlyi egyenleteket és a dinamikai peremfeltételeket. Néhány példán keresztül bemutattam a potenciális energia minimuma elvén alapuló megoldást kombinálva a Ritz-módszerrel és az eredményeket a Rayleigh-Betti-féle felcserélhetőségi tétel segítségével ellenőriztem. Az eredmények jó egyezést mutattak.

List of Figures

List of Tables

Publications

The following publications were made in the topic of the thesis.

Articles in journals

(1) Á. J. Lengyel and I. Ecsedi. An analytical solution for two-layered composite beams with imperfect shear interaction, *International Review of Mechanical Engineering*, 10(7):508–517, 2016.

(2) Á. J. Lengyel and I. Ecsedi. Analysis of bimetallic beam with weak shear connection. *Acta Technica Corviniensis – Bulletin of Engineering*, 9(3):85–90, 2016.

(3) Á. J. Lengyel and I. Ecsedi. Curved composite beam with interlayer slip loaded by radial load. *Curved and Layered Structures*, 2(1):50–58, 2015.

(4) Á. J. Lengyel and I. Ecsedi. Energy methods for curved composite beams with partial shear interaction. *Curved and Layered Structures*, 2(1):351–361, 2015.

(5) Á. J. Lengyel and I. Ecsedi. Static and dynamic analyses of composite beams with interlayer slip. *Journal of Computational and Applied Mechanics*, 10(1):25–40, 2015.

(6) Á. J. Lengyel and I. Ecsedi. An equilibrium problem of curved composite beam with interlayer slip. *Acta Technica Corviniensis – Bulletin of Engineering*, 8(2):57–60, 2015.

(7) Á. J. Lengyel and I. Ecsedi. Kétrétegű nem tökéletesen kapcsolt kompozit rudak rezgéseinek vizsgálata (Vibration analysis of two-layered composite beams with partial shear interaction, in Hungarian). *GÉP* LXV(1):34–38, 2014.

(8) Á. J. Lengyel and I. Ecsedi. Egy módszer a részlegesen kapcsolt kompozit rudak lehajlásának és igénybevételeinek számítására (A method for computation of deflection and inner forces of composite beams with partial shear interaction, in Hungarian), *Multidiszciplináris Tudományok: A Miskolci Egyetem Közleménye* 3(1):83–96, 2013.

(9) Á. J. Lengyel and I. Ecsedi. Normál és csúsztató feszültségek számítása részlegesen kapcsolt rétegezett kompozit rudakban (Computations of normal and shear stresses in composite beams with partial shear interaction, in Hungarian) *GÉP* LXIV(5):22–27, 2013.

(10) Á. J. Lengyel and I. Ecsedi. Analitikus módszer részlegesen kapcsolt, rétegezett kompozit rudak szilárdságtani feladatainak megoldására (An analytical method

for static problems of composite beams with partial shear interaction, in Hungarian), *Multidiszciplináris Tudományok: A Miskolci Egyetem Közleménye* 2(1):89–102. 2012.

Conference papers

(11) Á. J. Lengyel and I. Ecsedi. Complementary energy method for curved composite beams. *MultiScience – XXX. microCAD International Multidisciplinary Scientific Conference*, Section: D5 - Technical Mechanics, University of Miskolc, 21.04.2016–22.04.2016

(12) Á. J. Lengyel and I. Ecsedi. Kompozit rudak vizsgálata energia módszer segítségével (Analysis of composite beams by means of energy method, in Hungarian), *XII. Magyar Mechanikai Konferencia (XII. Hungarian Conference of Mechanics)*, Section: 12. Tartószerkezetek II., University of Miskolc, 25.08.2015–27.08.2015, paper 279.

(13) Á. J. Lengyel and I. Ecsedi. Composite beam with weak shear connection subjected to thermal load, *MultiScience – XXIX. microCAD International Multidisciplinary Scientific Conference*, Section: D2 – Mechanical engineering design and technologies, numerical modelling and laboratory measurements, University of Miskolc, 09.04.2015–10.04.2015, paper D2-3

(14) Á. J. Lengyel and I. Ecsedi. Elastic Stability of Columns with Weak Shear Connection, *MultiScience – XXVIII. microCAD International Multidisciplinary Scientific Conference*, Section: D4 – Mechanical modelling and finite element simulation, University of Miskolc, 10.04.2014–11.04.2014, paper D-37

(15) Á. J. Lengyel and I. Ecsedi. Stability analysis of composite beams with weak shear connection by a variational method, *Tavaszi Szél Konferencia 2014. (Spring Wind Conference 2014)*, Műszaki szekció – Analízis, modellezés és szimuláció (Technical section – Analysis, modelling and simulation), University of Debrecen, 21.03.2014–23.03.2014, p.: 423–431

(16) Á. J. Lengyel and I. Ecsedi. Statics of the Composite Beams having not Perfect Connection on Its Total Length, *XXVII. microCAD International Scientific Conference*, Section: O – Applied Mechanics, University of Miskolc, 21.03.2013–22.03.2013, paper O-8

(17) Á. J. Lengyel and I. Ecsedi. Vibrations of Composite Beams with Interlayer Slip, *8th International Conference of PhD Students*, Section: D – Engineering Science, University of Miskolc, 05.08.2012–11.08.2012, paper D-10

(18) Á. J. Lengyel and I. Ecsedi. Kompozit rudak lineáris analízise Ritz-módszer segítségével (Linear analysis of composite beams with weak shear connection by means of Ritz method), *OGÉT 2012: XX. Nemzetközi Gépészeti Találkozó*. Cluj-Napoca, Romania, 19.04.2012–22.04.2012 p.: 266–269

(19) Á. J. Lengyel and I. Ecsedi. Application of the Ritz method for the linear analysis of composite beams with interlayer slip, *XXVI. microCAD International Scientific Conference*, Section: O – Applied Mechanics, University of Miskolc 29.03.2012–30.03.2012, paper O-10

Bibliography

[1] N. M. Newmark, C. P. Siess, and I. M. Viest. Test and analyis of composite beams with incomplete interaction. *Proceedings of the Society of Experimental Stress Analysis*, 9(1):75–92, 1951.

[2] H. Granholm. *On composite beams and columns with particular regard to nailed timber structures.* Transaction No. 88, Chalmers Technical University, Göteborg, Sweden, 1949. (in Swedish).

[3] F. Stüssi. Zusammengesetzte Vollwandträger. *IABSE Publications*, 8:249–269, 1947.

[4] J. R. Goodman and E. P. Popov. Layered beam systems with interlayer slip. *Journal of the Structural Division, Proceedings of the American Society of Civil Engineers*, 94(11):2535–2548, 1968.

[5] A. O. Adekola. Partial interaction between elastically connected elements of a composite beam. *International Journal of Solids and Structures*, 4:1125–1135, 1968. doi: 10.1016/0020-7683(68)90027-9.

[6] H. Robinson and K. S. Naraine. Slip and uplift effects in composite beams. In *Proceedings of the Engineering Foundation Conference on Composite Construction (ASCE)*, pages 487–497, 1988.

[7] R. P. Johnson and I. N. Molenstra. Partial shear connection in composite beams for buildings. In *Proceedings of the Institution of Civil Engineers, Part 2*, volume 91, pages 679–704, 1991. doi: 10.1680/iicep.1991.17485.

[8] E. Cosenza and S. Mazzolani. Linear-elastic analysis of composite beams with partial shear interaction. In *Proceedings of the First Italian Workshop on Composite Structures, University of Trento*, 1993. (in Italian).

[9] U. A. Girhammar and V. K. A. Gopu. Composite beam-columns with interlayer slip – exact analysis. *Journal of Structural Engineering*, 119(4):1265–1282, 1993. doi: 10.1061/(ASCE)0733-9445(1993)119:4(1265).

[10] I. Ecsedi and A. Baksa. Static analysis of composite beams with weak shear connection. *Applied Mathematical Modelling*, 35(4):1739–1750, 2011. doi: 10.1016/j.apm.2010.10.006.

[11] U. A. Girhammar and D. Pan. Dynamic analysis of composite members with interlayer slip. *International Journal of Solids and Structures*, 30(6):797–823, 1993. doi: 10.1016/0020-7683(93)90041-5.

[12] D. R. Plum and M. R. Horne. Analysis of continuous composite beams with partial interaction. In *Proceedings of the Institution of Civil Engineers, Part 2*, volume 59, pages 625–643, 1975. doi: 10.1680/iicep.1975.3631.

[13] N. A. Jasim. Computation of deflections for continuous composite beams with partial shear interaction. In *Proceedings of the Institution of Civil Engineers: Structures and Buildings, Part 2*, volume 122, pages 347–354, 1997.

[14] N. A. Jasim and A. Atalla. Deflections of partially composite continuous beams: a simple approach. *Journal of Constructional Steel Research*, 49:291–301, 1999. doi: 10.1016/S0143-974X(98)00001-7.

[15] A. Dall'Asta and A. Zona. Non-linear analysis of composite beams by a displacement approach. In *Proceedings of the Fifth International Conference on Computational Structures Technology, Lueven (Belgium)*, pages 337–348, 2000.

[16] A. Zona. *Finite element modelling of composite beams.* PhD thesis, University of Ancona, Italy, 2003.

[17] G. Prathap and B. P. Naganarayanan. Stress oscillations and spurious load mechanisms in variationally inconsistent assumed strain formulations. *International Journal for Numerical Methods in Engineering*, 33(10):2181–2197, 1992. doi: 10.1002/nme.1620331011.

[18] A. Dall'Asta and A. Zona. Finite elements for the analysis of composite members with interlayer slip. In *Proceedings of the XVIII Italian Workshop on Steel (CTA), Venice (Italy)*, 2001.

[19] B. J. Daniels and M. Crisinel. Composite slab behavior and strength analysis. Part I: calculation procedure. *Journal of Structural Engineering, ASCE*, 119(1).

[20] Y. Arizumi, S. Hamada, and T. Kajita. Elastic-plastic analysis of composite beams with incomplete interaction by finite element method. *Computers and Structures*, 14 (5–6):453–462, 1981. doi: 10.1016/0045-7949(81)90065-1.

[21] A. Dall'Asta and A. Zona. Non-linear analysis of composite beams by a displacement approach. *Computers and Structures*, 80(27–30):2217–2228, 2002. doi: 10.1016/S0045-7949(02)00268-7.

[22] A. Dall'Asta, G. Leoni, and A. Zona. Some problems on the nonlinear analysis of composite beams by the finite element method. In *Proceedings of the XVII Italian Workshop on Steel (CTA), Naples (Italy)*, 1999.

[23] M. R. Salari, E. Spacone, P. B. Shing, and D. M Frangopol. Non-linear analysis of composite beams with deformable shear connectors. *Journal of Structural Engineering, ASCE*, 124(10):1148–1158, 1998. doi: 10.1061/(ASCE)0733-9445(1998)124:10(1148).

[24] M. R. Salari and E. Spacone. Finite element formulations of one-dimensional elements with bond-slip. *Engineering Structures*, 23(7):815–826, 2001. doi: 10.1016/S0141-0296(00)00094-8.

[25] A. Ayoub and F. C. Filippou. Mixed formulation of nonlinear steel-concrete composite beam element. *Journal of Structural Engineering, ASCE*, 126(3):371–381, 2000. doi: 10.1061/(ASCE)0733-9445(2000)126:3(371).

[26] A. Ayoub. A two-field mixed variational principle for partially connected composite beams. *Finite Elements in Analysis and Design*, 37(11):929–959, 2001. doi: 10.1016/S0168-874X(01)00076-2.

[27] A. Dall'Asta and A. Zona. Three-field mixed formulation for the non-linear analysis of composite beams with deformable shear connection. *Finite Elements in Analysis and Design*, 40(4):425–448, 2004. doi: 10.1016/S0168-874X(03)00071-4.

[28] C. Faella, V. Consalvo, and E. Nigro. An "exact" finite element model for the linear analysis of continuous composite beams with flexible shear connection. In *Proceedings of the XVIII Italian Workshop on Steel (CTA), Ancona (Italy)*, 1997. (In Italian).

[29] C. Faella, E. Martinelli, and E. Nigro. Steel and concrete composite beams with flexible shear connection: "exact" analytical expression of the stiffness matrix and applications. *Computers and Structures*, 80(11):1001–1009, 2002. doi: 10.1016/S0045-7949(02)00038-X.

[30] E. Cosenza and M. Pecce. Structural analysis of linear-elastic continuous composite beams with partial interaction. In *Proceedings of the XVI Italian Workshop on Steel (CTA), Ancona (Italy)*, 1997. (In Italian).

[31] P. Ansourian. Experiments on continuous composite beams. In *Proceedings of the Institution of Civil Engineers, Part 2*, volume 71, pages 25–51, 1982.

[32] J. C. Chapman and S. Balakrishnan. Experiments on composite beams. *The Structural Engineer*, 42(11):369–383, 1964.

[33] G. Fabbrocino, G. Manfredi, M. Pecce, and E. Cosenza. Nonlinear behaviour of composite beams in the hogging moment region: numerical study. In *Proceedings of the III Italian Workshop on Composite Construction, Ancona (Italy)*, 1998. (In Italian).

[34] G. Fabbrocino, G. Manfredi, E. Cosenza, and M. Pecce. Nonlinear behaviour of composite beams under negative moment: an experimental-theoretical comparison. In *Proceedings of the 2nd European Conference on Steel Structures EUROSTEEL '99, Prague (Czech Republic)*, 1999.

[35] R. P. Johnson and M. C. Hope-Gill. Applicability of simple plastic theory to continuous composite beams. In *Proceedings of the Institution of Civil Engineers, Part 2*, volume 91, pages 679–704, 1976.

[36] P. R. Barnard and R. P. Johnson. Plastic behaviour of continuous composite beams. In *Proceedings of the Institution of Civil Engineers*, volume 32, pages 180–197, 1965.

[37] L. C. P. Yam and J. C. Chapman. The inelastic behaviour of simply supported composite beams of steel and concrete. In *Proceedings of the Institution of Civil Engineers*, volume 41, pages 651–683, 1968.

[38] L. C. P. Yam and J. C. Chapman. The inelastic behaviour of continuous composite beams of steel and concrete. In *Proceedings of the Institution of Civil Engineers*, volume 53, pages 487–501, 1972.

[39] L. C. P. Yam. *Design of Composite Steel-Concrete Structures*. Surrey University Press, 1981.

[40] J. M. Rotter and P. Ansourian. Cross-section behaviour and ductility in composite beams. In *Proceedings of the Institution of Civil Engineers, Part 2*, volume 67, pages 453–474, 1979.

[41] J. M. Rotter and P. Ansourian. Design of ductile steel/concrete composite beams. In *Civil Engineering Transactions of The Institution of Engineers (Australia)*, volume 22, pages 202–208, 1980.

[42] E. Cosenza and S. Mazzolani. Short-term deflection of steel-concrete composite beams: the effects of the nonlinear behaviour of the shear connection. In *Proceedings of the First Italian Workshop on Composite Structures, University of Trento (Italy)*, 1993. (In Italian).

[43] R. I. M. Al-Amery and T. M. Roberts. Nonlinear finite difference analysis of composite beams with partial interaction. *Computers and Structures*, 35(1):81–87, 1990. doi: 10.1016/0045-7949(90)90258-4.

[44] D. J. Oehlers and G. Sved. Composite beams with limited-slip-capacity connectors. *Journal of Structural Engineering, ASCE*, 121(6):932–938, 1995. doi: 10.1061/(ASCE)0733-9445(1995)121:6(932).

[45] G. Fabbrocino, G. Manfredi, and E. Cosenza. Non-linear analysis of composite beams under positive bending. *Computers and Structures*, 70(1):77–89, 1999. doi: 10.1016/S0045-7949(98)00173-4.

[46] G. Manfredi, G. Fabbrocino, and E. Cosenza. Modelling of steel-concrete composite beams under negative bending. *Journal of Engineering Mechanics, ASCE*, 125(6):654–662, 1999. doi: 10.1061/(ASCE)0733-9399(1999)125:6(654).

[47] G. Fabbrocino, G. Manfredi, and E. Cosenza. Analysis of continuous composite beams including partial interaction and bond. *Journal of Structural Engineering, ASCE*, 126(11):1288–1294, 2000. doi: 10.1061/(ASCE)0733-9445(2000)126:11(1288).

[48] G. Fabbrocino, G. Manfredi, and E. Cosenza. Ductility of composite beams under negative bending: an equivalence index for reinforcing steel classification. *Journal of Constructional Steel Research*, 57(2):185–202, 2001. doi: 10.1016/S0143-974X(00)00008-0.

[49] M. A. Bradford and R. I. Gilbert. Nonlinear behaviour of composite beams at service loads. *The Structural Engineer*, 67(14):263–268, 1989.

[50] M. A. Bradford and R. I. Gilbert. Composite beams with partial interaction under sustained loads. *Journal of Structural Engineering, ASCE*, 118(7):1871–1883, 1992. doi: 10.1061/(ASCE)0733-9445(1992)118:7(1871).

[51] M. A. Bradford and R. I. Gilbert. Time-dependent stresses and deformations in propped composite beams. In *Proceedings of the Institution of Civil Engineers: Structures and Buildings*, volume 94, pages 315–322, 1992. doi: 10.1680/istbu.1992.20291.

[52] A. M. Tarantino and L. Dezi. Creep effects in composite beams with flexible shear connectors. *Journal of Structural Engineering, ASCE*, 118(8):2063–2081, 1992. doi: 10.1061/(ASCE)0733-9445(1992)118:8(2063).

[53] L. Dezi and A. M. Tarantino. Creep in composite continuous beam – I: theoretical treatment. *Journal of Structural Engineering, ASCE*, 119(7):2095–2111, 1993. doi: 10.1061/(ASCE)0733-9445(1993)119:7(2095).

[54] L. Dezi and A. M. Tarantino. Creep in composite continuous beam – II: parametric study. *Journal of Structural Engineering, ASCE*, 119(7):2112–2133, 1993. doi: 10.1061/(ASCE)0733-9445(1993)119:7(2112).

[55] L. Dezi, C. Ianni, and A. M. Tarantino. Simplified creep analysis of composite beams with flexible connectors. *Journal of Structural Engineering, ASCE*, 119(5):1484–1497, 1993. doi: 10.1061/(ASCE)0733-9445(1993)119:5(1484).

[56] L. Dezi, G. Leoni, and A. M. Tarantino. Algebraic methods for creep analysis of continuous composite beams. *Journal of Structural Engineering, ASCE*, 122(4):423–430, 1996. doi: 10.1061/(ASCE)0733-9445(1996)122:4(423).

[57] C. Amadio and M. Fragiacomo. A finite element model for the study of creep and shrinkage effects in composite beams with deformable shear connections. *Construzioni Metalliche*, (4):213–228, 1993.

[58] C. Amadio and M. Fragiacomo. A finite element model for short and long term analysis of steel-concrete composite beams in cracked phase. In *Proceedings of the XVII Italian Workshop on Steel (CTA), Naples (Italy)*, 1999. (In Italian).

[59] M. Fragiacomo, C. Amadio, and L. Macorini. Influence of viscous phenomena on steel-concrete composite beams with normal or high performance slab. *Steel and Composite Structures*, 2(2):85–98, 2002.

[60] L. Dezi, F. Gara, and G. Leoni. Long term behaviour of composite continuous two-beam decks with HCP slab. In *Proceedings of the XVII Italian Workshop on Steel (CTA), Naples (Italy)*, 1999. (In Italian).

[61] F. Mola, M. Mapelli, and R. Sicilia. Analysis of continuous composite beams with partial interaction by means of the algebraic simplified creep models. In *Proceedings of the IV Italian Workshop on Composite Construction, Palermo (Italy)*, 2000.

[62] H. G. Kwak and Y. J. Seo. Time-dependent behaviour of composite beams with flexible connectors. *Computer Methods in Applied Mechanics and Engineering*, 191 (34):3751–3772, 2002. doi: 10.1016/S0045-7825(02)00293-1.

[63] G. Ranzi. *Partial interaction analysis of composite beams: A direct stiffness approach*. VDM Verlag, 2009.

[64] H. Murakami. A laminated beam theory with interlayer slip. *Journal of Applied Mechanics, Transactions ASME*, 51(3):551–559, 1984. doi: 10.1115/1.3167673.

[65] X. Lin and Y. X. Zhang. A novel one-dimensional two-node shear-flexible layered composite beam element. *Finite Elements in Analysis and Design*, 47(7):676–682, 2011. doi: 10.1016/j.finel.2011.01.010.

[66] S. Jiang, X. Zeng, and D. Zhou. Novel two-node linear composite beam element with both interface slip and shear deformation into consideration: Formulation and validation. *International Journal of Mechanical Sciences*, 85:110–119, 2014. doi: 10.1016/j.ijmecsci.2014.05.006.

[67] Q. Nguyen, M. Hjiaj, and S. Guezouli. Exact finite element model for shear-deformable two-layer beams with discrete shear connection. *Finite Elements in Analysis and Design*, 47(7):718–727, 2011. doi: 10.1016/j.finel.2011.02.003.

[68] Q. Nguyen, E. Martinelli, and M. Hjiaj. Derivation of the exact stiffness matrix for two-layer Timoshenko beam element with partial interaction. *Engineering Structures*, 33(2):298–307, 2011. doi: 10.1016/j.engstruct.2010.10.006.

[69] S. Schnabl, M. Saje, G. Turk, and I. Planinc. Locking-free two-layer Timoshenko beam element with interlayer slip. *Finite Elements in Analysis and Design*, 43(9): 705–714, 2007. doi: 10.1016/j.finel.2007.03.002.

[70] Y. C. Wang. Deflection of steel-concrete composite beams with partial shear interaction. *Journal of Structural Engineering*, 124(10):1159–1165, 1998. doi: 10.1061/(ASCE)0733-9445(1998)124:10(1159).

[71] G. He, D. Wang, and X. Yang. Analytical solutions for free vibration and buckling of composite beams using a higher order beam theory. *Acta Mechanica Solida Sinica*, 29(3):300–315, 2016. doi: 10.1016/S0894-9166(16)30163-X.

[72] A. Chakrabarti, A. H. Sheikh, M. Griffith, and D. J. Oehlers. Analysis of composite beams with partial shear interactions using a higher order beam theory. *Engineering Structures*, 36:283–291, 2012.

[73] A. Chakrabarti, A. H. Sheikh, M. Griffith, and D. J. Oehlers. Analysis of composite beams with longitudinal and transverse partial interactions using higher order beam theory. *International Journal of Mechanical Sciences*, 59(1):115–125, 2012. doi: 10.1016/j.ijmecsci.2012.03.012.

[74] G. He and X .Yang. Finite element analysis for buckling of two-layer composite beams using Reddy's higher order beam theory. *Finite Elements in Analysis and Design*, 83:49–57, 2014. doi: 10.1016/j.finel.2014.01.004.

[75] C. Adam, R. Heuer, and A. Jeschko. Flexural vibrations of elastic composite beams with interlayer slip. *Acta Mechanica*, 125(1):17–30, 1997. doi: 10.1007/BF01177296.

[76] R. Heuer and C. Adam. Piezoelectric vibrations of composite beams with interlayer slip. *Acta Mechanica*, 140(3):247–263, 2000. doi: 10.1007/BF01182514.

[77] U. A. Girhammar, D. H. Pan, and A. Gustafsson. Exact dynamic analysis of composite beams with partial interaction. *International Journal of Mechanical Sciences*, 51(8):565–582, 2009. doi: 10.1016/j.ijmecsci.2009.06.004.

[78] Y. F. Wu, R. Xu, and W. Chen. Free vibrations of the partial-interaction composite members with axial force. *Journal of Sound and Vibration*, 299(4–5):1074–1093, 2007. doi: 10.1016/j.jsv.2006.08.008.

[79] N. Challamel and U. A. Girhammar. Lateral-torsional buckling of vertically layered composite beams with interlayer slip under uniform moment. *Engineering Structures*, 34(8):505–513, 2012. doi: 10.1016/j.engstruct.2011.10.004.

[80] F. Chen and P. Qiao. Buckling of delaminated bi-layer beam-columns. *International Journal of Solids and Structures*, 48(18):2485–2495, 2011. doi: 10.1016/j.ijsolstr.2011.04.020.

[81] P. L. Grognec, Q. H. Nguyen, and M Hjiaj. Exact buckling solution for two-layer timoshenko beams with interlayer slip. *International Journal of Solids and Structures*, 49(1):143–150, 2012. doi: 10.1016/j.ijsolstr.2011.09.020.

[82] S. Schnabl and I. Planinc. The influence of boundary conditions and axial deformability on buckling behavior of two-layer composite columns with interlayer slip. *Engineering Structures*, 32(10):3103–3111, 2010. doi: 10.1016/j.engstruct.2010.05.029.

[83] S. Schnabl and I. Planinc. The effect of transverse shear deformation on the buckling of two-layer composite columns with interlayer slip. *International Journal of Non-Linear Mechanics*, 46(3):543–553, 2011. doi: 10.1016/j.ijnonlinmec.2011.01.001.

[84] X. Liu, R. E. Erkmen, and M. A. Bradford. Creep and shrinkage analysis of curved composite beams including the effects of partial interaction. In *Proceedings of the Eleventh International Conference on Computational Structures Technology, Scotland*, 2012.

[85] R. E. Erkmen and M. A. Bradford. Nonlinear elastic analysis of composite beams curved in-plan. *Engineering Structures*, 31(7):1613–1624, 2009. doi: 10.1016/j.engstruct.2009.02.016.

[86] E. L. Tan. and B. Uy. Nonlinear analysis of composite beams subjected to combined flexure and torsion. *Journal of Constructional Steel Research*, 67(5):790–799, 2011. doi: 10.1016/j.jcsr.2010.12.015.

[87] U. A. Girhammar and D. Pan. Exact static analysis of partially composite beams and beam-columns. *International Journal of Mechanical Sciences*, 49(2):239–255, 2007. doi: 10.1016/j.ijmecsci.2006.07.005.

[88] E. G. Thomson, J. R. Goodman, and M. D. Vanderbilt. Finite element analysis of layered wood systems. *Journal of the Structural Division*, 101(12):2659–2672, 1975.

[89] S. P. Timoshenko and J. N. Goodier. *Theory of Elasticity*. McGraw-Hill, New York, 1970. 3rd edition.

[90] I. S. Sokolnikoff. *Mathematical Theory of Elasticity*. McGraw-Hill, New York, 1970. 2nd edition.

[91] W. C. Young and R. G. Budymas. *Roark's Formulas for Stress and Strain*. McGraw-Hill, New York, 2002. 7th edition.

[92] B. A. Boley and J. H. Weiner. *Theory of Thermal Stresses*. Dover Publications, New York, 1997.

[93] R. B. Hetnarski and M. R. Eslami. *Thermal Stresses – Advanced Theory and Applications*. Springer, Berlin, 2010.

[94] K. Washizu. *Variational Methods in Elasticity and Plasticity*. Pergamon, New York, 1968.

[95] J. M. Gere and S. P. Timoshenko. *Mechanics of Materials*. PWS Engineering, Boston, MA, 1984. 2nd edition.

[96] R. Solecki and R. J. Conant. *Advanced Mechanics of Materials*. Oxford University Press, Oxford, 2003.

[97] I. Ecsedi and K. Dluhi. A linear model for static and dynamic analysis of nonhomogeneous curved beams. *Applied Mathematical Modelling*, 29(12):1211–1231, 2005. doi: 10.1016/j.apm.2005.03.006.

[98] T. H. Richard. *Energy Methods in Stress Analysis: With an Introduction to Finite Element Techniques*. Ellis Horwood, Chichester, 1977.

[99] L. Elsgolts. *Differential Equation and the Calculus of Variations*. Mir Publishers, Moscow, 1977.